TOPOLOGICAL ANALYSIS OF THE TRANSHYDROGENASE IN *Escherichia coli* MEMBRANES USING PROTEOLYTIC PROBES

by

Raymond Cheuk Wa Tong

B.Sc., The University of British Columbia, 1986

A THESIS SUBMITTED IN PARTIAL FULFILLMENT OF

THE REQUIREMENTS FOR THE DEGREE OF

MASTER OF SCIENCE

in

THE FACULTY OF GRADUATE STUDIES

Department of Biochemistry

We accept this thesis as conforming

to the required standard

THE UNIVERSITY OF BRITISH COLUMBIA

March 1991

In presenting this thesis in partial fulfilment of the requirements for an advanced degree at the University of British Columbia, I agree that the Library shall make it freely available for reference and study. I further agree that permission for extensive copying of this thesis for scholarly purposes may be granted by the head of my department or by his or her representatives. It is understood that copying or publication of this thesis for financial gain shall not be allowed without my written permission.

Department of Biochemistry

The University of British Columbia
Vancouver, Canada

Date March 22, 1991

DE-6 (2/88)

ABSTRACT

Using proteolytic probes, the pyridine nucleotide transhydrogenase (EC 1.6.1.1) from Escherichia coli was analyzed for its native topography in the cytoplasmic membrane.

Before analyses could be performed, the isolation of transhydrogenase-enriched ISO (inside-out) cytoplasmic membrane vesicles was accomplished by modification of the procedure followed by Clarke (Clarke, D. M. and Bragg, P. D. (1985) *Eur. J. Biochem.* 149, 517-523) in purifying the enzyme from overexpressing E. coli JM83pDC21 cells. Two major changes were made. One was that the solubilization of the bacterial membrane and subsequent purification steps were omitted. The other was the separation of outer membranes from the cytoplasmic membrane preparation by sucrose gradient density centrifugation. This was essential owing to the contaminating presence of a 30 kD protein in the outer membrane of the original preparation. Transhydrogenase-enriched RSO (right-side-out) membrane vesicles were isolated by a different procedure using lysozyme-mediated breakage of E. coli spheroplasts and subsequent vesicular reformation.

To identify possible transhydrogenase fragments arising from proteolytic cleavage, anti-E. coli transhydrogenase polyclonal antibodies were generated in rabbits. Two sets of polyclonal antibodies were produced. One set cross-reacted with both the α (52 kD) and β (48 kD) subunits of the transhydrogenase. The other reacted with the α subunit only.

Trypsin and proteinase K were the main proteolytic probes used against both ISO and RSO cytoplasmic membrane vesicles, although chymotrypsin was also used in preliminary experiments with ISO membrane vesicles. Identification of fragments resulting from proteolytic cleavage of the enzyme was obtained using anti-transhydrogenase antibodies and by N-terminal sequencing and/or C-terminal

sequencing. In some of these experiments, isolation of the proteolytic fragments was necessary prior to analysis. This was done using a number of different methods. The particular methods applied, which included column chromatography strategies and elution procedures from SDS-Polyacrylamide gels, depended on the type of analysis carried out.

The analyses indicated that the α subunit has at least a 41 kD sequence extending from its N-terminus which is exposed to the cytoplasmic side of the membrane. This sequence may contain an active site of the enzyme. This is suggested by the binding of this fragment to a NAD-affinity column. The membrane-imbedded region of the α subunit anchoring the 41 kD region predicted by hydropathy plotting (Clarke, D. M., Loo, Tip W., Gilliam, S. and Bragg, P. D. (1986), *Eur. J. Biochem.* 158, 647-653) could not be detected by our methods. Susceptible tryptic cleavage sites along the 41 kD region were identified by partial proteolysis and may reflect areas in the subunit's tertiary or quaternary structure that are exposed to the surrounding medium. Major cleavage sites were at arg_{15}, lys_{227}, lys_{264}, arg_{268}, lys_{275}, arg_{355}, and arg_{361}. There do not appear to be significant portions of the subunit protruding into the periplasm as neither trypsin nor proteinase K had any effect on the subunit in RSO-oriented membrane vesicles.

Proteinase K experiments with ISO and RSO membrane vesicles suggest that a 20 kD portion of the β subunit is protected from cleavage and is imbedded in the membrane. The identity of this fragment could not be confirmed. Hydropathy analysis of the transhydrogenase gene-derived amino acid sequence (Clarke, D. M., Loo, Tip W., Gilliam, S. and Bragg, P. D. (1986), *Eur. J. Biochem.* 158, 647-653) suggests that this could be a sequence extending from the N-terminus of the β subunit. This is a hydrophobic sequence containing 7 possible transmembranous helices and having a theoretical molecular weight in the range of 20 kD. The proteinase K results also indicate that the rest of the β subunit is exposed to the cytoplasmic side of the

membrane rather than the periplasmic side. The results obtained here are consistent with hydropathy predictions made with regard to this subunit.

In addition, two different experiments indicate that an α-α subunit interaction may be present in the oligomeric structure of the membrane-bound enzyme (Hou, C., Potier, M. and Bragg, P. D. (1990), *Biochim. Biophys. Acta* 1018, 61-66). Substrates of the enzyme did not appear to affect the transhydrogenase's general conformation upon binding as detected by experiments using partial tryptic proteolysis. Partial trypsinolysis also revealed that selective detergent extraction of transhydrogenase-enriched ISO vesicles with Triton X-100 and sodium cholate did not affect the overall conformation of the membrane-bound enzyme despite greatly reducing the enzymatic activity.

TABLE OF CONTENTS

Page

Page

LIST OF TABLES

LIST OF FIGURES

Page

Page

LIST OF ABBREVIATIONS

AcNAD(+)(H)	3-Acetylpyridine adenine dinucleotide
ATP	Adenosine-5'-triphosphate
ATPase	ATP phosphohydrolase
Brij 35	Polyoxyethylene (23) lauryl ether
$Cu(OP)_2$	Copper-(*o*-phenanthroline)$_2$
DCCD	N, N'-dicyclohexylcarbodiimide
DEAE-	Diethylaminoethyl-
DNase	Deoxyribonuclease
DPPC	Diphenyl carbamyl chloride (inhibits chymotrypsin in trypsin preparations)
DTNB	5,5'-dithiobis(2-nitrobenzoic acid)
DTT	Dithiothreitol
EDTA	(Ethylenedinitrilo)-tetraacetic acid
E. coli	Escherichia coli
FAD	Flavin adenine dinucleotide
FCA	Freund's complete adjuvant
FIA	Freund's incomplete adjuvant
FPLC	Fast protein liquid chromatography
FSBA	*p*-fluorosulfonylbenzoyl-5'-adenosine
F_o	Proton channel unit of ATPase
H^-	Hydride ion equivalent
IEF	Isoelectric focusing
IgG	Gamma immunoglobulin
ISO	Inside-out
KBS	Potassium-buffered saline
kD	KiloDalton

K_{eqm}	Equilibrium constant
K_m	Michaelis constant
M_r	Molecular weight
NAD(+)(H)	Nicotinamide adenine dinucleotide
NADP(+)(H)	Nicotinamide adenine dinucleotide phosphate
NBD-Cl	4-chloro-7-nitrobenzo-2-oxa-1,3-diazole
NEM	N-ethylmaleimide
PAGE	Polyacrylamide gel electrophoresis
PCB^-	Phenyl dicarbaundecarborane
pI	Isoelectric pH
pK_a	Negative logarithm of the dissociation constant for the acid
PMSF	Phenylmethylsulphonylfluoride
pnt	Pyridine nucleotide transhydrogenase gene
psi	Pounds per square inch
PVDF	Polyvinylidene difluoride
RNase	Ribonuclease
RSO	Right-side-out
S. aureus	*Staphylococcus aureus*
SBTI	Soya bean trypsin inhibitor
SDS	Sodium dodecyl sulfate
TED	Buffer containing 50 mM Tris-H_2SO_4, 1 mM DTT, 1 mM EDTA, pH 7.8
TEMED	N,N,N',N'-tetraacetic acid
Tris	Tris (hydroxymethyl)-aminomethane
Triton X-100	Polyoxyethyleneglycol (9-10) p-t-octylphenol
Tween 20	Polyoxyethylene (20) sorbitan monolaurate
U	Units of enzymatic activity

v/v	Volume to volume ratio
V_{max}	Maximum enzymatic velocity
w/v	Weight to volume ratio
x g	Times gravity
ΔpH	Difference in pH across the membrane

ACKNOWLEDGEMENTS

I am greatly indebted to Dr. P. D. Bragg, for giving me the opportunity, the means and the financial support to work on this thesis. The patience, advice and encouragement that he proffered, was invaluable over the course of this study.

My heartfelt thanks to all the people that I worked with in our lab, both to the ones that remain and to those that have come, conquered and gone. I consider them all to be friends. To Dr. Ted Sedgwick, I thank for the assistance and wit with which he replied to my sometimes impertinent questions. To Cynthia Hou, I am grateful for her neverfailing help in matters of technical and grammatical importance. To Dr. Seeloch Beharry, I shall remember his good humour and empathy during our conversations. To Dr. Keith Withers, I thank for the general kindness and understanding with which he treated me. To Natalie Glavas, who skis and tells, the transhydrogenase torch is now yours. Last but not least, I thank David Chang who made the frustrations in my work bearable by regaling me with details of his own frustrating problems, which he insisted were worse than mine. When anything did work out, I was much comforted by his gracious reminders of the arsenic lining on the other side of every cloud. But I am most grateful for the fact that he was always there for me, since he never had any place else to go.

"Murphy was an optimist."

O'Toole

I INTRODUCTION

The pyridine nucleotide transhydrogenase in Escherichia coli and all mammalian cells is a membrane-bound enzyme that catalyzes the following hydride ion equivalent (proton + two electrons) transfer reaction:

$$NADH + NADP^+ \text{ <----> } NAD^+ + NADPH$$

An enzyme with this activity was first observed in extracts of Pseudomonas fluorescens by Colowick et al. (1). This enzyme was also subsequently shown to exist in mammalian tissues (2). In mammalian cells, the enzyme is located in the mitochondrial inner membrane (3-7). The mammalian enzyme was later demonstrated to belong to a class of transhydrogenases designated as AB-specific in contrast with the Pseudomonas enzyme which belong to the BB-specific class. Both classes have been reviewed (8-10). The class distinction will be elaborated on below. The E. coli counterpart, also in the AB-specific family, is located in the cytoplasmic membrane (12) and has many functional and structural similarities in common with the mammalian system.

A unique property shared by these AB-transhydrogenases is that they are functionally coupled to the energy generating systems of the cell (9). These include the ATPase enzyme and the electron transport chain who have most of their functional constituents imbedded in the same membrane as the transhydrogenase (13-15). That is in the presence of energy generated by such sources, the apparent equilibrium constant jumps from a value of 1 to 500 (16-17). In conjunction, energy stimulates the forward reaction rate (10) and inhibits the reverse rate. It is commonly believed that the mediating link between the exergonic reactions and the endergonic forward transhydrogenase reaction is a protonmotive force (18-21) acting across the membrane bilayer in the classical chemiosmotic manner (22-23). There is a long-existing controversy as to whether this protonmotive force is present in the form of a generally accessible pool of protons in the bulk aqueous phase of the periplasmic and

interior milieus (24, 56) or whether there is at least in part a localized and direct circuit of proton flow or energization between the coupled enzyme systems (25-32, 53, 55, 57). Despite this mechanistic dispute at the molecular level, there is little doubt membrane energization is a necessary prerequisite for enhanced transhydrogenase activity in the membranes of cells.

This energy drivable activity is, however, not typical of the BB-specific class of transhydrogenases. They are not linked with energy-yielding cellular processes like the AB-family. The nomenclature of the two classes does not, however, result from this important difference. Rather, it derives from differences in the stereospecificity of transfer of the hydrogen from the 4 position of the nicotinamide ring of NADH and NADPH. The BB-enzyme transfers the 4B-hydrogen of both NADH and NADPH to $NADP^+$ and NAD^+, respectively. The AB-enzyme transfers the 4A-H of NADH and 4B-H of NADPH to $NADP^+$ and NAD^+, respectively (33).

The BB-class is exclusively found in heterotrophic bacteria such as the aforementioned Pseudomonas fluorescens (1, 34-39). They are easily solubilized proteins and have other major differences in properties with the AB-class. Excepting the common chemical reactions that they catalyze, they seem to be distinctly different as a group, structurally, mechanistically, and in terms of their effectors and regulation. Because BB-enzymes are not energy-coupled and the thermodynamic and kinetic amplitudes and directions are therefore fixed in this regard, the physiological functions of these enzymes in the cell are not likely to be the same as those for the AB-enzymes.

The present thesis concentrates on the structural aspects of the AB-transhydrogenase found in E. coli. This structural analysis will hopefully serve as a beginning point for further studies in gaining a better understanding of the enzyme's functional properties. As a necessary prelude, the remainder of this introduction will therefore review the background of research in the AB-transhydrogenase field developed prior to and concurrent with the work detailed in this thesis.

A. Energy Linkage

As alluded to, coupling of the mitochondrial transhydrogenase to the respiratory chain or to ATP hydrolysis (40-43) manifests itself in an energy-dependent 5-10 fold increase rate of $NADP^+$ reduction by NADH (40-42) and a 500-fold increase in the apparent K_{eqm} (16-17). In addition, the enhanced reaction can be driven by a potassium ion gradient across the inner membrane with valinomycin present (44).

The ATPase-driven activity can work independent of the aerobically driven activity and vice versa as demonstrated in the observation that electron transport inhibitors do not inhibit the former activity (40-42), while ATPase F_o inhibitors such as oligomycin do inhibit this but do not inhibit the respiration-driven reaction (13, 40-41, 45-46). Furthermore, E. coli mutants missing ATPase activity cannot drive the transhydrogenase using ATP (47), but can still do so via respiration (48). Either energy-linked reaction can be abolished by oxidative phosphorylation uncouplers (13, 42-43, 49-51) or by the combined effects of valinomycin and nigericin in the presence of potassium ions (52). Both types of reagents have the net effect of equilibrating the proton pools on either side of the membrane with each other and thus dissipating the gradient. It is commonly envisioned that this gradient acts through proton pools that equilibrate with the bulk aqueous phases separated by the inner membrane (24). However, it has been found in submitochondrial particles that both uncouplers and oligomycin blocked the ATP-driven transhydrogenase less efficiently than the ATP-driven NAD^+ reduction by succinate (43, 53), while both reactions are equally sensitive to ATPase inhibitors (53- 54). This suggested that the ATPase may interact directly with the transhydrogenase (53, 55), although subsequent experiments performed by Persson et al on submitochondrial particles and transhydrogenase reconstituted vesicles say that this coupling was delocalized (56). In a later development, Chang observed that in everted E. coli membrane vesicles expressing higher than normal levels of transhydrogenase, uncouplers stimulated the aerobic-driven transhydrogenase activity while inhibiting, as expected, the ATPase-dependent

reaction (57). This suggests a non-bulk phase coupling for the aerobically-linked reaction in these cells, while the ATPase-linked reaction seems to be coupled indirectly through bulk phase or delocalized proton pools as fitting the chemiosmotic hypothesis. Alternatively, the anomalous observation with the aerobically-driven transhydrogenase reaction may be an artifactual effect having no in vivo relevance because it was shown that NADH oxidase activity was significanty decreased in these overexpressing cells. However, Chang did a number of experiments to limit the speculation in this regard by showing that there was no change in the composition of many other respiratory chain components and also that excess transhydrogenase sequestered in intracellular tubular membrane structures induced by a need to accomodate the overproduction (88), perform the same unique form of energization as the enzymes located on the cytoplasmic membrane (ie. the anomalous energization phenomenon is not localized exclusively in the special membrane structures). He also noted that certain respiratory chain inhibitors had no effect on the aerobically-linked transhydrogenase in both normal and overproducing cells.

Another consequence of energy coupling of the transhydrogenase is that a reversal of the energy-linked transhydrogenase reaction may be able to be used to drive ATP production. Despite unfavourable equilibrium conditions which tend to ATP hydrolysis in the linked reaction, ATP production was indeed observed under in vitro experimental conditions (58).

B. Reaction Mechanism and Regulation

Steady state kinetics of the enzyme in beef heart submitochondrial particles (59-61) and in E. coli membranes (62-63) revealed a reaction mechanism involving a short-lived ternary complex. This was evident from linearly convergent double reciprocal plots of initial velocities versus substrate concentrations (ie. same K_ms but different V_{max}s). It was also demonstrated that competitive relationships between NAD^+ and NADH and between $NADP^+$ and NADPH existed, whereas noncompetitive

relationships between NAD^+ and $NADP^+$ and between NADH and NADPH were the case. Also, inhibitors exist which are specifically competitive for binding with either NAD(H) or NADP(H) (64-65). Another supporting observation was that hydride ion transfer occurs directly between the 4A locus of NADH and the 4B locus of NADPH without exchange between substrate hydrogen and water hydrogen (33, 66-67). Therefore, the prevailing evidence suggests separate binding sites for NADP(H) and NAD(H) and a ternary enzymatic intermediate. The order of substrate binding appears to follow a random mechanism (68-69).

Therefore, there is no need to invoke a binary ping-pong mechanism involving a reduced enzyme intermediate. Initially, such a mechanism was suggested by the reports that partial transhydrogenase reactions could occur at the NAD(H) and NADP(H) binding sites. In the presence of NADPH, the bovine heart enzyme could catalyze a hydride ion exchange reaction between the 4A locus of NADH and the 4A locus of NAD^+ (66). This argues against NADH binding to the NADP(H) binding site because one would expect the specific removal of the 4B hydrogen from NADH analogous to the 4B hydrogen of NADPH removed during "normal" transhydrogenation. This reduction of NAD^+ by NADH was thereby proposed to represent a partial reaction of the normal NADPH->NAD^+ transhydogenation which would involve a reduced enzyme intermediate. This idea was later put into doubt by an alternative explanation of the results observed above, using the catalytic amounts of NADPH in the reaction as a central point in the explanation (68, 70). This version did not require the involvement of a reduced enzyme intermediate and is explained below by analogy after discussion of a similar observation involving the NADPH->$NADP^+$ partial reaction.

Wu and Fisher saw similiar effects in an NADPH->$NADP^+$ partial reaction in the bovine heart transhydrogenase (71). The transfer of hydrogen between the nucleotides was between 4B loci, not from the 4A locus of NADPH to the 4B locus of $NADP^+$ as expected if the NADPH was indeed bound to the NAD(H) binding site. They

naturally thought a transiently reduced enzyme intermediate was involved. That is the enzyme would bind NADPH at its proper active site, remove the hydride ion from NADPH, release the "hydrideless" first product, bind a new $NADP^+$ molecule and then transfer its temporarily-bound hydride ion to the $NADP^+$ recipient, etc.. As a consequence, they thought that a similiar mechanism may be occuring in the NADPH–>NAD^+ transhydrogenase. Recent results by Enander and Rydstrom do not support this conclusion as they found the NADPH->$NADP^+$ reaction required catalytic amounts of NADH (67). Again, a reduced enzyme intermediate is not necessary in the explanation if such is the case. One could propose that NADH bound to its normal site would transfer its hydride ion to $NADP^+$, replenish itself by reduction by an incoming NADPH molecule that replaces the nascent product and thereby continue its catalytic conversion of $NADP^+$ molecules to NADPH without being stoichiometrically consumed. In figurative terms, the NAD(H) in this mechanism functionally replaces the reduced enzyme intermediate in the other explanation. This also explains by analogy, the strange stereochemistry of the NADH->NAD^+ partial reaction mentioned in the previous paragraph. In that case, the enzyme-bound NADP(H) molecule is the "catalyst" for the NADH->NAD^+ partial reaction. In addition, the idea of a binary ping-pong mechanism being involved in transhydrogenation is doubtful since there is no evidence of groups on the enzyme that are reducible (72-73).

It was found that when energy is applied, there is a significant reduction in the Michaelis constant value from 40 uM to 6.5 uM for $NADP^+$ in the beef heart transhydrogenase reaction, while the Michaelis constant for NAD^+ increases from 28 uM to 43.5 uM (59-60). Ergo, energy promotes binding of $NADP^+$ (and NADH) and release of NAD^+ (and NADPH). This occurs with a concomitant increase in the maximal velocity of the forward reaction. Since energy does not affect the maximal reverse reaction rate but only decreases the enzyme's affinity for its substrates (NAD^+ mainly), the primary reason for the increased forward reaction rate is this increased dissociation of NAD^+ (and following suit, NADPH).

These energy-linked changes in affinity may also account for the effects of certain inhibitors and effectors of the transhydrogenase such as Mg^{2+} ions and protons (17). An energy-linked increase in Mg^{2+} inhibition was observed. Also, increased pH enhanced the effect by Mg^{2+}. Later, it was shown that Mg^{2+} is a competitive inhibitor of $NADP^+$ (74) and thus, reflects the enzyme's increased affinity for $NADP^+$ under energization. Solute protons were also shown to compete with the extent of inhibition by Mg^{2+} (74) and may do so by increasing the affinity of the enzyme for $NADP^+$ as was observed (75). Experiments performed by Rydstrom indicated that protons act directly in the regulation of the enzyme's kinetic properties by acidifying selected region(s) of the enzyme which accompanies energization of the submitochondrial particles (75). The involvement of protons in the energized reaction mechanism is thus, central to how the enzyme is coupled and was explored in depth by many research groups. This is discussed further in section E of this introduction.

C. Purification of Transhydrogenase

The mitochondrial transhydrogenase was first purified from beef heart by two groups, Rydstrom (72) and Fisher (73). Rydstrom used sodium cholate with ammonium sulphate to extract the membrane proteins from submitochondrial particles. This extract was subject to DEAE-Sepharose and hydroxyapatite chromatography. The result was an enzyme preparation showing a homogeneous protein of molecular weight of 97 kD. On the other hand, Fisher extracted submitochondrial particles with sodium perchlorate to take off the extrinsic proteins and then solubilized the intrinsic proteins using lysolecithin. The transhydrogenase was subsequently purified by passage of the solubilized material through an alumina gel, a calcium phosphate gel, and NAD-affinity columns. This enzyme was found to be of 110 kD molecular weight. Both Rydstrom and Fisher's purification schemes were labor intensive and produce low yields of enzyme.

Wu et al. designed a simpler and higher yielding procedure involving extrinsic protein removal by a NaCl wash, membrane extraction with Triton X-100, NADH-elution chromatography on an agarose-immobilized NAD-affinity column (76). SDS-Page indicated that a homogeneous preparation of high specific activity and yield had been obtained, but this purification could not be achieved by others including Persson et al. (77).

Instead, Persson used cholate-ammonium sulphate fractionation followed by DEAE-Sepharose and fast protein liquid chromatography which resulted in a greater purity, a better reproducibility, and a larger yield than previous procedures (77).

The E. coli enzyme was first partially purified by Liang and Houghton (78) using ion exchange and gel filtration chromatography of deoxycholate extracts of membranes. SDS-Page revealed two major proteins of 94 and 50 kD as well as a number of minor ones. Because transhydrogenase synthesis is repressed in cells grown in complex media with large amounts of amino acids (79), this allows selective induction of transhydrogenase production. By using ^{3}H-Casamino acids and ^{14}C-labelled leucine in the repressive and inductive stages, respectively, of transhydrogenase synthesis and by measuring the incorporation ratio of the two labels into proteins, it was shown that induction of enzyme synthesis corresponded to incorporation of ^{14}C into the 94 and 50 kD proteins (78). The relationship between these two protein bands is unclear, but the experimenters postulated that the 94 kD molecular weight component represented the intact enzyme because of its similarity in size to the mitochondrial enzyme. They believed that the lower molecular weight component was a cleavage product. An alternative explanation as suggested by them was that the higher molecular weight species is an exceptionally stable dimer of the 50 kD species.

Clarke and Bragg first partially purified the E. coli enzyme (80) using a Tris-buffer wash of membranes to remove extrinsic proteins followed by extraction using sodium deoxycholate/KCl. This material was adsorbed onto phenyl-Sepharose and

eluted with Triton X-100 and Brij 35. The eluant was absorbed on a DEAE-Bio-Gel A column and eluted with a NaCl gradient elution. A pooled sample of transhydrogenase-containing fractions was subjected to gel filtration chromatography followed by NADH-elution chromatography from an agarose/hexane/NAD-affinity column. This purification procedure was not entirely satisfactory as yields were low and the purity varied greatly from run to run.

The fact that transhydrogénase constitutes only a minor amount of the total cytoplasmic membrane protein (in fact, 0.1 to 0.5%) in the native E. coli membrane adds to the difficulty of purification (81). This was overcome by increasing transhydrogenase expression through cloning of the transhydrogenase encoding gene, pnt, into a multicopy pUC13 plasmid (82). The cloned fragment, a 3.05-kilobase fragment from the 35.4 min location of the E. coli genome, in the pUC plasmid conferred to its host a 70-fold overproduction of the enzyme. The elevated level of activity was a criterion for screening out clones bearing the pnt gene. The protein products were found to be two polypeptides of molecular weights 50 and 47 kD as indicated by SDS-Page. Both polypeptides were shown to be necessary for transhydrogenase activity.

The increased expression of pDC21, the pnt-containing plasmid, by increasing the level of transhydrogenase in host E. coli cells afforded Clarke and Bragg a simple purification procedure with high yields and better purity (80) . Membranes from overexpressing cells were pre-extracted with Triton X-100 and sodium cholate before solubilization in sodium deoxycholate/KCl. The solubilized material was centrifuged through a 1.1 M sucrose solution. The enzyme purified this way consisted of two subunits, α and β, of apparent molecular weights, 50 and 47 kD, respectively. It was found that upon storage or heating, the two solubilized subunits aggregated to form a 95-100 kD species which is of similar size to Liang and Houghton's high molecular weight component obtained in their purification (78). The presence of both subunits in the 95-100 kD species was shown by peptide mapping (82).

D. Reconstitution of Transhydrogenase

In order for the functional and structural properties of the enzyme to be elucidated in a less ambiguous but still relevant setting, it was necessary to purify the enzyme and to reconstitute it into liposomes. The functional and structural studies with the reconstituted enzyme will be expounded on in later sections of this introduction, so the subject at hand will deal with the methods of reconstitution and of how to determine whether the reconstitution is a functional one.

Hojeberg and Rydstrom (72) were the first to reconstitute the purified bovine heart enzyme into phosphatidylcholine vesicles. NADPH ---> NAD^+ transhydrogenation by these vesicles resulted in an uncoupler-sensitive intake of lipophilic anions suggestive of the establishment of a membrane potential, positive in the vesicle's interior. Uncouplers enhanced the catalytic reaction rate. Thus, a functional enzyme was reconstituted in this system.

Others reconstituted the enzyme by dialysis of transhydrogenase with sodium cholate and phosphatidylcholine to form small unilamellar proteoliposomes (83-85). Again, these vesicles showed acidification of the vesicle's internal space upon transhydrogenase mediated reduction of NAD^+ by NADPH. As well, uncouplers enhanced the reaction rate in both directions as expected. In the absence of uncouplers, the inhibition of transhydrogenation results from the formation of a pH gradient across the vesicular membrane (8). Uncouplers relieve the enzymatic inhibition by allowing proton cycling across the membrane.

Clarke and Bragg functionally reconstituted the purified E. coli enzyme with egg yolk phosphatidylcholine (80) using the cholate dilution method (84). They found uncoupler sensitive inhibition of catalytic activities and proton movements working here as well. Proton movements as indicated by fluorescent pH probe measurements were correlated with the hydride ion transfer reactions in the coupled state.

The respiratory control ratio is the ratio of transhydrogenase activity in the presence to that in the absence of uncouplers (84). This ratio indicates the degree to which the enzyme had been reconstituted properly in terms of coupled function. This control in a properly reconstituted vesicle may be obliterated by detergents such as Triton X-100 and lysophosphatidylcholine (84-85). If detergent-effected lysis of proteoliposomes in this manner does not reveal any latent transhydrogenase activity, one could say that the enzyme is functionally and unidirectionally reconstituted. Given that pyridine nucleotides are not membrane permeable, the enzyme molecules must be incorporated asymmetrically with their active sites accessible to the external medium. Therefore, it is ideal before studies are carried out with reconstituted vesicles that this criterion is met. It was so found in the reconstitution methods mentioned above.

E. Electrogenic and Proton Pumping Properties

Mitchell first proposed that transhydrogenase is a transmembrane proton pump by observing transhydrogenase-catalyzed transport of solute protons in tightly coupled submitochondrial particles (18). He found that hydride ion transfer between NADPH and NAD^+ generated proton uptake at 0.2 protons/$NADP^+$ formed. The reverse reaction led to proton extrusion. Mitchell and Moyle subsequently determined the proton uptake per $NADP^+$ formed to be 2 for intact rat liver mitochondria (86). Using phenyl dicarbaundecarborane (PCB^-), a lipophilic anion, to monitor electrogenic changes across submitochondrial particles, NAD^+ reduction by NADPH resulted in the uptake of the anion and the opposite transhydrogenation resulted in its efflux (8). Based on this and similar findings in E. coli vesicles (87), it was proposed that the proton pump was reversible.

Direct evidence on the proton translocation properties of the enzyme had to await a system where the influence of other proteins could be negated. And it was in using enzymes reconstituted into lipid vesicles that uptake of tetraphenylboron,

another permeant lipophilic anion, was observed (72) and could be expunged by uncouplers (83-85). Although this indicated an electrogenic activity of the enzyme, the ion species involved is strongly suggested to be protons because of an internal (84) and external pH shift (83-85). This shift was sensitive to both uncouplers (83-85) and nigericin (84). Valinomycin in the presence of a high internal potassium concentration resulted in substantial internal proton accumulation and a transient stimulation of NAD^+ reduction by NADPH (85). A high external potassium concentration had the opposite effect on the catalytic activity. The same group of researchers show that an artificially imposed "high to low" proton concentration gradient from outside to inside stimulated NAD^+ reduction by NADPH (85). These results indicate that both membrane potentials (as shown exquisitely by the potassium gradient/valinomycin experiments) and pH gradients regulate the transhydrogenase in membrane vesicles. However, Earle and Fisher using valinomycin and nigericin demonstrated that reconstituted transhydrogenase is probably controlled for the most part, by membrane potential and very little by pH difference (84). Nevertheless, it seems proton movements are the direct molecular links to enhanced hydride ion transfer by transhydrogenase.

Protonal movements were also indicated by the distribution of fluorescent pH probes, 9-aminoacridine (77, 83-84) and 9-amino-6-chloro-2-methoxyacridine (85), where proton uptake by transhydrogenation was accompanied by a quenching of the fluorescence as the probes "follow" the protons into the vesicle. The preparations used in these experiments were of homogeneously purified transhydrogenase enzymes incorporated back into liposomes. In the absence of artificially imposed ion gradients, ionophores, uncouplers, or membrane continuity caused by physical disruption, all conditions that favor enhanced or free proton movements through the transhydrogenase, these preparations show little or no catalytic activity as expected. This indicates that the transhydrogenase activity in this case is limited by a pH gradient and/or a membrane potential. However, Clarke using 9-aminoacridine in his studies,

found that the E. coli proton pump is regulated primarily by a pH gradient rather than by a membrane potential (88).

Protons moving into vesicles as a result of the enzyme's catalytic activity can also be monitored inside the vesicles by a trapped pH indicator, dextran-linked fluorescein (84) and outside the vesicles by a sensitive pH electrode (89). Using a pH electrode, it was determined that 1 proton was taken up per $NADP^+$ formed in reconstituted vesicles (89). Recently, a value of 0.5 was reported (90). The discrepancy is difficult to explain but it may be that the higher value is correct since the lower value may arise from uncoupling or improper reconstitution of the transhydrogenase in these preparations.

Supporting evidence that the transhydrogenase indeed acts as a proton pump is seen in the enzyme's sensitivity to N,N'-dicyclocarbodiimide (DCCD) which probably acts by disabling the proton channel (91-92). This effect has also been observed in the mitochondrial ATPase (93) and in the cytochrome oxidase (94). Dontsov and others demonstrated in submitochondrial particles that lipophilic anion uptake catalyzed by the enzyme is inhibited by DCCD but not by oligomycin (95). Pennington and Fisher's treatment of the enzyme with DCCD inactivated the hydride ion transfer activity in addition to the proton translocation activity (91). One interesting outcome of this group's experimentation with DCCD was the determination that it took 2 molecules of this inhibitor per molecule of transhydrogenase monomer to totally inactivate the catalytic activity and only one molecule of DCCD per enzyme monomer to knock out the proton translocating activity. This suggests that the proton translocation and catalytic activities are not obligatorily linked or that DCCD separates in part proton pumping from hydride ion transfer, two possible conclusions supported by similar findings of Persson et al. (77). On the other hand, Clarke concluded that proton translocation and catalytic activities are obligatorily linked after observing DCCD's inhibition of proton pump activity and transhydrogenation in the E. coli

enzyme (80). He found one DCCD molecule covalently modifying one active enzyme unit was sufficient to block both activities carried out by the enzyme totally and equally.

Pennington and Fisher in their work with the mitochondrial enzyme also found that DCCD inactivation could be influenced by NADP(H) even though the binding site for DCCD was proposed to be elsewhere from the active site (91). In contrast, Phelps and Hatefi stated that AcNAD$^+$ (an NAD$^+$ analogue) and NADH rather than NADP(H) prevented the enzyme from being inactivated by DCCD, which suggests that DCCD may be binding at or close to the NAD(H) binding site (96-97). A similiar case was observed for the E. coli transhydrogenase (80). NADH protected the enzyme against DCCD inhibition whereas NADP$^+$ and to a lesser degree NADPH, increased the rate of this inhibition.

Sulfhydryl groups have been suggested to act in transhydrogenase-dependent proton translocation via a thiol-disulfide interchange (98). Inactivation/modification of two classes of sulfhydryls, one situated in or near the NADP(H)-binding site and one peripheral to the active sites (99), indicated that they are not involved in proton translocation (8, 100). In addition, the enzyme would still generate a membrane potential upon methane thiolation of both classes of sulfhydryls (100). This however does not discount the possible role of buried sulfhydryls that are exposed upon denaturation (8) in contributing to the proton translocation process. Also a thiol-disulfide interchange may not be the way sulfhydryl groups act as a link in proton movement, since a conformationally induced change in its and/or other residues' apparent pKa values may in fact bring about proton transfer through the protein (101). More on this will be said later.

F. Sequence and Structural Properties of Transhydrogenase

As indicated previously, the mitochondrial enzyme has a minimal molecular weight between 97 to 115 kD. The amino acid composition has been determined for the purified enzyme and its polarity index (percentage of charged and polar amino

acids) is approximately 40% (76). This value indicates that the transhydrogenase is more nonpolar than most water soluble proteins (102).

Cross-linking studies were performed on the purified bovine heart enzyme to elucidate any possible oligomeric arrangement in its structure (103). Crosslinking of the enzyme with bifunctional reagents such as dimethyl adipimidate, dimethyl pimelimidate, dimethylsuberimidate, and dithiobis (succinyimidyl propionate) gave a dimeric species as observed on SDS-Page. No higher molecular weight aggregates were observable. Crosslinking was prevented and activity was lost after 6 M urea denaturation. This plus the cross-linking results obtained from studies on the membrane-bound enzyme (104) indicated that the enzyme exists in the mitochondrial membrane as a homodimer.

The reconstituted enzyme was shown to be a transmembrane protein (105). Encapsulating the impermeant photoprobe, N-(4-azido-2-nitrophenyl)-2-aminoethylsulfonate, inside the vesicles, resulted in a covalently modified enzyme that was inhibited. Externally added AcNAD$^+$ (an NAD$^+$ analog) increased the inhibition rate several-fold, whereas the other substrates had no effect. Isotopic labelling with the photoprobe was enhanced by AcNAD$^+$ and NADP$^+$, decreased by NADH, and not affected by NADPH. These findings clearly show that the reconstituted enzyme is transmembranous. In addition, the transmembranous nature and orientation of the membrane-bound enzyme was determined by evaluating the effects of proteolytic treatment on the structural integrity of the enzyme in right-side-out mitoplasts and inside-out oriented submitochondrial particles prepared from rat liver cells (106). Transhydrogenase fragments from partial cleavage by a nonspecific protease, proteinase K, were detected by polyclonal antibodies raised against the purified bovine heart enzyme. The upshot from this study was that the 110 kD membrane-bound transhydrogenase contained a 23 kD core of proteolytically inaccessible residues within the membrane bounded by a 52 kD extramembranous domain sticking into the matrix and a 35 kD cytoplasm-facing domain.

As can be seen from the photoprobe labelling and inactivation studies above, binding of substrates can affect the transhydrogenase's conformation. Ligand-induced changes in enzyme conformation have also been detected in proteolytic, thermostability and other chemical modification studies. NADPH protected the mitochondrial enzyme from thermal inactivation while $NADP^+$ caused it to be more labile to thermal perturbation (107-108). The other two substrates had no observable effect. Similar but not identical substrate binding effects were uncovered by trypsin inactivation studies (107). Ernster et al. originally demonstrated the high sensitivity of transhydrogenase to trypsin inactivation (109). Low NAD(H) concentrations protected the bovine heart enzyme from trypsin inactivation whereas in liver, they did not (107). NADPH enhanced trypsin inactivation of both enzymes, while $NADP^+$ did not have any significant effect. As an aside, Yamaguchi and Hatefi discovered similiar although not identical results with the purified bovine heart transhydrogenase and they subsequently identified cleavage of a highly susceptible lys_{410}-thr_{411} bond (see below) that was accelerated by NADPH to account for the high trypsin sensitivity (111). Also, the presence of NADPH resulted in a clearly evident cleavage product of 48 kD formed by the breaking of the arg_{602}-leu_{603} bond, which is not observed to any great extent in the absence of NADPH. These results taken together indicate different conformational states that are possible for the unliganded enzyme, the NAD(H)-bound enzyme, the NADPH-bound enzyme and the $NADP^+$-bound enzyme.

Sulfhydryl modification studies using 5,5'-dithiobis(2-nitrobenzoic acid) (DTNB), N-ethylmaleimide (NEM) and other such reagents on purified and functionally reconstituted bovine heart enzymes seem to confirm the different ligand-induced conformational states suggested above (112). The results in general are that $NADP^+$ and NADPH affected enzymatic inactivation by the different sulfhydryl modification reagents, in opposite fashions whereas NAD^+ and NADH had no effects. Yamaguchi independently obtained similar results using NEM and found in addition that the NADP(H) effects result from binding at their active site (101). Quantification of the

sulfhydryls modified by the different reagents revealed in general that reactive sulfhydryl groups were less accessible in the $NADP^+$-enzyme complex and more accessible in the NADPH-enzyme complex (112).

The E. coli enzyme could be inhibited by arginine-reactive phenylglyoxal and 2,3-butanedione in borate buffer (63). $NADP^+$, NAD^+ and high concentrations of either reduced nucleotides protected the enzyme from 2,3-butanedione inhibition. Low concentrations of the reduced nucleotides stimulated the 2,3-butanedione inhibition rate. The trypsin inactivation studies showed a similar pattern of substrate binding effects. Therefore, E. coli appears from these results to have different conformational states for the unliganded enzyme, the enzyme bound by oxidized substrates, and the enzyme bound by the reduced substrates.

The amino acid sequences from bovine mitochondria have been determined via gene cloning and sequencing (113). The enzyme shows great sequence homology with the E. coli enzyme (51.8 %) (81, 113). The N-terminal and C-terminal portions line up with the E. coli α and β subunits respectively. The greatest homology appears to be in the C-terminal end of the mitochondrial and β subunit sequences (from ser_{308} to β C-terminus) with 67.7 % identity. Hydropathy plots predict as many as 14 transmembranous segments for the mitochondrial transhydrogenase located in the central, hydrophobic, one third of the sequence (113).

The NAD(H) and NADP(H) binding sites of the bovine enzyme were determined by *p*-fluorosulfonylbenzoyl-5'-adenosine (FSBA) affinity labelling to be at the hydrophilic regions of the molecule near the N- and C- termini, respectively (114). Specifically, FSBA -boundat tyr_{245} (putative NAD(H) binding site) and alternatively, at tyr_{1006} (putative NADP(H) binding site). Although the putative substrate binding sites are extremely far apart in the primary sequence, the binding sites might come close together in the folded 3-dimensional configuration. Evidence supporting that there may be a short distance separating the NAD(H) and NADP(H) binding sites came from Kozlov et al. (115). This group found that the 7-nitrobenzofurazan-4-yl derivative of

dephospho-coenzyme A inhibited the mitochondrial enzyme competitively with respect to both binding sites. The kinetics of the inhibition revealed that one molecule of the inhibitor bound simultaneously to both nucleotide binding sites.

Vicinal cysteines present at or near the $NADP^+$-binding site were indicated to be important for activity (112). Experimental formation of an intramolecular disulfide cross-link was observed upon copper-(*o*-phenanthroline)$_2$ complex ($Cu(OP)_2$) and DTNB inactivation of bovine heart transhydrogenase. Dithiothreitol could reverse this disulfide cross-link. It was found that two exposed DTNB-reactive sulfhydryl groups are cross-linked by $Cu(OP)_2$. $NADP^+$ protected the enzyme from inactivation and sulfhydryl group cross-linking. In some disagreement, Persson et al. using 4-chloro-7-nitrobenzo-2-oxa-1,3-diazole (NBD-Cl) as the sulfhydryl-modifying and enzyme-inactivating reagent, discovered that the presence of substrates enhanced exposure of, rather than protected, reactive sulfhydryl groups which they interpreted to be peripheral to the NAD(P)(H)-binding sites (116). In addition, this group noticed that photo-induced transfer of the NBD-adduct to nearby lysine(s) in partially inhibited transhydrogenases resulted in inhibition of the residual activity. They suggested at least one lysine near a reactive sulfhydryl residue was essential for activity. In other work, glutamate or aspartate (77, 92, 96, 101, 117), lysine (118), arginine (119), and cysteine (90, 100) have all been suggested to be essential residues.

Yamaguchi and Hatefi identified a specific cysteine residue whose sensitivity to NEM was enhanced in the presence of NADPH (101). This cysteine was that at the 893rd amino acid position (from the N-terminal). Interestingly enough, it is located 113 residues upstream from the FSBA-modifiable tyrosine in the NADP(H) binding domain of the enzyme. From studying the effect of pH on NEM inhibition rate, they found that this NEM-sensitive cysteine changed its apparent pK_a of about 9.1 to $\pm$ 0.4 units depending on the redox state of the NADP(H) bound to the enzyme. That is, when bound to $NADP^+$, the apparent pK_a of cys_{893} is raised to 9.5 units while NADPH binding decreases the pK_a to 8.7 units. The smaller sized methylmethanethiosulfonate

inhibited no more than 75% of the transhydrogenase activity when it modifies cys_{893} whereas NEM modification of the same residue gives near complete inactivation (101). Therefore, the cysteine residue appeared not to be essential and the effect of NEM was probably a steric one. The extrapolation from this is that cys_{893} does not interact catalytically with $NADP^+$ or NADPH to promote the enzyme's activity. The opposite effects of $NADP^+$ and NADPH on cys_{893}'s pK_a may then be ascribed to the different manner in which these ligands affect the enzyme's conformation and consequently, the environment of cys_{893}. This has important mechanistic implications regarding proton pumping. That is, it is not difficult to envision such ligand induced conformational changes affecting other appropriate prototropic residues of the protein on opposite sides of the membrane, thereby resulting in proton uptake on one side and proton release on the other. However, it is wise to keep in mind that cys_{893} is the first instance that such a pk_a shift phenomenon brought about by ligand altered conformational states, has been demonstrated for any energy-transducing enzyme of the mitochondrial or bacterial oxidative phosphorylation system.

The probable site on the primary sequence responsible or at the least, affecting proton pumping was identified by [^{14}C]DCCD labelling and subsequent sequencing of the proteolytically obtained radioactive peptide (120). This revealed that unlike most energy-transducing enzymes in which the DCCD-binding glutamic or aspartic acid residue is located in a hydrophobic, membrane-spanning domain (121), the bovine transhydrogenase-bound DCCD at glu_{257} is located in the hydrophilic stretch in the NAD(H)-binding domain, 12 amino acids downstream from the FSBA binding site.

The sequence of the transhydrogenase gene in E. coli (Figure 1) (81) has shown that in this organism, the enzyme is composed of two types of subunits, α with a calculated M_r of 53,906 and β with a calculated M_r of 48,667 which agrees well with the molecular weights estimated from SDS-Page.

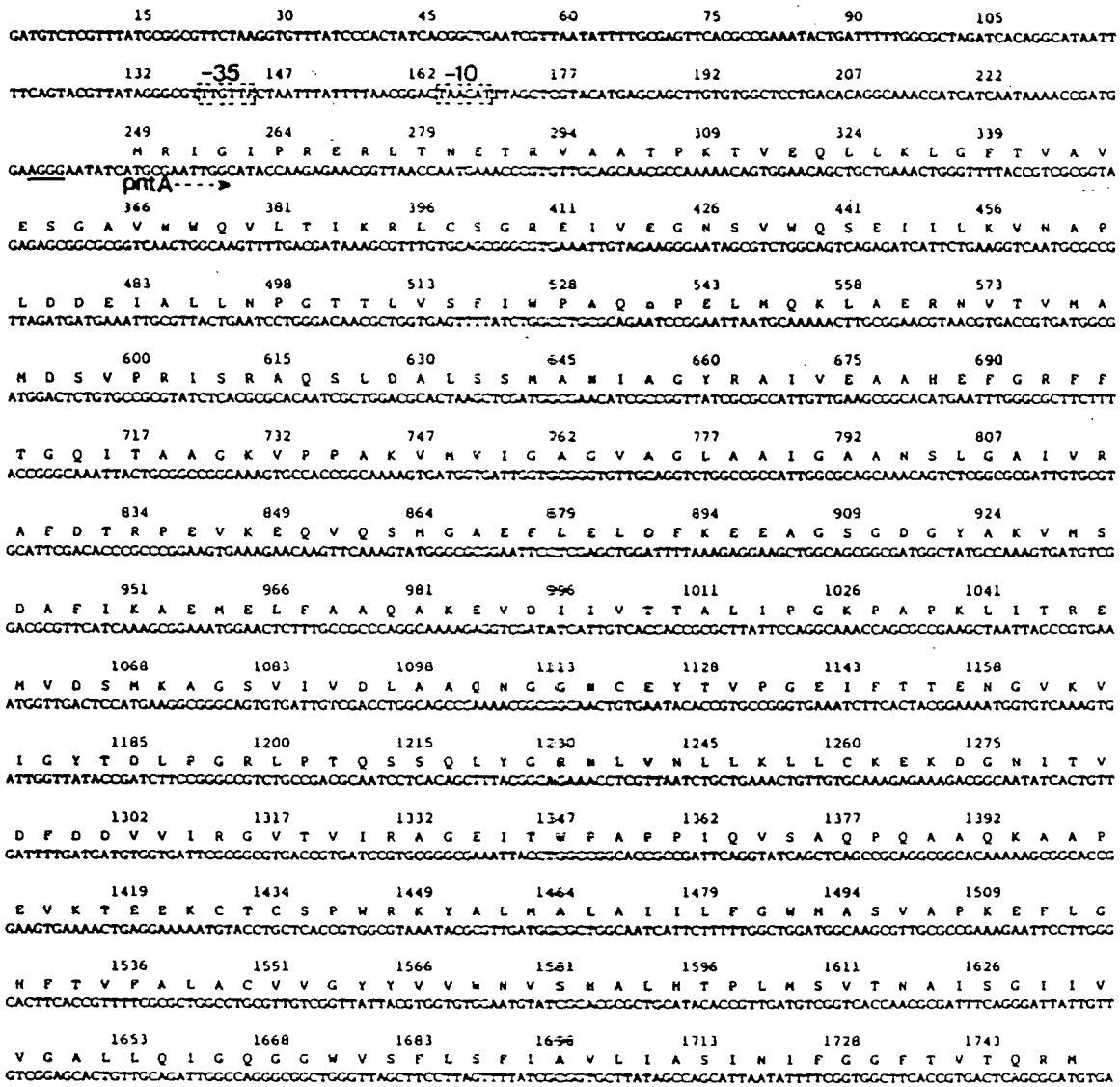

Figure 1: Nucleotide Sequence of the Cloned pnt Gene Region

The pnt gene cloned into a pUC 13 plasmid and subsequently renamed pDC21, was sequenced and expressed in E. coli JM83 cells by Clarke (81). The genes coding for the α and β subunits are labeled as pntA and pntB, respectively. These labels are marked above the proposed points of translation initiation. Proposed ribosomal-binding sites have been underlined. Promotor sequences are boxed and labelled -10 and -35. The amino acid sequences of the translated products are indicated above the DNA sequences from which they derive.

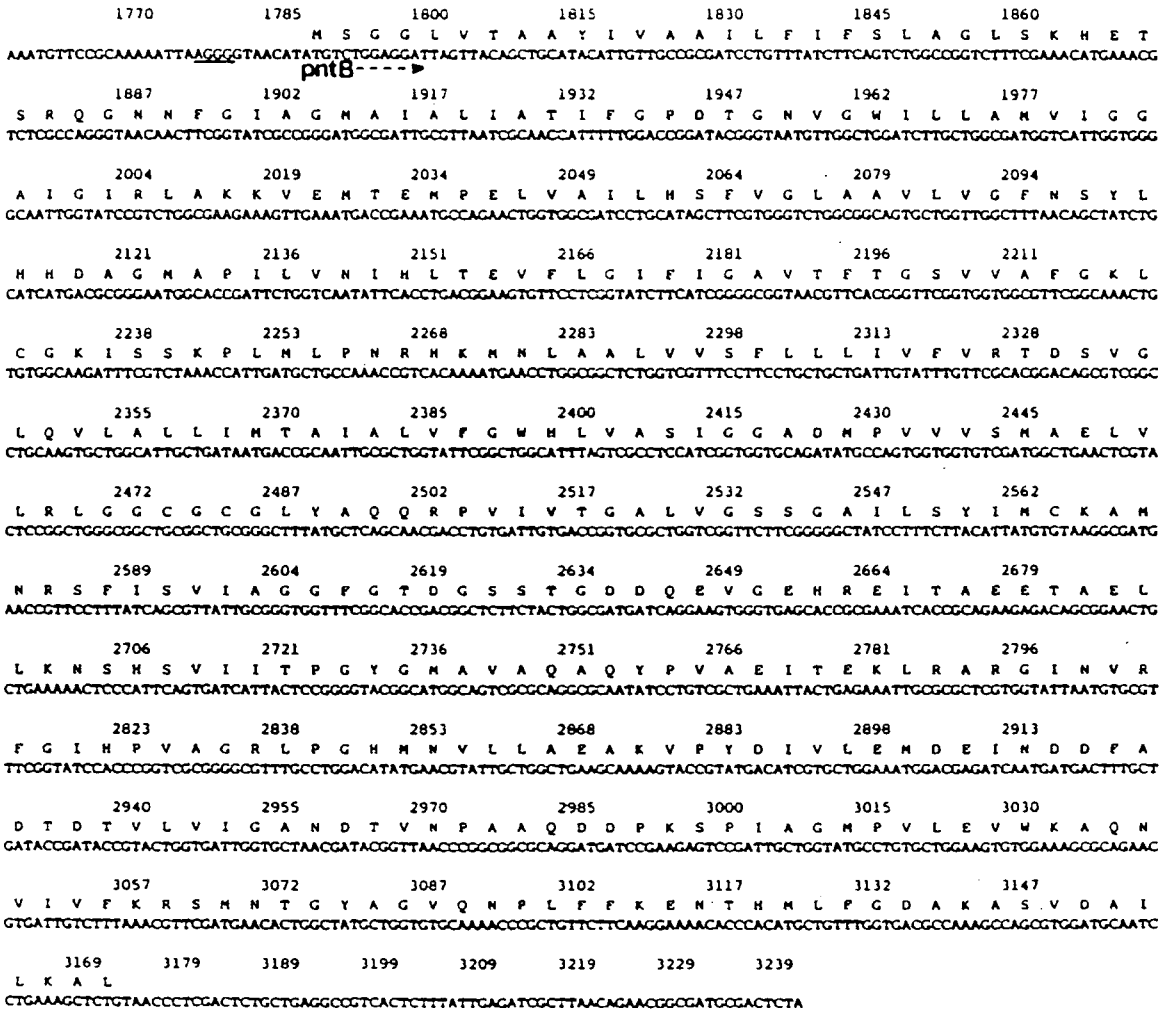
pntB

The amino acid composition was also calculated. The polarity indices of 38% for α and 33% for β is lower (81) than the 40% calculated for the bovine mitochondrial enzyme (76) and is more in line with the polarity of intrinsic membrane proteins (102).

Although the reliability of predictions made from hydropathy plots is unknown because of the lack of a database of membrane proteins with known structures, the hydropathy plots of the E. coli enzyme subunits (Figure 2) (81) was determined and indicate that the first 200 or so amino acid residues of the β subunit is organized into seven possible hydrophobic transmembranous segments separated by short polar regions containing some charged residues. The first six segments are also separated by regions in which a reverse-turn can be predicted (81, 122). The remaining 250 or so amino acid residues toward the C-terminal show no hydrophobic sequences long enough to cross the membrane. Many charged residues are present in this region. The α subunit has four possible transmembranous domains all located in a series extending 100 or so amino acids from the C-terminal end. Garnier et al.'s method of analysis for secondary structure (122) would predict that this region has largely β structure rather than membrane-spanning α-helices. The remaining 80% or so of the α subunit at the N-terminal end contains many charged amino acid residues although another potential membrane-spanning segment can be seen in this region. Within this segment is a short sequence of twenty amino acids which shares homologies with the FAD and $NAD(P)^+$-binding folds of lipoyl dehydrogenase, glutathione and mercuric reductases (123). This may be a possible substrate binding site. Also, this short twenty amino acid sequence shows high homology to the corresponding segment on the bovine mitochondrial sequence, and the latter is located between 38 and 58 residues upstream from the FSBA-modifiable NAD(H)-binding site (114, 120). The DCCD modifiable site is another 12 residues downstream from the FSBA modifiable site in the mitochondrial enzyme. If DCCD covalently attaches to a similar area in the E. coli enzyme, that would be in the α subunit. Indeed, [^{14}C]DCCD labelling of the E. coli

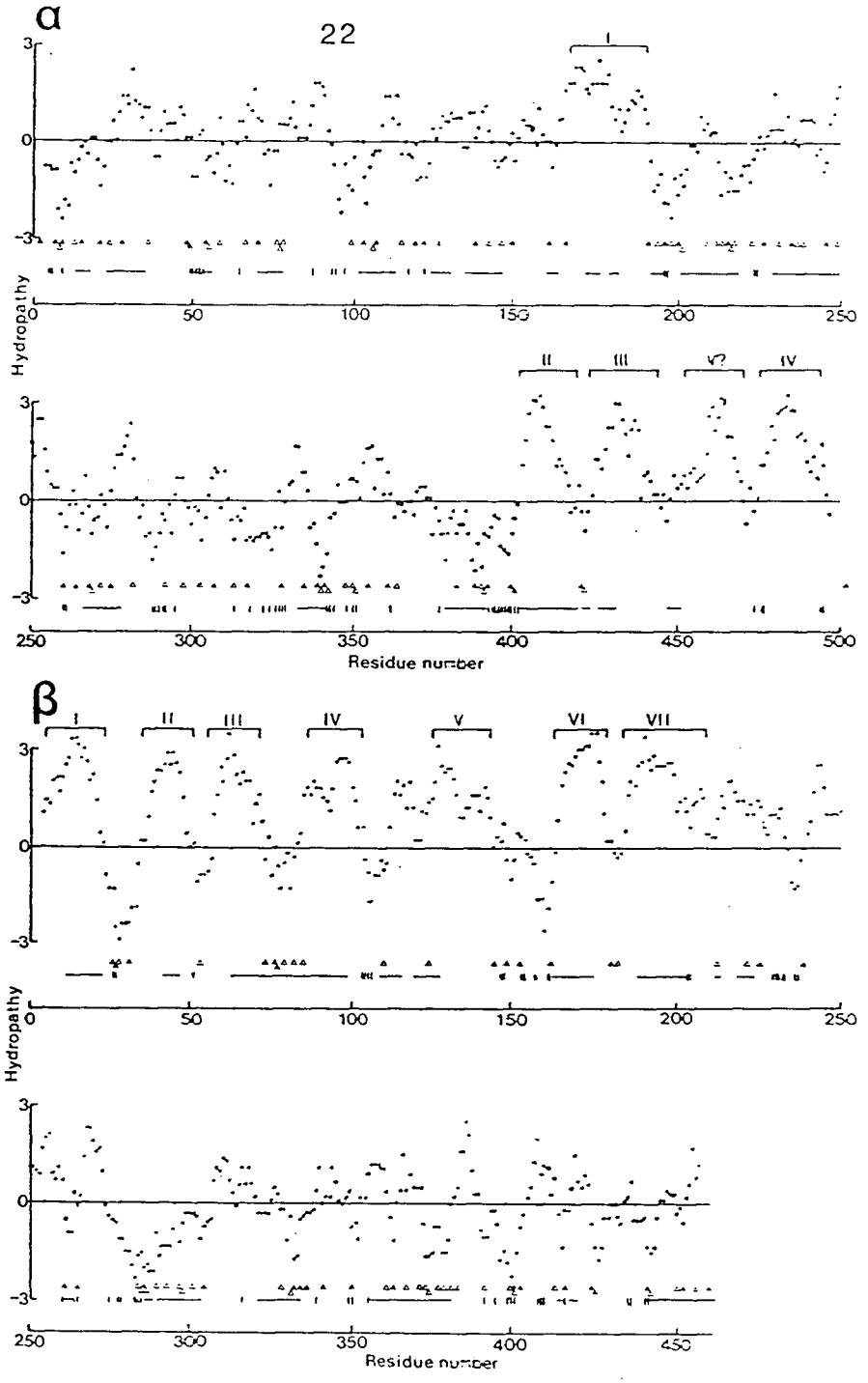

Figure 2: Hydropathy Plots of the Transhydrogenase Subunits

The hydropathy plots of the α and β subunit have been labelled as such above their respective figures. The plots were done by Clarke (81), based on the method of Kyte and Doolittle (11). The positions of basic residues (▲), acidic residues (Δ) and regions of predicted alpha helix (-) and beta sheet (IIIIII) are indicated. Secondary structure was determined by the procedure of Garnier et al. (122). Possible transmembranous segments are indicated as I-V for the α subunit and I-VII for the β subunit.

transhydrogenase resulted in the α subunit being preferentially labelled (80). The DCCD binding site was not further localized by these workers.

Homyk and Bragg (63) concluded from studying the kinetics of 2,3-butanedione modification of arginyl residues that there may be an allosteric site for binding NADH on the E. coli transhydrogenase. Clarke and Bragg (80) found NADH, but not AcNADH, specifically stimulated the enzyme catalyzed reduction of $AcNAD^+$ by NADPH and protected the enzyme from DCCD inactivation. The protection by NADH may mean that DCCD binds to the enzyme at or near the allosteric NADH-binding site. This may be the case because the DCCD binding site in the mitochondrial enzyme is situated only 12 amino acid residues downstream from the FSBA-modifiable NAD(H)-binding site (114, 120). If one were to believe the homologous alignment of the N-terminal of the mitochondrial enzyme with the α subunit of the E. coli enzyme (81, 113), the DCCD-modified mitochondrial site is then located just 50 to 70 residues downstream of the E. coli "twenty amino acid" sequence which shares homology with the active sites of other nucleotide binding proteins as stated previously. Therefore, there are two possible sites near the DCCD-binding site for allosteric NADH binding. One binds FSBA (mitochondrial enzyme) (114, 120). The other has nucleotide-binding fold homology (E. coli enzyme) (123). This is still speculation based on many unvalidated assumptions. Concrete evidence obtained from site-determining experiments similar to those performed on the mitochondrial enzyme must still be obtained to determine whether the allosteric NADH molecule and DCCD bind in the same or proximal region(s). An alternative explanation is that NADH binding to the allosteric site induces a long range conformational change that makes the DCCD-binding site less accessible. In contrast, $NADP^+$ and to a lesser extent NADPH appear to induce a conformational change which makes the DCCD-binding residue more available for modification and the accompanying enzymatic inhibition (80).

Similar to the results obtained for the rat liver enzyme (108), the degree of trypsin inactivation increased with the presence of NADPH whereas the other

substrates had no effect (88). In good agreement with this, sulfhydryl group modification by NEM on either the E. coli enzyme or the mitochondrial counterpart was stimulated by NADPH whereas $NADP^+$ protected the enzyme against NEM modification (107, 124).

The intact, active enzyme unit in the membrane appears to be an $\alpha_2\beta_2$ oligomer having a calculated molecular weight of 205,146 Daltons (125). Crosslinking of the purified and membrane-bound E. coli enzymes with a series of bifunctional crosslinking reagents and the formation of interchain disulfide bonds with cupric 1,10-phenanthrolinate, resulted in crosslinked dimers of α_2, $\alpha\beta$, and β_2, the trimer $\alpha_2\beta$, and a little bit of the $\alpha_2\beta_2$ tetramer. ^{60}Co gamma radiation inactivation analysis determined the molecular size of the intact enzyme unit to be 217 kD with an 11% standard error. This is within agreement with the 205,146 Dalton molecular size determined for the $\alpha_2\beta_2$ tetramer from the amino acid composition of the cloned transhydrogenase subunits (81).

G. Lipid Dependence of Transhydrogenase

The mitochondrial transhydrogenase can be inactivated by organic solvents such as acetone (2, 126), detergents including bile salts, sodium cholate/ammonium sulphate (2, 126-128), and phospholipases (2, 128), indicating a need for lipid for proper activity. Beef-heart transhydrogenase extracted with tertiary amyl alcohol could be reactivated with lecithin (129). Others found delipided enzyme preparations could be restored to activity by mitochondrial mixed phospholipids (73), phosphatidylcholine, phosphatidylethanolamine, lysolecithin (128), or soybean phosphatidycholine (73). Cardiolipin stimulated the activity as well, but at high concentrations it was inhibitory. The concentrations of the various phospholipids necessary for half-maximal stimulation were very near the phospholipid concentration in submitochondrial particles (128).

Cholate/ammonium sulphate treatment inactivated the E. coli enzyme (124). Various phospholipids including cardiolipin and phosphatidylglycerol could restore the activity of this preparation. Singh and Bragg found that phospholipase A inactivated the E. coli enzyme (130). Although it seems that lipids are necessary for activity, Singh found that the bulk of the phospholipids do not appear to affect transhydrogenase activity as bulk lipid phase changes cannot be correlated to "transition temperature" changes in the enzyme's activity. This does not rule out the possibity that limited amounts of lipid localized around the enzyme, are essential for activity, be the interaction specific or nonspecific. The nonspecificity of phospholipid types which can restore activity in delipided enzyme preparations (73, 128-129) suggests the latter possibility.

H. Energy-Coupling Reaction Mechanisms and Models

The mechanism by which transhydrogenation is linked to membrane energization is largely unknown. It has been widely accepted that the transhydrogenase reaction is coupled to proton translocation across native mitochondrial membranes according to the following reaction (85):

$$NADPH + NAD^+ + n\,H_{matrix} \quad <---> \quad NADP^+ + NADH + n\,H_{cytosol}$$

where *n* is the number of protons translocated per hydride transferred. Values ranging from 0.2 to 2 have been determined for *n*, as mentioned previously (18, 86, 89). Mitchell first came out with a loop mechanism to account for the protonmotive coupling to the enzymatic activity (Figure 3) (23). His idea was that the enzyme is reduced by a hydride ion equivalent donated by NADPH and a proton from the cytosolic side of the membrane to form a reduced enzyme intermediate. The hydride ion is then transferred to NAD^+ and the proton is released into the mitochondrial matrix.

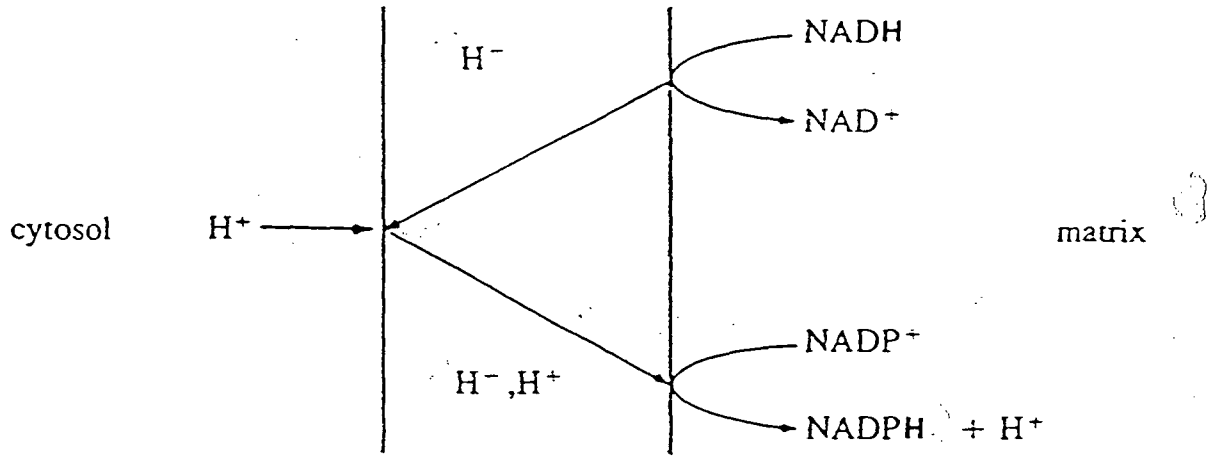

Fig. 3: Proposed Loop Mechanism for Protonmotive Coupling to Transhydrogenation in Mitochondria

The loop mechanism was proposed by Peter Mitchell (23). H^+ and H^- represent protons and hydride ion equivalents. NAD(P)(H) represent the natural pyridine nucleotide substrates and products of the transhydrogenase.The area enclosed by the two vertical lines represent the inner membrane.

Skulachev, taking into account ligand-induced conformational changes of the enzyme, proposed an alternative scheme (21). He thought that the transhydrogenase had catalytic and proton translocating domains separate from each other. A proton-binding site was proposed to be near but not at the NADP(H) binding site. Hydride ion transfer from NADPH to NAD^+ would leave $NADP^+$ occupying the NADP(H) binding site, which induces a conformational reorientation of the proton-binding site so that it faces the other side of the membrane. This is followed by proton release into this new milieu.

Enander and Rydstrom, knowing that the mitochondrial enzyme exists as a dimer with proton pumping abilities, proposed an even more detailed mechanism (Figure 4) (67). Their proposal considered the observation that some oligomeric proteins can exert what is termed half-of-the-sites reactivity (131-132). In this situation, only some monomer(s) of the complex are catalytically active at a given time, while other(s) are not. In the case of the dimeric transhydrogenase, one monomer (arbitrarily denoted I) is involved in the replacements of the products (NADH and $NADP^+$) with the substrates (NAD^+ and NADPH) in their respective binding sites as a proton binds to the side of the monomer facing the exterior of the vesicle. At the same time, the other monomer (II) reduces an already bound and "waiting" NAD^+ with a hydride ion equivalent from bound NADPH which drives the pumping of its own already bound proton into the interior. This monomer (II) can then replace the nucleotide products for new substrates and bind a new proton on the exterior side while at the same time causing monomer (I) to undergo hydride ion transfer and release of the proton into the interior. This scheme therefore involves alternation of different steps of the reaction mechanism between the two monomers. That is, there is a staggered effect where at any one time, one monomer is proceeding with one step of the mechanism while the other is proceeding with the second step. Of course, this mechanism suggests "communication" between the two monomers and conformation changes may be very important here. This half-the-sites reactivity is suggested by modification studies with

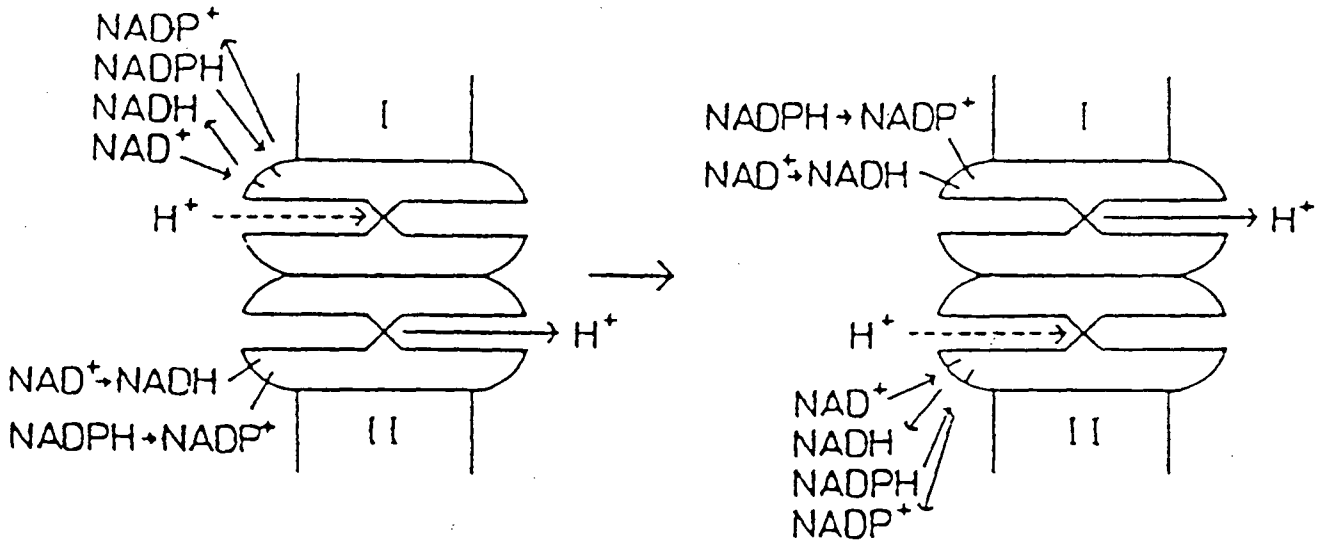

Fig. 4: Proposed Half-the-Sites Reactivity Mechanism for Protonmotive Coupling to Transhydrogenation in Mitochondria

The half-the-sites reactivity mechanism was proposed by Enander and Rydstrom (67). H^+ represent protons. NAD(P)(H) represent the natural pyridine nucleotide substrates and products of the transhydrogenase.The area enclosed by the two vertical lines represent the inner membrane. The transhydrogenase is represented as a dimer with the individual monomers labelled as I and II.

[^{14}C]DCCD and NADH-active-site-binding [^{3}H]FSBA, which when covalently bound to their respective sites in the dimeric bovine enzyme, inhibit the catalytic activity (96, 120, 133). It was found that with either reagent, complete inactivation occured with incorporation of 1 mole of inhibitor per mole of dimer.

Pennington and Fisher proposed a gated mechanism in which conformational changes also play a role (Figure 5) (91). They envisioned that the dimeric unit as a whole forms a single proton channel which spans the inner membrane of the mitochondrion. In the unliganded enzyme state, the proton-binding domain is inaccessible to protons on both sides of the membrane. The binding of NADPH and NAD^+ induces a conformational change, wherein the proton-binding domain is exposed to the matrix side. Hydride ion transfer causes a second conformational change which sees the proton-binding domain now exposed to the cytosolic side of the membrane. Enzymatic products are released back into the matrix and the proton is dissociated from its binding domain into the cytosol. This results in the enzyme returning to its closed unliganded conformation.

Both the Enander/Rydstrom and Pennington/Fisher models are consistent with the 1 to 1 stoichiometry of protons translocated per hydride ion transferred found in reconstituted transhydrogenase vesicles (89). However, the finding that 1 mole of DCCD per mole enzyme monomer was required for complete inhibition of proton translocation (91) is more consistent with the Enander/Rydstrom model, where both monomers in the active dimer each possess a proton channel, rather than with the Pennington/Fisher model where a common channel is shared by the two monomers. However, the Enander/Rydstrom model cannot explain why binding of one DCCD molecule to one monomer does not knock out the translocation of protons in the other monomer since in their scheme, the two monomers seem to depend tightly on each other in order for the half-of-the-sites reactivity mechanism to work. Perhaps, an elaboration of the Enander/Rydstrom model is required.

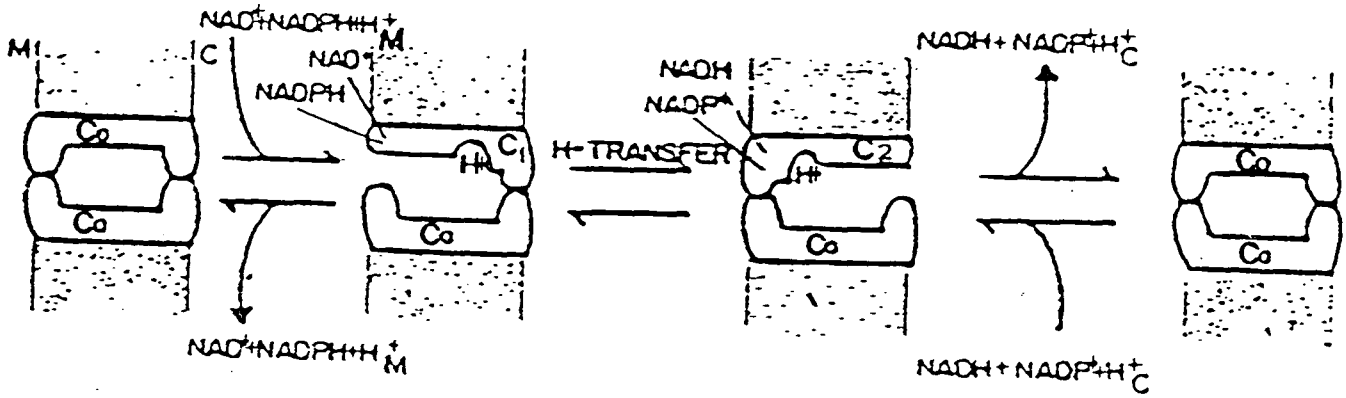

Fig. 5: Proposed Conformationally Gated Channel Mechanism for Protonmotive Coupling to Transhydrogenation in Mitochondria

The conformationally gated channel mechanism was proposed by Pennington and Fisher (91). H^+ represent protons. NAD(P)(H) represent the natural pyridine nucleotide substrates and products of the transhydrogenase. C_0, C_1, and C_2 represent the different transhydrogenase conformations. The area enclosed by the two vertical lines represent the inner membrane. C and M represent the cytoplasmic and the matrix side respectively. The transhydrogenase is represented as a dimer.

However, no matter what the final mechanistic model is, large energy-induced conformational changes must be involved as shown by Hatefi et al. (134). The partial reaction, NADPH + [^{14}C]NADP$^+$ <---> NADP$^+$ + [^{14}C]NADPH, catalyzed by transhydrogenase in submitochondrial particles is at all times in thermodynamic equilibrium because there is basically no difference in the nature and concentration of the substrates and products. However, membrane energization increases the forward reaction rate manifold. Since energy cannot be conserved in the products, energy utilization by this reaction must result in large entropic increases which was interpreted by the experimenters to mean that the enzyme undergoes great energy-induced conformation changes during catalysis.

Because of the lack of knowledge about the E. coli enzyme, Clarke (Figure 6) (88) could only come up with a sketchy working hypothesis for a mechanism in this organism. He based it on findings that the enzyme is a proton pump and may exist in three different conformations arbitrarily labelled E_1, E_2 and E_3. The E_1 resting conformation is transformed to E_2 after binding NADP$^+$. Upon hydride ion transfer, the enzyme changes to the E_3 conformation. Simultaneously, a proton is translocated from the outer surface of the membrane to the inner one. The direction of the reaction would be determined by substrate/product ratio and by the existing pH gradient.

I. Physiological Importance of Transhydrogenase

The physiological function of the transhydrogenase is still much a matter of debate. In mitochondria, it has been implicated in supplying NADPH for 11β-hydroxylation in steroid metabolism (135-140) and for other biosynthetic reactions (10). The enzyme may also indirectly regulate the route of isocitrate oxidation (141-144), providing NADPH reducing equivalents for extramitochondrial NADPH-dependent reactions via an α-ketoglutarate-isocitrate shuttle system (141, 145), and/or participate in a hydroperoxide-inactivation pathway (146-147).

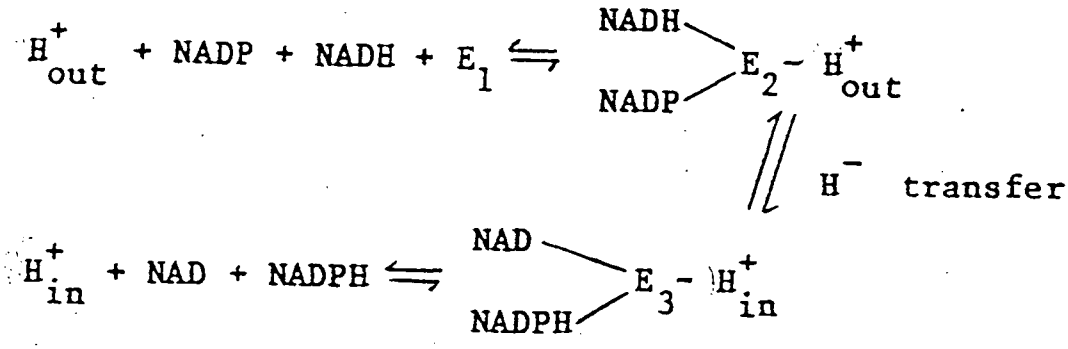

Fig. 6: Proposed Mechanism of Transhydrogenation in E. coli Cells

This mechanism was proposed by Clarke (88). H^+ and H^- represent protons and hydride ion equivalents respectively. NAD(P)(H) represent the natural pyridine nucleotide substrates and products of the transhydrogenase. E_1, E_2, and E_3 represent the different transhydrogenase conformations. "in" and "out" represent the cytoplasmic and the periplasmic side of the cytoplasmic membrane, respectively. Details of the mechanism are found in the Introduction.

In E. coli, Bragg et al. suggested a role in which the enzyme provided NADPH for amino acid biosynthesis (79). They and subsequently others (78, 148-150) observed that the presence of amino acid(s) in the growth medium markedly decreased the level of the enzyme in the cell. The enzyme could be derepressed by the removal of amino acid(s) from the growth medium, but this recovery was inhibited by rifampicin or chloramphenicol added to the induction medium (148-149). This inhibition indicates that de novo protein synthesis is necessary for heightened levels of activity, and the induction effect is not a result of activation of preexisting enzyme.

Gerolimatos and Hanson argued that transhydrogenase could provide only a small fraction of the NADPH necessary for amino acid biosynthesis (149). However, it is possible that in E. coli strains lacking the hexose monophosphate shunt or having higher levels of transhydrogenase, the enzyme may be providing NADPH for synthesis of amino acids (149). This group found another possible role for the enzyme by observing that in E. coli mutants constitutively synthesizing leucine, isoleucine, and valine, the addition of leucine to the growth medium effectively repressed both leucine transport and transhydrogenase activity. This coregulation of activities indicated to these experimenters that transhydrogenase may play a role in branched-chain amino acid transport. In addition, they found that in the absence of extraneously added leucine, an E. coli strain with altered leucyl-tRNAs also showed repressed levels of the transhydrogenase. Their belief was that leucyl-tRNA was the regulator of the enzyme. Nevertheless, this branched-chain amino acid transport role of transhydrogenase does not explain the repression by amino acids other than leucine. That is, besides alanine and methionine which effectively increases the intracellular leucine levels (151).

In another proposal, the E. coli enzyme was believed to function in the ammonia assimiliation pathway (152). E. coli grown on glucose and different concentrations of NH_4Cl showed a parallel pattern of changes in transhydrogenase and glutamate dehydrogenase activities as a function of ammonia concentration. Both enzymes

under these conditions could be repressed by extraneously added glutamate, which is the normal product of ammonia incorporated into α-oxoglutarate by the NADPH dependent glutamate dehydrogenase reaction. This coregulation of the transhydrogenase and an enzyme involved in ammonia assimiliation implies a possible role of the enzyme in this pathway. Although the above observations were repeated by Clarke (88), he also did a further experiment to rule out the direct involvement of transhydrogenase in providing NADPH for ammonia assimiliation by glutamate dehydrogenase. He found that an E. coli mutant lacking transhydrogenase activity and depending solely on the glutamate dehydrogenase pathway for ammonia assimiliation, did not require glutamate for growth.

An active transhydrogenase does not appear to be critical for cell viability as E. coli mutants missing this activity will grow normally under many different growth conditions (88, 153-155). It appears that transhydrogenase is not an essential source of NADPH for the cell. This is not surprising as other enzymes such as glucose 6-phosphate dehydrogenase and NAD-specific malic enzyme can also contribute to the NADPH pool.

J. Objective of This Thesis

Because of the transhydrogenase's interesting membership in the "club" of enzymes that are affected directly by membrane energization and because of its relatively simple structure and limited functional complexities, many research groups have studied it in an effort to affirm, disprove, or refine the chemiosmostic theory of Mitchell since it is widely held presently to be the model best fitting most of the data in the field of membrane bioenergetics. The E. coli transhydrogenase system has many advantages over other biological systems both as a model and as a practical tool to discover new and different aspects in the membrane protein bioenergetics area. Yet little work has been performed on it and very little was known about the E. coli enzyme

until very recent times. The cloning of and the development of a simpler purification procedure for the genetically obtained product in this lab has given us relatively copious amounts of material with which to study.

The present thesis will examine the topographical, conformational and structural facets of the native, membrane-situated transhydrogenase from E. coli. It is a widely-accepted operational hypothesis that a membrane protein's structure is related to its function. Alas, the results presented here have only a limited contribution to the final goal of revealing the enzyme's functional nitty-gritties. It is hoped that with the work of others in the future, the enzyme's grand design and its role in the bioenergetics of the cell will be discovered.

II MATERIALS AND METHODS

A. Materials

All chemicals were purchased from commercial sources and were either of reagent or analytical grade. Special chemicals and materials were obtained from the following suppliers if not otherwise mentioned in the methods:

Difco	-Bactotryptone, agar, and yeast extract, antibiotic medium 3
Sigma	-NAD(H), NADP(H), AcNAD$^+$, ampicillin, L-proline, D(+)glucose,
Tris	(Trizma base), bovine pancreas DNase I and RNase A, DL-
dithiothreitol,	Triton X-100, sodium cholate, sodium deoxycholate, chicken egg
white	lysozyme, glycine, papaya latex papain, bovine pancreas DPPC-
treated	trypsin, SBTI, Tritirachium album proteinase K, bovine pancreas α-chymotrypsin, PMSF, dodecyl-β-D-maltoside, benzylated cellulose dialysis tubing, Ponceau S, L-norleucine, pepstatin A, N6-linked
NAD	agarose
Biorad	-Most polyacrylamide gel electrophoresis reagents, alkaline
phosphatase	conjugated goat anti-rabbit IgG, nitrocellulose membranes,
gelatin,	Tween 20, AG11A8 ion retardation resin
Pharmacia	-Low molecular weight protein standards, pH 4.0-6.5 ampholytes, Sephadex G-75, prepacked Superose 12 and MonoQ columns
BDH	-4-nitrophenyldisodium orthophosphate plus most common and
inorganic	chemicals
Fisher	-Sodium citrate, ferric citrate, potassium cyanide, bromophenol
blue,	phosphoric acid, sodium azide
Promega Biotec	-5-bromo-4-chloro-3-indoyl phosphate/nitro blue tetrazolium
alkaline	phosphatase development system (BCIP/NBT)
Gibco Labs.	-Fetal calf serum

Millipore	-Immobilon-P transfer membranes
J.T. Baker Chem.	-Thiamine, 2-mercaptoethanol, pyridine
Pierce	-Baker's yeast carboxypeptidase Y
Merck	-Coomassie Brilliant Blue R250
Calbiochem	-L-cysteine, Freund's complete and incomplete adjuvant
Miles Labs. Inc.	-Staphylococcus aureus V8 protease
Spectrum Med. Ind.	-Spectropor 1 membrane tubing
Amicon	-Centricon-10 microconcentrators
UBC Physics Dept.	-Liquid nitrogen

B. Growth of Escherichia coli

E. coli strains of JM83pDC21F$^-$ ara Δ lac pro str A thi φ80d lac Z ΔM15, and the parent strain of JM83 were used in this study. These strains were stored at -50° to -70°C in Bacto Antibiotic Medium 3 with 25% glycerol for the long-term. For short-term storage, cells were maintained at 4°C as circular colonies on agar media with Bacto Antibiotic Medium 3 and 100 ug/ml ampicillin.

Cell cultures were started on autoclaved Bacto Antibiotic Medium 3 made up according to the supplier's instructions, with 50 ug/ml ampicillin present. They were incubated overnight at 37°C.

The cultures were then transfered to either autoclaved LB (Luria-Bertani) or M9 minimal salts media. They were incubated at 37°C with aeration by shaking at 250 rpm in a New Brunswick Scientific Controlled Environment Incubator Shaker. The LB medium consists of the following: 1% Bacto-tryptone, 0.5% Bacto-yeast extract, 1% NaCl, pH 7.5. The M9 medium consists of the following: 0.7% K_2HPO_4, 0.3% KH_2PO_4, 0.05% sodium citrate, 0.02% $MgSO_4 \bullet 7H_2O$, 0.1% $(NH_4)_2SO_4$, 1 mg/ml thiamine, 50 mg/ml proline, 12 mM ferric citrate, 0.4% glucose, pH 7.4. The plasmid pDC21F$^-$ strains were selected for by addition of 100 ug/ml ampicillin into both types of medium.

The cultures were harvested when they reached an absorbance at 600 nm ranging from 1.0 to 1.5 which is at early to mid-log phase growth. The cells were pelleted by centrifugation at 4,400 x g for 20 min. The pellets were washed by resuspending in 0.9% NaCl followed by centrifugation at 4,400 x g for 20 min, twice. The resulting cell pellets were either used immediately or stored at -50 °C.

C. Isolation of ISO Cytoplasmic Membrane Vesicles

All steps were performed at 0 to 4°C. Approximately 3 g of LB derived cell pellets were first suspended at 0.1 to 0.5 g/ml (wet weight) in vesicle buffer (50 mM Tris-H_2SO_4, 10 mM $MgCl_2 \cdot 6H_20$, 1 mM DTT, 1 mM EDTA, 1 mM DNase I, pH 7.8). They were then lysed by passage through an ice-cold AMINCO French Pressure Cell at 20,000 psi, three times to make crude ISO membrane vesicles. Unbroken cells and debris were removed by centrifugation at 12,100 x g for 20 min. The resulting supernatant was layered onto 0.77 M/1.44 M sucrose 2-step discontinuous density gradients and centrifuged at 63,900 x g for 13 hours using a 60Ti fixed angle rotor. The light brown material that banded at the gradient interface was collected with a syringe. This is the cytoplasmic membrane fraction. The whitish outer membrane fraction that sedimented to the bottom of the tube. The cytoplasmic membrane suspension was diluted 2-5 fold with TED buffer (50 mM Tris-H_2SO_4, 1 mM EDTA, 1 mM DTT, pH 7.8) and centrifuged at 178,000 x g for 2 hours to pellet the membrane and remove any soluble proteins. Further purification could be attained by treatment of the membranes with 1% Triton X-100 in TED buffer, centrifugation at 178,000 x g for 2 hours, followed by retreatment of the membrane fraction with 50 mM sodium cholate in TED and centrifugation at 178,000 x g for 2 hours. The detergent-extracted pellet was washed by resuspension in TED buffer and centrifugation at 178,000 x g for 2 hours, twice. The final membrane pellet was suspended at 0.2-1 g membranes/ml TED buffer and kept at -20°C or used immediately.

In early experiments, the sucrose gradient centrifugation step was not performed in the preparation of ISO membrane vesicles. In some experiments, the detergent-extraction steps were eliminated or the concentrations of detergents used were different from those given above. When working with less or more than 3 g of cells, the basic steps were followed with minor logistic adjustments.

D. Isolation of RSO Cytoplasmic Membrane Vesicles

The efficient and reproducible method of Witholt et al. for making E. coli spheroplasts (156) was used with minor modifications and from these spheroplasts, right-side-out membrane vesicles were prepared. All steps were performed at 0 to 4°C. Cells were first grown in LB or M9 media according to the previously mentioned procedures. Washed cell pellets were resuspended in 200 mM Tris-HCl, pH 8.0 at 10-40 mg wet weight/ml. The suspension was diluted with an equal volume of 1.0 M sucrose in 200 mM Tris-HCl, pH 8.0. Then, 0.5% (v/v) of 0.1 M EDTA, pH 7.6 was added to the diluted suspension. A 10 mg/ml lysozyme stock solution was used to add lysozyme to a final concentration of 60 ug/ml. After 30 min, the incubated mixture was diluted two-fold with distilled water. $MgCl_2 \bullet 6H_2O$ was added to 20 mM final concentration. DNase and RNase were both added to 50 ug/ml final concentrations. The mixture was kept for 15 min and the decrease in absorbance at 600 nm was monitored over the 15 min interval to check that cell disruption did indeed occur. Unbroken cells and large cell debris were pelleted out by centrifugation at 4,400 x g for 20 min. The supernatant was centrifuged at 95,600 x g for 2 hours. The sedimented right-side-out vesicles were washed once by centrifugation at 95,600 x g for 2 hours after resuspension in 50 mM potassium phosphate, pH 7.5. The washed pellet was finally resuspended at 80 mg wet weight per mL of 50 mM potassium phosphate, pH 7.5. The suspension was quick-frozen and stored in liquid nitrogen.

E. Protein Concentration Determinations

Protein concentrations were determined by the Lowry method (157). Bovine serum albumin in 1% NaCl was used as the standard over the range of 0 to 500 ug protein. The Folin-Ciocalteau reagent was diluted 1:2. Absorbance readings were measured at 500 or 660 nm. Experimental determinations of protein concentrations were performed at least twice on each sample.

F. Energy-Independent Transhydrogenase Activity Assays

Energy-independent assays of transhydrogenase activity were based on the method of Kaplan (158). A 0.1 mL sample of a properly diluted membrane vesicle suspension was mixed with 0.9 mL of assay buffer (50 mM NaH_2PO_4 , pH 7.0, 1 mM DTT, 0.5 mM EDTA-disodium salt, 1 mM KCN, 1 mM NADPH, 1 mM $AcNAD^+$) at room temperature to start the reaction. The reduction of $AcNAD^+$ by NADPH was measured as the absorbance increase at 375 nm using a Perkin-Elmer Lambda 3A spectrophotometer. The reference blank was 0.1 mL of a sample in buffer not containing the enzyme or membrane vesicles mixed with 0.9 mL of assay buffer. The extinction coefficient for AcNADH is 5.1 mL/umol/cm. The path length is 1 cm. One unit of enzyme activity represents the conversion of 1 mmol of $AcNAD^+$ to AcNADH per min.

G. SDS Polyacrylamide Gel Electrophoresis (SDS-Page)

SDS-Polyacrylamide gel electrophoresis of proteins, based on the method of Laemmli (159), was performed according to the manufacturers' instructions using one of the following three systems: Bio-Rad Mini-Protean II, Bio-Rad Model 220 Vertical Slab, and Hoefer SE 600 Vertical Slab gel electrophoresis apparatus. The Mini-Protean II system gave gels which were 7 cm in vertical length, 8 cm across and 0.75 or 1 mm thick. The Bio-Rad Model 220 Vertical Slab gels were 12 x 14 x 0.075 or 0.15

cm in size. The dimensions of the Hoefer SE 600 Vertical Slab gel were 14 or 16 x 14 x 0.075 or 0.15 cm. The separating gels were poured at varying concentrations depending on the range of protein sizes to be separated. They contained 0.375 M Tris-HCl (pH 8.8), 0.1% SDS, and 8-15% acrylamide (prepared from a 30% (w/v) acrylamide and 0.8% (w/v) N,N'-methylenebisacrylamide stock solution). Polymerization was effected by the addition of freshly prepared 10% (w/v) ammonium persulfate to a final concentration of 0.05% and the addition of 0.1% (v/v) TEMED. The stacking gel was poured as a 4% polyacrylamide gel with 0.125 M Tris-HCl (pH 6.8) and 0.1% SDS. Polymerization was initiated by adding ammonium persulfate (from a 10% (w/v) stock) to a 0.03% final concentration and TEMED to a 0.2% (v/v) final concentration. The samples were depolymerized by the addition of an equal volume of twice concentrated SDS sample buffer (0.125 M Tris-HCl (pH 6.8), 4% SDS, 10% β-mercaptoethanol, 0.002% bromophenol blue and 20% glycerol). Samples containing transhydrogenase or its fragments were incubated at 37°C for 10 min prior to their loading and electrophoresis. The running buffer contained in the lower and upper buffer reservoirs consisted of 0.025 M Tris, 0.192 M glycine, and 0.1% SDS. Electrophoresis of the Mini-Protean II gels was performed at 200 V for 30 to 45 min at ambient temperature. The electrophoresis of the other two, larger and longer vertical slab gels was carried out at 40 mA per slab for 1 to 1.5 hours with cooling. Protein gels were then stained with Fairbank's stain (0.1% (w/v) Coomassie Brilliant Blue R, 25% (v/v) isopropanol and 10% (v/v) acetic acid) for 30 min to 1 hour. The gels were destained with 10% (v/v) acetic acid. They were dried down onto Whatman 3MM chromatography paper for 1 hour under vacuum heating at 80°C in a Bio-Rad model 224 gel slab dryer.

H. Isoelectric Focusing Gel Electrophoresis

Isoelectric focusing gels were prepared according to a modification of the O'Farrell procedure (160). Each gel contained 8 M urea, 4.0 % (w/v) acrylamide, 0.107 % (w/v) N,N'-methylene-bis-acrylamide, 1.33 % (w/v) Triton X-100, 5.0 % (v/v) pH 4.0-6.5 ampholytes, and 0.1% (v/v) TEMED. The acrylamide in the presence of the other ingredients, was polymerized as a 14 x 14 x 0.075 cm sized gel after addition of 0.05% (w/v) ammonium persulfate. The polymerized gel was placed into a Hoefer SE 600 Vertical Slab gel electrophoresis apparatus. Samples to be electrofocussed were depolymerized by the addition of an equal volume of twice concentrated SDS sample buffer (0.125 M Tris-HCl (pH 6.8), 4% SDS, 10% β-mercaptoethanol, 0.002% bromophenol blue and 20% glycerol). Approximately 30 ug of protein sample was loaded into a well of the gel. The upper anode and lower cathode chambers were filled with freshly prepared 0.01 M H_3PO_4 and deaerated 0.05 M NaOH, respectively. The gel was run at room temperature and at maximum voltage and current settings of 100 V and 3 mA for approximately 16 hours.

To determine pIs of bands indirectly after electrofocusing, an empty lane was cut out after identifying the acidic or basic end. To identify the pH gradient down this lane, the gel strip was cut into 1.5 cm segments from top to bottom. Each segment was incubated with 1.5 ml of distilled water for 1.5 hours after which the pH was measured using a meter. The location of bands on the sample lanes can then be correlated with their pH environments and thus approximate pI values can be determined.

The rest of the gel was soaked in 50% ethanol and 10% acetic acid for a 1 day period with 2-3 changes of the solution in order to remove ampholytes. The deampholined gel was then stained with Fairbank's stain (0.1% (w/v) Coomassie Brilliant Blue R, 25% (v/v) isopropanol and 10% (v/v) acetic acid) for 1 hour, destained with 10% (v/v) acetic acid, and dried down on Whatman 3MM chromatography paper

while under vacuum heating at 80°C for one hour in a Bio-Rad model 224 gel slab dryer.

I. Peptide mapping

Peptide mapping was performed according to the procedures of Cleveland et al. (161). 10% SDS-Page of proteins and Fairbank's staining were accomplished as outlined previously. Desired polypeptide bands were excised from stained gels with a razor blade and trimmed to 5 mm. Each band or gel slice contained approximately 10 ug of protein. Gel slices were soaked in buffer B (0.125 M Tris-H_2SO_4, pH 6.8, 0.1% (w/v) SDS, 1 mM EDTA) for 30 min. Gel slices could be stored temporarily at -20°C. Gel slices were loaded into 5.4 mm wide wells of a 14 x 14 x 0.15 cm 15% (w/v) SDS-Page gel with a 5 cm 4% stacking gel, both prepared according to the previously described recipes. The wells contained buffer B with 20% (w/v) glycerol. Excess buffer B-20% glycerol was removed after gel slice(s) addition. The gel slice(s)-containing wells were overlaid with 10 ul of buffer B having 10% (w/v) glycerol and a given amount of protease (eg. S. Aureus V8 protease or papain). In the case of papain, a 1 mg/ml stock containing 5 mM cysteine and 1 mM EDTA was used. The samples were then overlaid with SDS-Page running buffer. Electrophoresis was started at 40 mA/slab until the blue colored front neared the bottom of the stacking gel. The current was switched off at this point for 30 min. The electrophoresis was resumed at 100 mA/slab until the blue front reached approximately 1 cm from the bottom of the separating gel. The gel was removed and stained with Fairbank's stain (0.1% (w/v) Coomassie Brilliant Blue R, 25% (v/v) isopropanol and 10% (v/v) acetic acid) for 1 hour. The gel was then destained with 10% (v/v) acetic acid with 2% (w/v) glycerol. It was finally dried onto Whatman 3MM chromatography paper while under vacuum heating at 80°C for one hour in a Bio-Rad model 224 gel slab dryer. A black and white

photographic record of the gel may be made before drying and possible cracking of the gel.

J. Generation of Anti-Transhydrogenase Polyclonal Antibodies

The transhydrogenase was purified in order to provide as specific an antigenic agent as possible for raising polyclonals in rabbits. All purification steps were performed at 0-4^{o}C. ISO membrane vesicles from E. coli JM83pDC21F^{-} cells were prepared as mentioned. Triton X-100 and sodium cholate was not used in preextraction of the preparation. The membranes were solubilized with 15 mM sodium deoxycholate, 15 mM sodium cholate, and 1 M KCl in TED buffer by stirring for 10 min. Unsolubilized material was removed by centrifugation at 178,000 x g for 45 min. The supernatant was layered onto a 1.44 M sucrose cushion containing 2.3 mM sodium cholate, 2.3 mM sodium deoxycholate and 1 M KCl (all in TED buffer). This was centrifuged at 178,000 x g for 16 hours. 1.4 mL fractions were collected. The pellet was resuspended in 2 mL of TED. The fractions were analyzed by 10% SDS-Page for purity. A portion of the purified transhydrogenase fraction containing 0.3 mg of protein was diluted 13-fold with 0.1% SDS in TED buffer to give a volume of 0.65 mL. This was emulsified by adding 2 volumes of Freund's complete adjuvant (FCA) in dropwise fashion into a vortexing transhydrogenase solution, giving an approximate total volume of 2 mL. FCA was replaced with Freund's incomplete adjuvant (FIA) after the first few injections. Emulsification was ensured by repeated passage of the sample through a 18 gauge hypodermic needle. The mixture was deemed emulsified enough for injection into a rabbit when a droplet of the emulsion placed onto water was not dispersed when agitated slightly.

Preimmune serum was collected prior to injection as a control. The injections and bleedings of rabbits was carried out by a service provided by the University of British Columbia Animal Care Unit. The first few injections were done subcutaneously

at 4 sites into a young rabbit. Two sites are located on either side of the back around the scruff of the neck and the other two are situated on either side of the back near the rear haunches. The second booster shot was performed 20 days after the first and subsequently the boosters were done at 30 day intervals. After the first few injections when significant abcesses were noticed, the rabbit was injected intramuscularly with FIA emulsified antigen at two sites in behind the hind legs.

The rabbit was bled at approximately 2 week intervals after injections. After delivery from the Animal Care Unit, the blood was allowed to stand at room temperature for 1 hour. Then it was stored at 4^{o}C overnight. The serum was separated from the clot by centrifugation at 2000 x g for 5 to 10 min. 10 to 20 mL of serum were usually obtained in this manner. Six and one half monthes after the 1st injection, the rabbit was sacrificed and a full body bleed was performed to obtain 200 mL of blood serum.

K. Titering of Polyclonal Antibodies

The rough titering of the rabbit antisera obtained at various times was performed using an enzyme-linked immunosorbent assay. The antigen (0.33 ug of purified solubilized transhydrogenase in a 1 ul volume) was coated onto each well of a flexible, 96-well, polystyrene, flat-bottomed assay plate. The antigenic solutions in these wells were dried down by heating at 60^{o}C for 1 hour or by leaving at room temperature overnight. The plate wells were then rinsed with water once. The wells were quenched or blocked with 2% gelatin in KBS buffer (137 mM NaCl, 1.5 mM KH_2PO_4, 7.2 mM Na_2HPO_4, 0.02% NaN_3, 2.7 mM KCl, 0.05% Tween 20) for 1 hour at room temperature. They were rinsed once with KBS. 50 ul aliquots of serially diluted antiserum were added to sequential wells in a row across the plate. This was repeated on different rows for the different antisera solutions. The dilutions ranged from undiluted, 2x, 4x and so on to 2048x. The antigen/primary antibody mixes were

incubated for 1 hour. The wells were then washed of unattached substances by rinsing with KBS 3 to 4 times. 100 ul of alkaline phosphatase-conjugated goat anti-rabbit immunoglobulin (diluted in KBS according to supplier's recommendation) was added to every well and incubated for 1 hour. The nonbinding materials were removed by 3 to 4 washes with KBS. 100 ul of substrate solution was added to each well. The substrate solution consisted of 0.1% (w/v) 4-nitropheny disodium orthophosphate in a diethanolamine buffer (1% (v/w) diethanolamine, 0.3 mM sodium azide, 0.05 mM $MgCl_2 \bullet 6H_2O$, pH 9.8). The reactions were stopped after 40 min with 50 ul of 2 M NaOH per well and the individual absorbances of the solutions were read at 405 nm using a Bio-Tek Instruments Microplate EL309 Autoreader. The dilution giving maximum colour development was deemed the optimum dilution factor for the antiserum.

L. Immunoblots

Samples with and without transhydrogenase subunits or fragments were subjected to SDS-polyacrylamide gel electrophoresis as described previously. The gel was then equilibrated in transfer buffer (25 mM Tris, 192 mM glycine, 20% (v/v) methanol) for 30 min and the proteins then transferred onto blot-qualified nitrocellulose paper or Immobilon PVDF transfer membranes by electrophoretic elution (162) using a Bio-Rad Trans-Blot cell according to the manufacturer's instructions. The electrotransfer was performed at 60 V for 5 hours or 70 V for 3 hours with cooling by running water at ambient temperature.

The transferred proteins were immunostained as described by Harlow and Lane (110). The trans-blotted nitrocellulose membrane was "blocked" to prevent non-specific binding to antibodies by incubation in 5% fetal calf serum in KBS buffer for 60 min at room temperature or at 4 °C overnight . It was washed thrice with KBS and incubated with the primary antibody, 32-fold diluted rabbit anti-transhydrogenase or

64-fold diluted rabbit anti-α subunit antisera for 30 to 60 min at room temperature. It was washed three more times with KBS and incubated with the secondary antibody, alkaline phosphatase-conjugated goat anti-rabbit IgG (diluted as prescribed by the supplier) for 30 to 60 min. The membrane was washed thrice more with KBS and equilibrated in alkaline phosphatase substrate buffer (100 mM Tris (pH 9.5), 100 mM NaCl, 5 mM $MgCl_2$) for 5 min. Colour development was accomplished by addition of nitro blue tetrazolium and 5-bromo-4-chloro-3-indoyl phosphate to final concentrations of 0.44% and 0.33% (v/v), respectively. The reaction was stopped by washing the membrane with distilled water after 10 to 15 min or when the immunostain had reached a sufficient intensity.

M. Proteolytic Digestions of ISO and RSO Membrane Vesicles

E. coli JM83pDC21 inside-out and right-side-out membrane vesicles were treated alike except for the buffer used in the digests. TED buffer, pH 7.8, was used to suspend the ISO vesicles to a concentration of 1.5 mg protein/ml, while 50 mM potassium phosphate, pH 7.5 was used to suspend the RSO vesicles to an approximate concentration of 0.1 mg/ml. All proteolytic digestions were performed at room temperature. Trypsin was added to the ISO and RSO vesicle suspensions at a protein molar ratio of 1 : (65 or 270) and 1 : 6.5, respectively. Proteinase K was added to the ISO and RSO vesicle preparations at a protein weight ratio of 1 : 180 and 1: 18, respectively. Aliquots containing 0.36 mg and 0.036 mg protein, from proteolytically treated ISO and RSO vesicles respectively were removed after different times of incubation. The action of trypsin was stopped with the addition of a "double the trypsin weight" amount of soya bean trypsin inhibitor (SBTI) , while proteinase K activity was stopped with the addition of "44-fold the proteinase K weight" amount of phenylmethylsulfonylfluoride (PMSF) from a 50 mM stock solution made in methanol. All stopped reactions were put on ice for 15 min. They were then diluted 20 or 28x with

5 mM $MgCl_2$. The diluted material was centrifuged at 194, 000 x g at 4°C for 2 hours. The pellets were resuspended at their original undiluted concentrations with their original buffers and stored at -20°C. The supernatants were lyophilized. The lyophilizates were resuspended at their original undiluted concentrations with distilled water and stored at -20°C until further analysis.

Chymotrypsin was added to a 1.5 mg protein/ml ISO vesicle preparation at a protein weight ratio of 1 : 36. Aliquots from the proteolytically treated ISO vesicles containing 0.36 mg protein were removed after different times of incubation and chymotrypsin action was stopped by the addition of "44-fold the chymotrypsin weight" amount of phenylmethylsulfonylfluoride (PMSF) from a 50 mM stock solution made in methanol. All stopped reactions were put on ice for 15 min. They were then diluted 20-fold with 5 mM $MgCl_2$. The diluted material was centrifuged at 194, 000 x g at 4°C for 2 hours. The pellets were resuspended at their original undiluted concentrations in their original buffers and stored at -20°C. The supernatants were lyophilized. The lyophilizates were resuspended at their original undiluted concentrations in distilled water and stored at -20°C until further analysis.

N. Detergent Effects on Conformation as Detected by Trypsinolysis

All steps prior to partial tryptic digestion analysis were performed at 4°C. ISO membrane vesicles containing 0.4 mg protein and suspended to 1 mg/ml was treated successively with 0.05% Triton X-100 in TED and 2.5 mM sodium cholate in TED. After 5 min of mixing with Triton X-100, the extracted membrane pellet was sedimented at 178,000 x g for 2 hours. The pellet was washed with TED buffer by resuspension and centrifugation at 178,000 x g for 2 hours. The washed pellet was treated with sodium cholate, mixed as before and centrifuged at 178,000 x g for 2 hours. The detergent-extracted pellet was washed as before. The final membrane pellet was suspended at 4.8 mg protein/ml TED buffer and kept at -20°C for tryptic and other

analyses. A portion of the untreated membranes was also saved at 4.8 mg protein/ml TED.

Both the native and detergent-extracted membranes, containing 0.48 mg protein in 100 ul total volume each, were treated with 4 ug DPPC-trypsin. After 5 min, 8 ug of SBTI was added to each reaction to inhibit the trypsin. The mixtures were left in ice for 15 min. Each mixture was made up to 8 ml with distilled water. The diluted material was centrifuged at 160, 000 x g at 4^{o}C for 2 hours. The pellets were resuspended at their original undiluted concentrations in TED buffer and stored at -20^{o}C. The supernatants were removed and lyophilized. The lyophilizates were resuspended at their original undiluted concentrations with distilled water and stored at -20^{o}C until SDS-Page analysis.

O. Tryptic Digestions of Substrate-Bound Transhydrogenase

Purified ISO membrane vesicle suspended at 10.2 mg/ml were dispensed in aliquots containing 2.55 mg or 0.051 umole protein and incubated with 0.104 umoles of AcNAD^{+}, NAD^{+}, NADH, NADP^{+}, or NADPH in separate tubes for 10 min. In effect, the transhydrogenase in each tube was incubated with a 20-fold excess of one substrate or substrate analog. 0.37 nmoles of DPPC-trypsin was added to start each individual reaction. After 10 min of incubation, the reactions were stopped by the addition of 1.0 nmole SBTI each. The mixtures were left in ice for 15 min. Each mixture was made up to 7 ml with 5 mM $MgCl_2$. The diluted material was centrifuged at 194, 000 x g at 4^{o}C for 2 hours. The pellets were resuspended at their original undiluted concentrations in TED buffer and stored at -20^{o}C. The supernatants were lyophilized. The lyophilizates were resuspended at their original undiluted concentrations with distilled water and stored at -20^{o}C until SDS-Page analysis.

P. Sephadex G-75 Gel Filtration Chromatography

The possible oligomeric nature and size of the soluble tryptically-released fragments from the membrane-bound transhydrogenase were analyzed by gel filtration chromatography on Sephadex G-75. 20 g Sephadex G-75 was pre-swollen and mixed to a slurry with 180 ml of 50 mM Tris-HCl, pH 7.8, 1 mM EDTA, 1 mM DTT, 0.1 M NaCl, 0.02% NaN_3. It was packed at 4°C into a Pharmacia 2.5 x 45 cm column to a bed height of 35 cm. The gel was equilibrated by passage of three bed-volumes of the abovementioned Tris-HCl buffer through it. The column was set up for an upward flow elution with the sample applied at the bottom of the column and pushed through the column and out the top at a flow rate of 15-18 ml/hour with a peristaltic pump.

The sample applied was 1 ml of concentrated supernatant, containing the recommended range of 5-20 mg protein, obtained after partial tryptic digestion as outlined below. Purified ISO membrane vesicles containing 12.3 mg or 0.25 umole protein in TED buffer were treated with 3.7 nmoles of DPPC-trypsin. After 5 min of incubation at room temperature, the reactions were stopped with the addition of 10 nmole SBTI. The mixture was left in ice for 15 min and was then made up to 8 ml with distilled water. The diluted material was ultracentrifuged at 194, 000 x g at 4°C for 2 hours. The supernatant was lyophilized. The lyophilizates were resuspended in 1 ml distilled water and kept at 4°C until application to column. The sample was applied into the column at half the operating flow rate. Immediately after sample application, 2 ml of 10% w/v sucrose in TED was applied. The normal operating speed of 15-18 ml/hour was restored 1 min after this. 1.5 ml fractions were collected. The fractions were temporarily stored at 4°C until A_{280} measurements and SDS-Page analysis could be carried out.

Pharmacia low molecular weight calibration proteins with blue dextran were used to calibrate the Sephadex G-75 column. The protein components in this calibration mix were BSA, ovalbulmin, chymotrypsinogen A, ribonuclease A. They

were applied to the column as a 2 ml mixture containing 4 mg of each component, in the same manner as above.

Q. Superose 12 Gel Filtration Fast Protein Liquid Chromatography

Soluble protein fragments released into the supernatant after tryptic treatment of JM83pDC21 ISO membrane vesicles were analyzed and partially purified using Superose 12 gel filtration FPLC. The sample applied was in TED or 50 mM Tris-HCl, pH 7.8 buffer solubilized with 1% SDS. Large suspended particles were removed by centrifugation at 10, 000 x g for 10 min. 200 ul to 1 ml of supernatant containing not more than 5 mg protein and not exceeding 30 mg/ml in protein concentration were applied. One prepacked Pharmacia Superose 12 HR 10/30 FPLC column or two of these columns connected in series were used in the purifications. The FPLC system consisted of Pharmacia components: GP-250 gradient programmer, P-500 pumps, mixer, pre-filter, manual valve V-7, UV-1 single path monitor control and optical units with a HR 10 flow cell, REC-481 single channel chart recorder, and Frac-100 fraction collector. The column was equilibrated with two bed volumes (50 ml) of a 50 mM Tris-HCl buffer, pH 7.8 with 1% SDS, 0.1 M NaCl prior to sample application. After sample application, elution was effected by pumping the same buffer used for equilibration at a flow rate of either 0.2 or 0.5 ml/min through the column(s). The back pressure was not allowed to exceed 3 MPa for one column and 4 MPa for the two serially connected columns during the run. Absorbance at 280 nm was monitored as 0.5 ml fractions were collected. Fractions were stored at -20^{o}C. In case of increased back-pressure or after 5 runs, the column(s) were cleaned and regenerated according to the manufacturer's instructions. Columns were stored by equilibration in 20% ethanol.

R. MonoQ Ion Exchange Fast Protein Liquid Chromatography

The Pharmacia FPLC system mentioned previously was also used here in an attempt to effect fast, high resolution Mono Q anion exchange chromatography of soluble protein fragments that were released into the supernatant upon tryptic treatment of JM83pDC21 ISO membrane vesicles. The sample applied was in TED or 50 mM Tris-HCl, pH 7.8 buffer with or without 1% dodecyl-β-D-maltoside. Large suspended particles were removed by vacuum filtration through a 0.22 um filter. 500 ul of supernatant containing not more than 20 mg protein total was applied to a prepacked Pharmacia Mono Q HR 5/5 anion exchange FPLC column. The column had been equilibrated with 50 mM Tris-HCl buffer, pH 7.8 with or without 1% dodecyl-β-D-maltoside until the A_{280} baseline was stable prior to sample application. After sample application, elution was effected using a 0-0.5 M or a 0-1 M NaCl gradient. The elution flow rate was 1.0 ml/min and the back pressure was 1.6 MPa. Absorbance at 280 nm was monitored as 1.0 ml fractions were collected and stored at -20^{o}C. The column was cleaned and regenerated after the runs according to the manufacturer's instructions. Columns were stored by equilibration in 20% ethanol.

S. Isolation of Proteolytically Released Transhydrogenase Fragments

Proteolytically released fragments from the membrane-bound transhydrogenase were obtained as indicated previously. The soluble fragments were isolated in three possible manners :

1. Superose 12 gel filtration FPLC was used as outlined previously.

2. The soluble fragments obtained from proteolytic treatment of JM83pDC21 ISO membrane vesicles, containing 33 mg of protein, with 270 ug of DPPC-trypsin were first subjected to 10% SDS-Page. This was done at a protein concentration of approximately 1-5 ug/band/lane and using 40 mA of current for each slab until the bromophenol blue dye front had just reached the gel bottom. The gel was washed

three times with distilled water and then placed in 0.2 M KCl cooled to 4°C to reversibly stain the SDS-Page gel. White protein bands appeared after prolonged cooling. The desired bands were excised as small gel pieces and equilibrated with 5 ml of 0.1% SDS. This mixture was shaken overnight using a Burrell model 75 wrist action shaker to allow diffusive elution of the protein fragments from the gel. The eluant was separated from the residual gel pieces by decanting and brief centrifugation at 10,000 x g. The eluant was temporarily kept at 4°C while another 5 ml of 0.1% SDS was added to the residual gel pieces. These were incubated with shaking as above for approximately 24 hours. The eluant was removed and added to the first batch. The combined eluants sample was filtered through a 0.45 um Acrodisc filter. The filtrate was treated in two possible ways. In the first method, it was dialyzed against 400 ml of 0.1% SDS at 4°C with three changes of the dialysis solution over 48 hours. The dialysis membrane used was either Spectropor 1 with a molecular weight cut-off of 6-8 kD or Sigma benzylated cellulose tubing with a molecular size cut-off at 2.0 kD. An alternate method of removing gel contaminants such as glycine from the filtered eluant was to exchange the buffer with fresh 0.1% SDS using Centricon-10 microconcentrators. 2 ml aliquots of the filtered eluant were each centrifuged at 8,800 x g for 30 min through a 10 kD molecular weight cut-off Centricon-10 filter in a Beckman JA-20 rotor. The concentrates were each resuspended with approximately 2 ml of fresh 0.1% SDS and recentrifuged as above. This was repeated a total of twice to give 1.5 ml final total volume. This material was combined with the dialyzed material, lyophilized and stored at -20°C as a powder of 40-80 ug protein.

3. The soluble fragments obtained from proteolytic treatment of JM83pDC21 ISO membrane vesicles were subjected to SDS-polyacrylamide gel electrophoresis as described previously. The gel was then equilibrated in electrotransfer buffer (25 mM Tris-acetate, pH 8.3, 20% (v/v) methanol) for 30 min and subsquently blotted onto Immobilon PVDF transfer membranes by electrophoretic elution (162) using a Bio-Rad

Trans-Blot cell according to the manufacturer's instructions. The electrotransfer was performed at 60 V for 5 hours or 70 V for 3 hours with cooling by running water at ambient temperature. The transfer membrane was rinsed with distilled water and stained with 0.01% (w/v) Coomassie Brilliant Blue R, 0.09% (w/v) Ponceau S and 50% (v/v) methanol overnight. The membrane was destained rapidly with 50% (v/v) methanol, 10% (v/v) acetic acid and air-dried. The purplish protein bands were excised to the smallest dimensions possible and saved as membrane pieces at 4°C. The nonsoluble, E. coli membrane-bound fragments obtained from proteolytic treatment of JM83pDC21 ISO membrane vesicles were isolated in a similar fashion except the transfer buffer contained only 25 mM Tris-acetate, pH 8.3 and the SDS-Page gel was not equilibrated in transfer buffer prior to electrotransfer.

T. Amino-Terminal Sequencing

Protein samples in the lyophilized form were sent to the University of Victoria's Protein Microchemisty Centre in the Department of Biochemistry and Microbiology for amino-terminal sequencing. Sequence analysis was done using an Applied Biosystems 470A gas phase sequencer with on-line PTH-analyzer and 900A system controller and data analyzer. At least 20 picomoles of protein per sample was sent and analyzed.

U. SDS Removal By AG11A8 Ion Retardation Chromatography

SDS was removed from proteins by passage through a Biorad AG11A8 ion retardation resin according to the manufacturer's instructions. The capacity of the AG11A8 resin was 2.2 mg SDS/g resin. AG11A8 resin (6 g) was mixed with 15 ml distilled and deionized water into a slurry. The slurry was poured into a 0.8 x 10 cm Econo-column to a bed volume of 4.8 cm^3. A 1 ml sample containing protein with 1% SDS was carefully pipetted onto the top of the resin bed. The sample was eluted with

deionized distilled water at a flow rate of 0.5 ml/min. 0.5 ml fractions were collected and the absorbance was monitored at 280 nm. The column was regenerated by washing with five bed volumes (50 ml) of 1.0 M NH4Cl followed by 20 bed volumes of deionized distilled water. The column was stored in 10, 000-fold diluted habitane (chlorhexidine gluconate, 4% w/v) at 4°C.

V. Carboxy-Terminal Sequencing

Protein fragments purified by Superose 12 gel filtration FPLC in 50 mM Tris-HCl, pH 7.8, 1% SDS buffer were freed from SDS and exchanged into deionized distilled water by AG11A8 ion retardation chromatography. The fractions containing purified fragments were pooled and lyophilized. The protein powder was redissolved in digestion buffer (0.1 M pyridine acetate, pH 5.6, 1% SDS, 0.1 mM norleucine internal standard) to 20 uM concentration. 4 nmol of the protein fragment was used in one carboxy-terminal sequencing experiment. This amount of protein in 200 ul of digestion buffer was incubated at 42°C for 20 min. 25 ul was withdrawn into 5 ul glacial acetic acid. 23 pmole of carboxypeptidase Y from a 1 mg/ml solution with 1 mM EDTA and 25 ug pepstatin/ml, was added to the mixture to serve as a zero time point. To the experimental protein sample, 0.16 nmol of carboxpeptidase Y was added from the 1 mg/ml stock solution to start the digestion of the carboxy-terminal region of the protein. At different time points, 25 ul of the reaction mix was removed and added to 5 ul glacial acetic acid to stop the reaction.

The samples taken at different times were lyophilized and submitted for micro amino acid analyses at the Protein Microchemistry Centre at the University of Victoria. The analyses were performed on an Applied Biosystems model 420A derivatizer-analyzer system. Acid hydrolysis was necessarily avoided prior to amino acid analysis. Approximately 500 pmole of "starting" protein per sample was submitted but only a portion of each sample was used for analyses. To determine the carboxy-terminal

sequence, the pmole content of the individual amino acids that appeared in the analyses was plotted against the duration of carboxypeptidase Y action.

W. NAD-Affinity Chromatography

0.1 mg of a purified 41 kD polypeptide fragment in 2 ml of deionized, distilled water was adsorbed onto an N6-NAD agarose affinity column maintained at 4°C. The column had a bed volume of 2.75 ml and a total of 3-8 umol of linked NAD^+. It had a theoretical capacity for 110-340 mg of a 41 kD polypeptide assuming that one molecule of this binds to one molecule of NAD^+. Prior to sample application, the column was equilibrated with six bed-volumes of a 10 mM sodium phosphate, pH 7.4 buffer containing 1 mM EDTA and 1 mM DTT. After sample application, the column was washed with four bed volumes of equilibration buffer. This was followed by elution with four bed-volumes of equilibration buffer containing 10 mM NADH. "Presample, postsample, and postNADH" samples were collected in batches.

III RESULTS

A. Isolation of Transhydrogenase-Enriched ISO Cytoplasmic Membrane Vesicles

1. Without Sucrose Density Gradient Centrifugation

Initially, in approaching the isolation of transhydrogenase-enriched ISO cytoplasmic membrane vesicles, the rationale used followed that of Clarke and Bragg (80) in purifying the enzyme from their overexpressing E. coli JM83pDC21 cells. The difference being that solubilization of the bacterial membrane and subsequent purification steps were not necessary.

Reconstitution of the solubilized and purified enzyme into a phospholipid membrane system was considered labour intensive and time consuming which would could result in lower yields and decreased enzyme activity. In addition, the homogeneity of structural orientation and integrity in the membrane vesicles could not be completely guaranteed in such a system. It was believed that a slightly less pure but more native enzyme-membrane situation was sufficient for the purposes of this thesis.

With the high concentration of the enzyme in the JM83pDC21 membrane, it was believed that selective detergent extraction of the isolated membrane would be sufficient to remove the other membrane proteins. Lane 3 of Figure 7 shows that in the crude membrane preparation obtained after French pressure lysis of JM83pDC21 cells, the α and β subunits of the transhydrogenase are the most intensely staining bands in the SDS-Page gel, although there are still significant amounts of other proteins. Extraction with Triton X-100 removed most of these other proteins as well as some of the α and β subunits (Lane 5, Figure 7) leaving these subunits and an equally intense staining 30 kD band in the membrane (Lane 4, Figure 7). Although sodium cholate removed some high molecular weight proteins

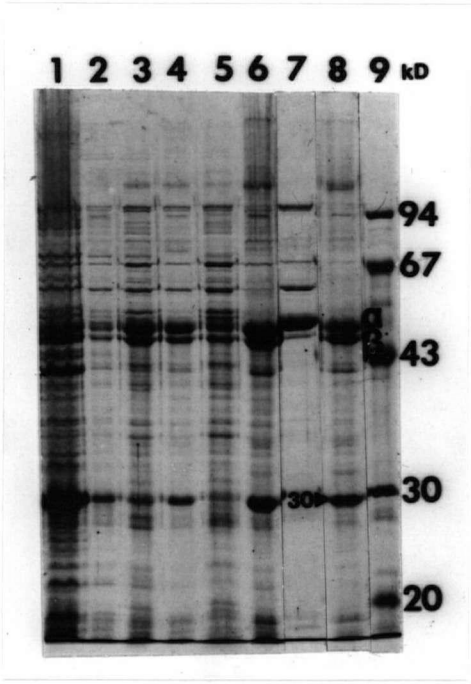

Fig. 7: SDS-10% Polyacrylamide Gel Electrophoresis of Fractions at Various Stages of the Partial Isolation of Transhydrogenase-Enriched ISO Membrane Vesicles

A sample was removed at various stages of the ISO membrane vesicle isolation procedure and analyzed by SDS-Page as described in Materials and Methods. Lane 1, 0.5 mg of intact JM83pDC21 cells; lane 2, French-pressed cell lysate; lane 3, 0.3 mg of crude ISO membrane vesicles; lane 4, 0.4 mg of ISO membrane vesicles after Triton X-100 extraction; lane 5, supernatant after Triton X-100 extraction and centrifugation; lane 6, ISO membrane vesicles containing 28 ug protein after Triton X-100 and sodium cholate extraction; lane 7, supernatant after sodium cholate extraction and centrifugation; lane 8, ISO membrane vesicles containing 30 ug protein after Triton X-100, sodium cholate, and 5 M urea extraction; lane 9, molecular weight markers.

(Lane 7, Figure 7) from the membrane, the 30 kD protein band is still unacceptably present in the membrane fraction (Lane 6, Figure 7). Even treatment of the membrane with 5 M urea was not able to remove the 30 kD protein (Lane 8, Figure 7). The presence of this protein constituent in the membrane could complicate the topographical analysis of the membrane-bound transhydrogenase using proteolytic enzymatic probes and SDS-Page as the detection system for the released fragments. The initial hope was that this 30 kD protein was in fact, a polypeptide fragment shortened by intrinsic proteolysis of either the α and β subunits occuring during the isolation procedure. If such was the case, the addition of protease inhibitors may have been necessary. With this in mind, peptide mapping using partial proteolysis was deemed the quickest and easiest route of identifying the origin of this protein constituent.

2. Peptide Mapping of 30 kD Polypeptide

If the 30 kD polypeptide was indeed derived from one or the other of the transhydrogenase subunits, partial proteolytic digestion of the 30 kD band would release peptides that are the same size as the partial proteolytic products of one of the subunits. This similarity of fragmentation would be most sharply evident at the lower molecular weights. Such was not the case when S. aureus V8 protease was used in a peptide mapping experiment following the methodology of Cleveland et al. (161). As one can see on the SDS-Page gel of Figure 8, the fragmentation pattern of the 30 kD band (lane 7) was dissimiliar to that of both the α and β subunits (lanes 5 and 6, respectively). Similar results were obtained using papain as the protease (data not shown). Although these results do not prove conclusively that the 30 kD band is not a fragment from a transhydrogenase subunit, it led the author to another supposition for its identity. Perhaps, the membrane preparation contained outer membrane fragments and the 30 kD polypeptide is an outer membrane protein.

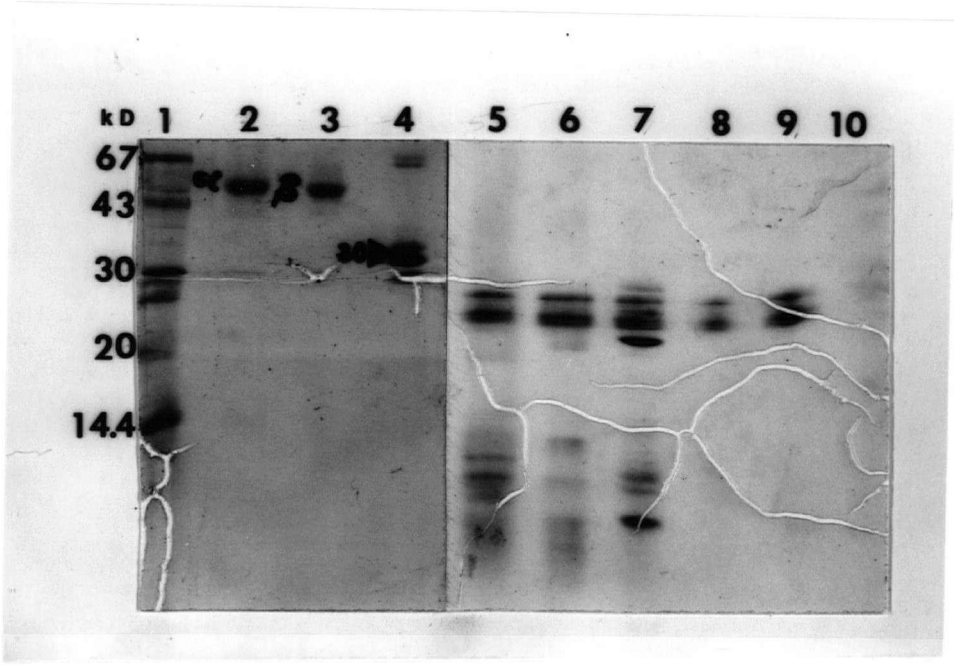

Fig. 8: Partial Proteolysis of the 30 kD Membrane Protein and the α and β Subunits of the Transhydrogenase

The 30 kD protein and the α and β subunits of the transhydrogenase were subjected to Cleveland digestion (161) using Staphylococcus aureus V8 protease on a 15% SDS-Page gel according to the procedure in Materials and Methods. Lane 1, molecular weight markers; lanes 2, 3, and 4 are the α and β subunits and the 30 kD protein, respectively; lanes 5, 6, and 7 are the α and β subunits and the 30 kD protein treated with 2.5 ug of S. aureus V8 protease; lanes 8 and 9 are 2.5 and 5.0 ug, respectively of the S. aureus V8 protease alone; lane 10 is an empty lane.

Therefore, it should be possible to have a cytoplasmic membrane preparation without the 30 kD band if the outer membrane could be separated from it.

3. With Sucrose Density Gradient Centrifugation

To effectively remove the two bacterial membranes from each other, a discontinous sucrose gradient centrifugation step was introduced into the membrane preparation procedure prior to selective detergent extraction. Theoretically, the gradient would separate the membranes based on their different densities. The bottom of the discontinuous gradient had a density of 1.22 g/ml and top had a density of 1.10 g/ml. The outer membrane being more dense than 1.22 g/ml would pellet out, while the cytoplasmic membrane having an intermediate density would collect sharply in the interphase band.

Lane 3 of the SDS-Page gel in Figure 9 shows the multitude of proteins present in the cell lysate. This fraction has a very low specific transhydrogenase activity of 0.86 U/mg protein (Table I). After sucrose gradient centrifugation, the interphase membrane material contained mainly the transhydrogenase subunits with a few comparatively faint bands (Lane 5). This fraction has a 3.8-fold increase in specific activity from the crude cell lysate, but only 15.3% of the total activity was recovered (Table I). The 30 kD polypeptide has been effectively separated with the outer membrane pellet fraction (Lane 4). Note that some α and β subunits representing a residual specific activity of 0.13 U/mg protein (Table I) is also removed with the outer membrane fraction. Perhaps some cytoplasmic membrane vesicles are still associated strongly with the outer membrane. Extraction with Triton X-100 and sodium cholate removes further proteins from the ISO cytoplasmic membrane vesicles as detected by SDS-Page (Lane 6 and 7 respectively). However, after Triton X-100 extraction, the membrane-bound enzyme activity is greatly reduced (Table I). The detergent may have two effects. One could be to alter the enzyme conformation. Another is the possibility of a specific inhibition of the

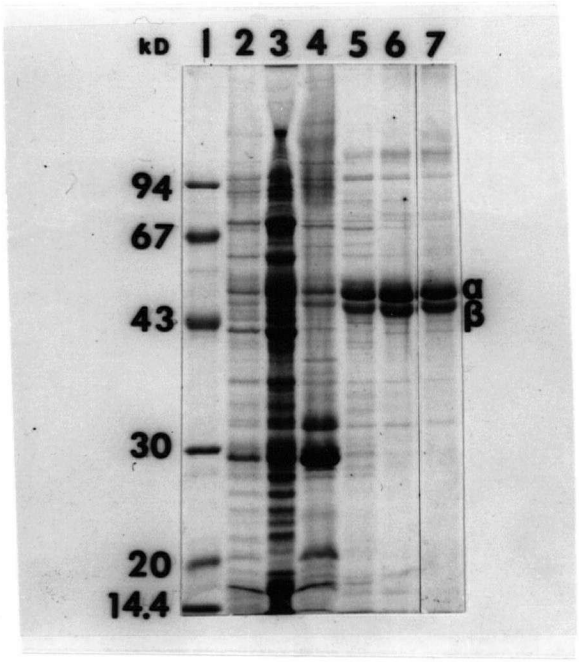

Fig. 9: SDS-10% Polyacrylamide Gel Electrophoresis of Fractions at Various Stages of the Purification by Sucrose Density Gradient Centrifugation of Transhydrogenase-Enriched ISO Cytoplasmic Membrane Vesicles

A sample was removed at various stages of the isolation procedure and analyzed by SDS-Page as described in Materials and Methods. Lane 1, molecular weight markers; lane 2, intact JM83pDC21 cells containing 10.5 ug protein; lane 3, French-pressed cell lysate containing 59.4 ug protein; lane 4, sucrose density gradient centrifugation pellet containing 44.5 ug protein; lane 5, sucrose density gradient centrifugation interphase material (ISO cytoplasmic membrane vesicles); lane 6, ISO cytoplasmic membrane vesicles after Triton X-100 extraction; lane 7, ISO cytoplasmic membrane vesicles containing 14 ug protein after Triton X-100 and sodium cholate extraction.

Table I: Isolation of Transhydrogenase-Enriched ISO Cytoplasmic Membrane Vesicles

		Transhydrogenase Activity	
Fraction	Protein	Total	Specific
	mg	%	U/mg protein
Whole cells	undetermined	undetermined	0.17
Crude membranes + soluble proteins	326	100	0.86
Sucrose gradient pellet (outer memb)	15.8	0.7	0.13
Sucrose gradient interphase, later spun down (cyto. memb)	13.6	15.3	3.23
Cytoplasmic membrane treated with 0.1% Triton X-100	2.2	0.15	0.21
Triton X-100 extracted cytoplasmic membrane treated with 5 mM sodium cholate	0.53	0.021	0.11

Membranes were prepared from 3.3 g of JM83pDC21 cells. Cells were lysed by a French Press. After removal of unbroken cells and large cell debris, the lysate or crude membrane mixture was centrifuged through a discontinuos sucrose density gradient. The interphase material was removed and pelleted by centrifugation. This membrane preparation was then extracted sequentially with 0.1% Triton X-100 and 5 mM sodium cholate. Experimental details of this isolation and determinations of enzyme activities and protein concentrations are described in Materials and Methods.

activity. More about this is discussed in Section D, Subsection 1.3 of the Results part of this thesis.

B. Isolation of Transhydrogenase-Enriched RSO Cytoplasmic Membrane Vesicles

Lane 2 of Figure 10 shows the SDS-Page gel of an aliquot of a transhydrogenase-enriched RSO cytoplasmic membrane vesicle preparation isolated as described in Materials and Methods. The α and β subunits are as indicated. There are two other bands, both of higher molecular weight than the transhydrogenase subunits, in this preparation. The material banding at about 94 kD could be a dimeric aggregate of the subunits that was not depolymerized by SDS. The other, which banded below 67 kD, may be another cytoplasmic membrane protein. As RSO membranes are quite labile and sensitive to reorientation, they were not treated or purified any further. These vesicles had no observable transhydrogenase activity (data not shown), which is consistent with a RSO orientation as the active site is on the cytoplasmic face of the enzyme.

C. Generation of Anti-Transhydrogenase Polyclonal Antibodies

In order to more clearly identify the transhydrogenase fragments arising from proteolytic cleavage, anti-E. coli transhydrogenase polyclonal antibodies were generated from rabbits as outlined in Materials and Methods. Anti-mitochondrial transhydrogenase antibodies were found by Clarke (82) to be ineffective against the E. coli enzyme.

Two sets of rabbit generated anti- transhydrogenase polyclonal antibodies were produced. One set was against both subunits and the other was specifically against the α subunit. The anti-α,β polyclonals reacted strongly in an immunoblot

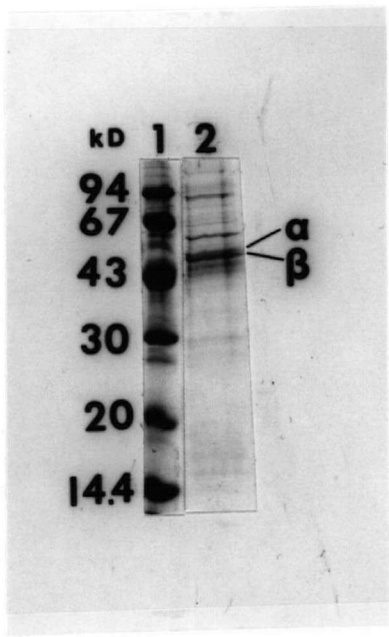

Fig. 10: Isolation of Transhydrogenase-Enriched RSO Membrane Vesicles from E. coli JM83pDC21 Cells

0.43 g of RSO membrane vesicles were prepared from 1.05 g of E. coli JM83pDC21 cells according to the procedure outlined in Materials and Methods. An aliquot of the membrane preparation containing 0.86 ug protein was analyzed by 12 % SDS-Page (lane 2) as described in Materials and Methods. Lane 1, molecular weight markers.

with both subunits (Lane 2, Figure 11) of a purified soluble transhydrogenase preparation (Lane 1) graciously donated by Natalie Glavas of this lab. The anti-α,β polyclonals also reacted strongly with both subunits (Lane 4) in a crude fraction of a JM83pDC21 membrane preparation (Lane 3), although there are some fainter cross-reactant proteins in this immunoblot. Considering the multitude of proteins present in the crude lysate membrane fraction, it is probably not surprising that some of these would cross-react with the anti-α,β polyclonals. In addition, the polyclonal antibody set more than likely contains a number of different antibodies that reacts with different epitopes or antigenic determinants of the transhydrogenase, which will react with similar epitopes on other proteins. The anti-α polyclonal set, in addition to reacting with the α subunit strongly, cross-reacts with a number of different proteins in the crude membrane lysate (Lane 5). But, more importantly, it did not react with the β subunit. The cross-reactivity of the polyclonals was not an obstacle for the writer's analysis of whether reacting proteolytic fragments arose from transhydrogenase cleavage, as long as the membranes were relatively enriched in transhydrogenase. In a transhydrogenase-enriched ISO cytoplasmic membrane preparation (Lane 6, Figure 14), the anti-α,β polyclonals reacted effectively with both subunits (Lane 8, Figure 14) and the anti-α polyclonals reacted very strongly with the α subunit (Lane 7, Figure 14).

The anti-α,β polyclonals was titered to 32x dilution and the anti-α set was titered to 64x dilution (data not shown). These gave the maximum reaction under the conditions outlined in the Materials and Methods of this thesis.

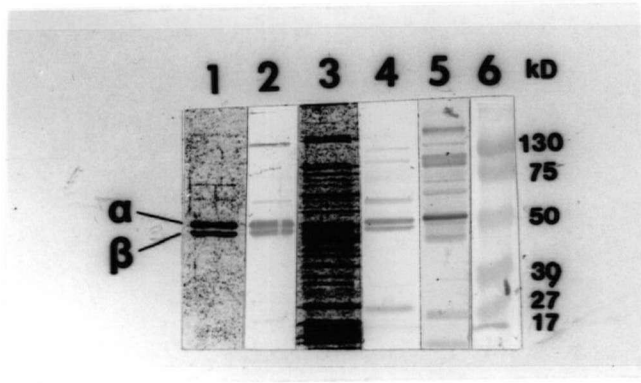

Fig. 11: Generation of Anti-Transhydrogenase Polyclonal Antibodies

Two sets of antisera having anti-transhydrogenase polyclonal antibodies were produced from rabbits as outlined in Materials and Methods. One set reacts with both subunits of the transhydrogenase while the other reacts with α and not β. Lane 1 is the SDS-10% polyacrylamide gel electrophoresis of 3 ug of purified soluble transhydrogenase. Lane 2 is the immunoblot of a similar transhydrogenase sample using the anti-α,β polyclonal antibody set. Lane 3 is the SDS-Page of a JM83pDC21 French-Pressed cell lysate sample containing 8 ug of protein. Lane 4 is the immunoblot of this cell lysate using the anti-α,β polyclonal set. Lane 5 is a similar immunoblot except with the anti-α polyclonal set as the primary antibody solution in the blot. Lane 6 is the prestained molecular weight markers on Immobilon-PVDF immunoblotting paper. Preparation of the antigen samples for immunoblotting and SDS-Page as well as these detection methodologies are detailed in Materials and Methods.

D. Proteolytic Digestion of ISO and RSO Cytoplasmic Membrane Vesicles

1. Trypsin Effects on ISO Vesicles

Figure 12M and 12S show a typical time course for partial tryptic digestion of transhydrogenase-enriched ISO cytoplasmic membrane vesicles. During the time span of this experiment, the α subunit is preferentially digested whereas the β subunit does not appeared to be affected (Lanes 7-10, Figure 12M). Prolonged digestion or digestion with increased amounts of trypsin does not diminish the amount of β in the membrane (data not shown). Therefore, it may be that most if not all of the β subunit is not protruding from the cytoplasmic face of the membrane or that the β subunit protrudes, but arranged in a manner so that its arginines or lysines are not accessible for tryptic attack. The α subunit is so accessible to trypsinolysis from the cytoplasmic face of the membrane that it completely disappears before 5 minutes of digestion (Lane 8, Figure 12M). Concomitant with the disappearance of α is the sequential appearance of protein bands of 41, 29, and 16 kD in that order in the fraction released from the membrane (Lanes 7-10, Figure 12S). This suggests that these polypeptides may be derived by cleavage of the α subunit. If this is the case, α subunits are already digested before 1 minute as the 41 kD fragment is already released into solution at the 1 minute time point (Lane 7, Figure 12S). In similar tryptic experiments, the further appearance of protein bands of 12 kD (Lane 2, Figure 17S or Lane 18, Figure 14) and 11 kD (Lane 1, Figure 21) was observed . In addition, on some occasions without any apparent differences in conditions, there appeared fragments of 39 and 27 kD in addition to the always present 41 and 29 kD fragments (Lane 2, Figure 17S). These fragments will be discussed in the context of their amino-terminal sequencing results. No significantly intense membrane-bound fragment bands were observable (Lanes 7-10, Figure 12M). This may not mean

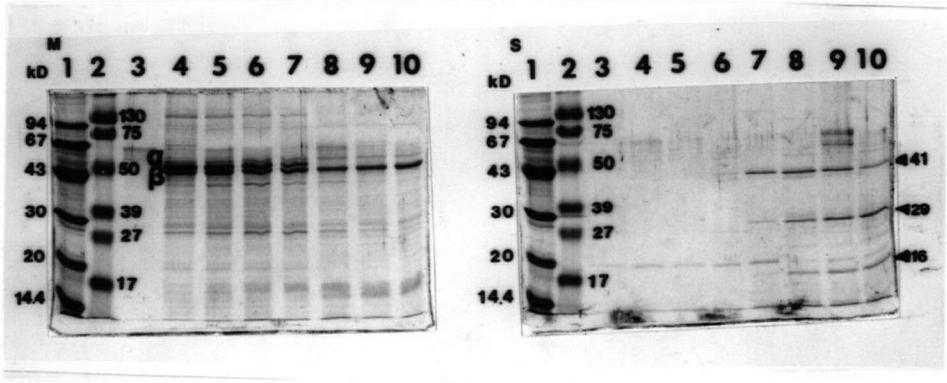

Fig. 12: Tryptic Digestion of ISO Cytoplasmic Membrane Vesicles

12% SDS-Page of the fractions from tryptic digestion of E. coli JM83pDC21 ISO cytoplasmic membrane vesicles: after DPPC-trypsin addition, aliquots were removed after different times of incubation and SBTI was added to stop the reaction. Membranes (M) and released fragments (S) were separated by ultracentrifugation. In this experiment, trypsin was added at a ratio of 1 ug to 120 ug of membrane protein. Lanes 1 and 2, molecular weight markers; lane 3, reaction without membranes stopped after 30 minutes; lane 4, reaction without trypsin but with SBTI after 30 minutes; lane 5, reaction with SBTI-inactivated trypsin added at zero time; lane 6, reaction with SBTI added to membranes first, followed immediately by trypsin addition at zero time; lanes 7, 8, 9, and 10 are reactions stopped with SBTI after 1, 5, 15, and 30 minutes, respectively. See Materials and Methods for details of protocols.

there are no such fragments. Perhaps such a hydrophobic fragment may not stain well with Coomassie Brilliant Blue R.

When a similar time course experiment was performed with 4-fold less trypsin (to membrane protein ratio), similar results were obtained except the 41kD fragment was observed to be associated with the membrane fraction at the zero and 5 minute time samples (Lanes 8, 9, Figure 13) and then with the released fraction at the 15, 30, 60 minute time samples (Lanes 15-17, Figure 13). It appears that the 41 kD fragment remains or adheres to the membrane for some time after cleavage of the α subunit before being released from the membrane. The nature of this interaction could be of a protein-protein sort which is possible given the oligomeric nature of the enzyme (125). That is, an α-α interaction may be at play here. A single proteolytic cut of the α-α dimer would not release the 41 kD polypeptide until the second α subunit was cut. This is one possible explanation for the time dependency of the release of the 41 kD polypeptide from the membrane. This point will be discussed further in conjunction with other results. In this experiment, it appears that there is cutting of the α subunit at the zero time point (Lanes 3, 8, Figure 13). This time point involves the addition of trypsin first to the membrane suspension followed immediately by the soya bean trypsin inhibitor. This shows the rapidity of the tryptic attack as it would be expected that the trypsin inhibitor would take only a short time before inhibiting trypsin activity. Another point to note that under the milder conditions of tryptic digestion of this experiment, the 16 kD fragment cannot be observed at any time point or is in such a low amount comparatively that it is not stained.

To determined whether 41, 29, 16 and 12 kD bands were indeed from the α subunit of the transhydrogenase, solutions removed after tryptic digestion of membranes (Lane 18, Figure 14) were Western blotted using polyclonal antibodies against the E. coli transhydrogenase. Anti-α polyclonals reacted strongly against the 41, 29, and 12 kD fragments but not the 16 kD fragment (Lane 19, Figure 14). This could mean the 16 kD fragment is not an α fragment or that it is an α fragment which

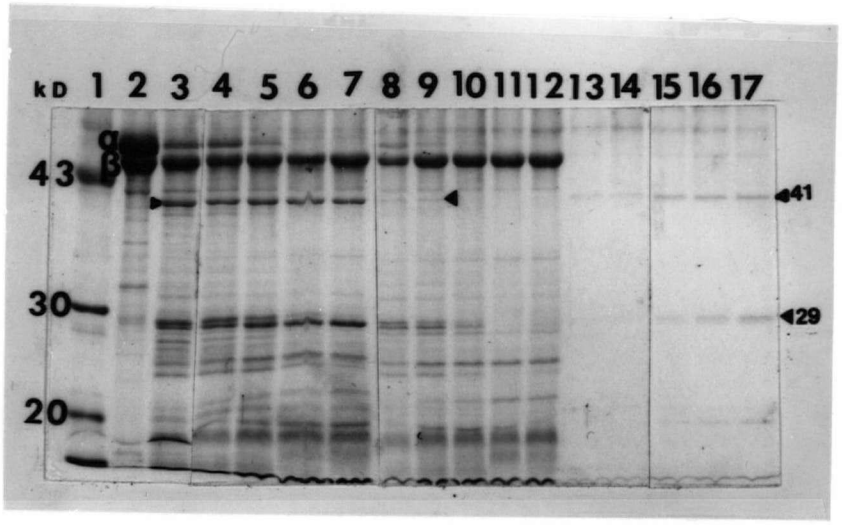

Fig. 13: Light Tryptic Digestion of ISO Cytoplasmic Membrane Vesicles

10% SDS-Page of the fractions from tryptic digestion of E. coli JM83pDC21 ISO cytoplasmic membrane vesicles: after DPPC-trypsin addition, aliquots were removed after different times of incubation and SBTI was added to stop the reaction (lanes 3-7). Membranes (lanes 8-12) and released fragments (lanes 13-17) were separated by ultracentrifugation. In this experiment, trypsin was added at a ratio of 1 ug to 500 ug of membrane protein. Lane 1, molecular weight markers; lane 2, untreated membranes; lanes 3, 4, 5, 6, and 7 are reactions stopped with SBTI after 0, 5, 15, 30, and 60 minutes, respectively; lanes 8, 9, 10, 11, and 12 are membrane fractions which were removed after reactions were stopped at 0, 5, 15, 30, and 60 minutes; lanes 13, 14, 15, 16, and 17 are supernatant fractions which were removed after reactions were stopped at 0, 5, 15, 30, and 60 minutes. The "zero" time samples come from a mixture where trypsin was added to the membranes first, followed immediately by SBTI addition. See Materials and Methods for details of relevant protocols.

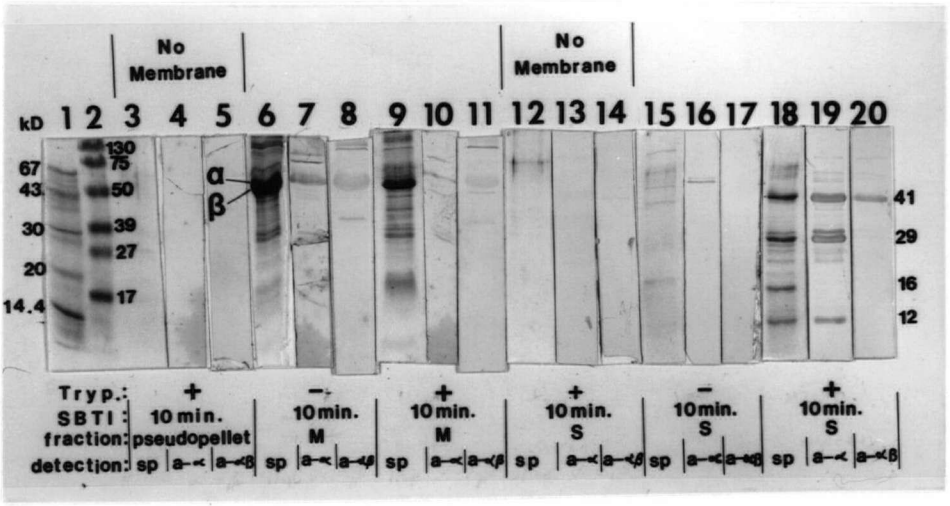

Fig. 14: Antibody Identification of Transhydrogenase Fragments from Tryptic Cleavages

Immunoblots and SDS-Page of the fractions from tryptic digestion of E. coli JM83pDC21 ISO cytoplasmic membrane vesicles: DPPC-trypsin was added (+) or not added (-) to membrane vesicles at a ratio of 1 ug to 255 ug of membrane protein and SBTI was added after 10 minutes to stop the reaction as indicated. Membranes (M) and released fragments (S) were separated by ultracentrifugation. Also, a tryptic incubation was performed under the above conditions in the absence of membranes (indicated by "No Membrane"). No pellet was observed after centrifugation of this solution; nevertheless, the sides and bottom of the centrifuge tube was scraped thoroughly and resuspended (indicated above by "pseudopellet"). 15% SDS-Page of the different fractions are indicated by lanes marked "sp". Immunoblots of these fractions using anti-α and anti α,β polyclonals are indicated as "a-α" and "a-αβ", respectively. Lanes 1 and 2 show molecular weight markers. See Materials and Methods for details of relevant protocols.

does not contain epitopes that the polyclonals can recognize. Interestingly, the anti-α,β polyclonals reacted only with the 41 kD fragment (Lane 20, Figure 14). This polyclonal set probably does not contain antibodies which recognize epitopes of the 29 and 12 kD α fragments like the anti-α polyclonals. Note the 16 kD fragment was not recognized either by anti-β antibodies in the anti-α,β set. The origin of this fragment was determined later to be from the α subunit based on amino-terminal sequencing results (Table III).

No membrane-bound fragments after trypsin digestion (Lane 9, Figure 14) were reactive with either set of anti-transhydrogense polyclonals (Lane 10, 11, Figure 14); only the β subunit that is left intact after trypsin digestion reacted with the anti-α,β polyclonals. Again, the fact that no membrane-bound tryptically cleaved fragments were detected does not necessarily mean that no such fragments exist. The anti-α (or β) antibodies in these polyclonal sets may not recognize epitopes on these hydrophobic fragments.

2. Chymotrypsin Effects on ISO Vesicles

Partial chymotrypsin digestion of transhydrogenase-enriched ISO membrane vesicles show a similar digestion pattern as the tryptic pattern (Figure 15M and 15S). Firstly, the β subunit does not appear to be affected (Lanes 6-9, Figure 15M). Secondly, the 41 KD and 29 kD fragments were released into the solution in the same sequence (Lanes 6-9, Figure 15S) as the α band in the membrane diminished in intensity with time (Lanes 6-9, Figure 15M). However, this effect took 3-fold more chymotrypsin than trypsin (Figure 12) in terms of the protease to membrane protein amounts ratio used in the experiments. The significance of this observation was not investigated.

The similarity in fragment sizes could mean exposure to the external medium of short sequences of the α polypeptide chain containing vicinal basic and aromatic residues for tryptic and chymotryptic cleavages, respectively. Because of the

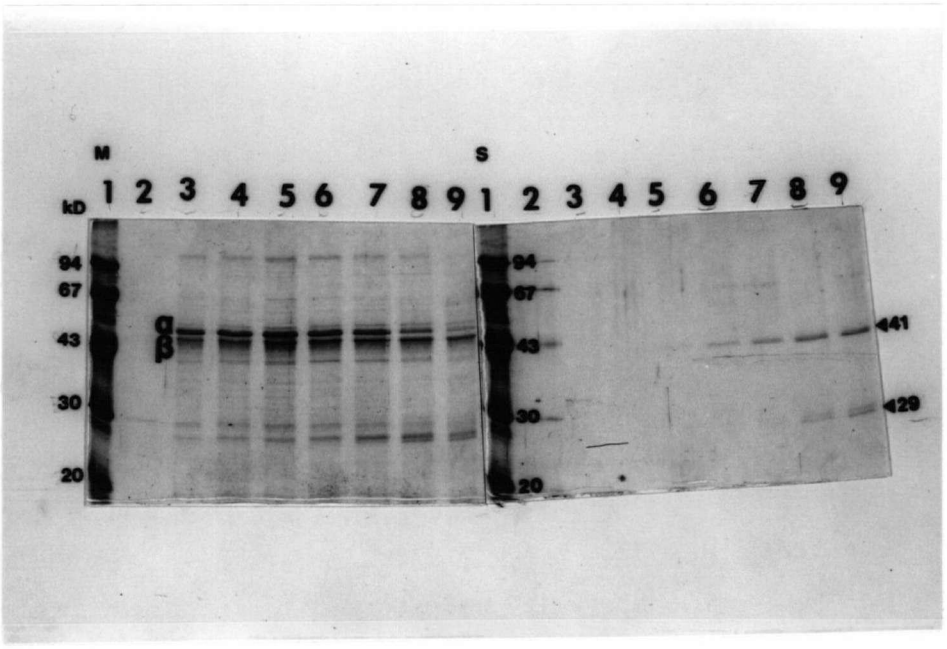

Fig. 15: Chymotryptic Digestion of ISO Cytoplasmic Membrane Vesicles

12% SDS-Page of the fractions from chymotryptic digestion of E. coli JM83pDC21 ISO cytoplasmic membrane vesicles: after chymotrypsin addition, aliquots were removed after different times of incubation and PMSF was added to stop the reaction. Membranes (M) and released fragments (S) were separated by ultracentrifugation. In this experiment, chymotrypsin was added at a ratio of 1 ug to 36 ug of membrane protein. Lane 1, molecular weight markers; lane 2, reaction without membranes stopped after 30 minutes; lane 3, reaction without chymotrypsin but with SBTI after 30 minutes; lane 4, reaction with PMSF-inactivated chymotrypsin added at zero time; lane 5, reaction with PMSF added to membranes first, followed immediately by chymotrypsin addition at zero time; lanes 6,7, 8, and 9 are reactions stopped with PMSF after 1, 5, 15, and 30 minutes, respectively. See Materials and Methods for details of protocols. Note in lane 2 of gel S, all bands result from an overspill of the molecular weight marker sample from lane 1 and must be discounted.

similarity of the chymotryptic results to the tryptic results, it was decided to pursue further investigation of the latter rather than the former.

3. Detergent Effects on Membrane-Bound Transhydrogenase Conformation

As most of the proteolytic experiments are performed on detergent-cleansed ISO membranes, the possibility of detergent disruption of the transhydrogenase prior to topographical probing was investigated. Membranes treated with increasing amounts of Triton X-100 or sodium cholate showed a progressive loss of total enzymatic activity and specific activity (Table II). Under similar experimental conditions, treatment with 0.05% Triton X-100 followed by 2.5 mM sodium cholate effectively inactivated the membrane-bound transhydrogenase (Table II).

A SDS-Page gel of this detergent extracted membrane fraction (Lane 2, Figure 16) was compared with one not treated with detergents (Lane 1, Figure 16). In both cases, the α and β subunits stained well. Therefore, both subunits are still present in the membrane after detergent extraction. The loss in specific activity may then be a result of two possibilities. One is inactivating conformational changes in the enzyme caused by the detergents. The other is more specific inhibition by the detergents without effecting major conformation changes. Trypsin was selected to probe the topology of the membrane-bound enzyme before and after detergent treatment (Lanes 5-12, Figure 16). The total reaction mixtures (Lanes 5, 6), the membrane fractions (Lanes 8, 9), and the solution fractions (Lanes 11, 12) for untreated and detergent treated membranes show a striking similarity in the fragmentation patterns. The only possible difference is that the amount of the soluble 41 kD fragment may be slightly less in the detergent treated membranes as detected by comparing stained intensities (Lanes 11,12). The difference was not however quantitated.

It was assumed, by using trypsin as a probe of conformational differences, that for the most part, no major conformational changes of the membrane-bound

Table II: Detergent Effects on Membrane-Bound Transhydrogenase

Fraction	Protein	Transhydrogenase Activity	
		Total	Specific
	mg	%	U/mg protein
Cytoplasmic membrane	2.19	100	5.99
after Triton X-100 extraction:			
0.01%	0.83	34.8	5.47
0.02%	0.10	2.5	3.33
0.04%	0.22	5.4	3.23
0.1%	0.15	1.9	1.70
after sodium cholate extraction:			
0.5 mM	0.68	19.1	3.75
1.0 mM	0.71	27.5	5.05
2.0 mM	0.78	21.4	3.62
5.0 mM	0.87	18.3	2.75
after 0.05% Triton X-100 and 2.5 mM sodium cholate:	0.50	0.61	0.16

Cytoplasmic membranes were prepared from JM83pDC21 cells. Cells were lysed by a French Pressure. After removal of unbroken cells and large cell debris, the lysate or crude membrane mixture was centrifuged through a discontinuos sucrose density gradient. The interphase material was removed and pelleted by centrifugation. Aliquots of this membrane preparation each containing 2.19 mg of protein and having a specific activity of 5.99 U/mg protein, were then extracted with different amounts of Triton X-100 and/or sodium cholate as indicated. Where the membrane is extracted with both detergents, Triton X-100 was added first and removed before subsequent sodium cholate extraction. Procedural details and determinations of enzyme activities and protein concentrations are described in Materials and Methods

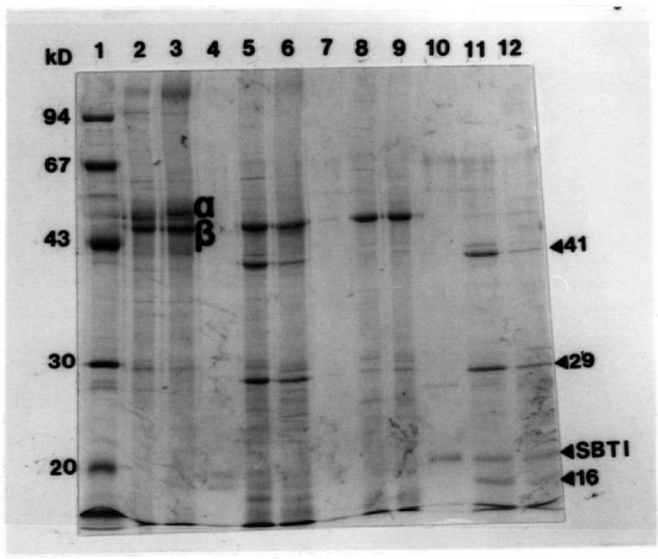

Fig. 16: Detergent Effects on Trypsin Digestion of ISO Cytoplasmic Membrane Vesicles

10% SDS-Page of the fractions from tryptic digestion of E. coli JM83pDC21 ISO cytoplasmic membrane vesicles (containing 0.4 mg protein) that were untreated or treated with 0.05% Triton X-100 and 2.5 mM sodium cholate in succession. DPPC-trypsin was added to both untreated and detergent-treated membrane samples at a ratio of 1 ug to 120 ug of membrane protein. DPPC-trypsin was also added to a control sample without membranes. SBTI was added after 5 minutes to stop all three reactions (lanes 4-6). Membranes (lanes 7-9) and released fragments (lanes 10-12) were separated by ultracentrifugation. Lane 1 shows molecular weight markers; lanes 2 and 3 are native and detergent-treated membranes, respectively, without trypsin; lanes 4, 5, and 6 are tryptic reaction mixes in the absence of membranes, with native membranes, and with detergent-treated membranes, respectively; lanes 7, 8 and 9 are membrane fractions from tryptic digestions in the absence of membranes, with native membranes, and with detergent-treated membranes; lanes 10, 11, and 12 are supernatant fractions from ultracentrifugation of tryptic reaction mixes without membranes, with native membranes, and with detergent-treated membranes, respectively. See Materials and Methods for procedural details.

transhydrogenase had occurred upon detergent extraction. The detergent may however cause small local conformational alterations which have a negative effect on the enzymatic activity. This may occur via selective removal of required lipids (2, 73, 124, 126-129). Alternatively, other workers (163) have found that Triton X-100 specifically blocks proton translocation via the transhydrogenase. If this is the explanation for the observed decrease in activity in our membranes, then hydride ion transfer catalyzed by the enzyme has to be well coupled to proton translocation. Despite the inactivation of the enzyme by the detergents used to clean up the transhydrogenase-enriched membranes, it was decided that this fact, for the purposes of this thesis, did not detract from the topographical interpretations made herein.

4. Substrate Effects on Membrane-Bound Transhydrogenase Conformation

To see if natural ligands of the transhydrogenase had any major effects on the enzyme conformation in the membrane, equal aliquots of a JM83pDC21 ISO membrane vesicle preparation were saturated with each of its four normal nucleotide substrates or an NAD^+ analog, 3-acetylpyridine NAD^+. Then the membranes were treated with equal amounts of trypsin in a partial proteolysis experiment. Figure 17 shows the results. The fragmentation patterns for all nucleotide-bound enzymes and the ligandless enzyme are basically the same. The $NADP^+$ result is not shown here but it also showed no difference from the ligandless enzyme. This suggests that as detected by partial trypsinolysis, there are no major conformational changes in the enzyme upon binding any of the substrates. This contradicts the well-documented results of others doing research in both the E. coli and mitochondrial transhydrogenase fields (63, 79, 88, 107-108, 111-112, 124). However, the conclusion was not verified by further experimentation using other means of probing enzyme conformation such as the use of different proteases. It may be simply that

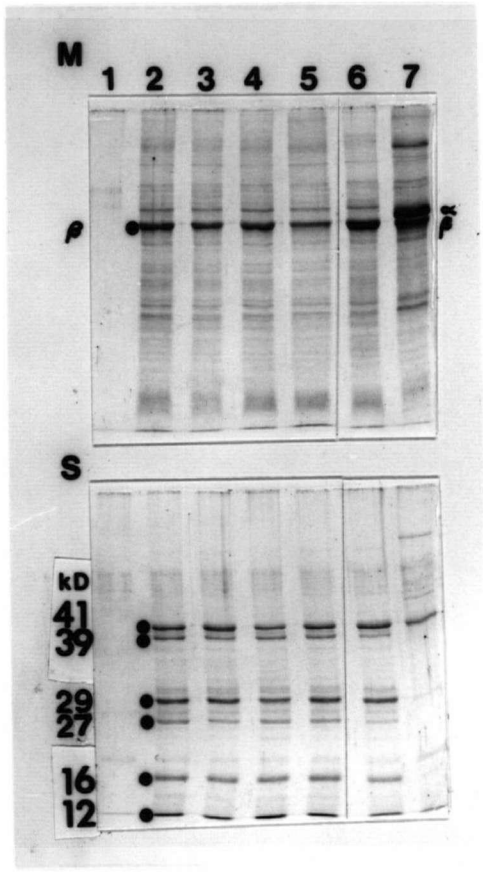

Fig. 17: Substrate Effects on Trypsin Digestions of ISO Cytoplasmic Membrane Vesicles

E. coli JM83pDC21 ISO cytoplasmic membrane vesicles were saturated with substrates (1 : 20 molar ratio) and then were treated with DPPC-trypsin so that the protease to membrane protein molar ratio was 1 : 138. SBTI was added after 10 minutes of reaction and the membranes (M) and released fragments (S) were separated by ultracentrifugation. Lane 1, trypsin and SBTI alone; lane 7, trypsin added to membranes, followed immediately by SBTI addition. Trypsin treatment without substrate (lane 2), with 3-acetylpyridine NAD^+ (lane 3), NAD^+ (lane 4), NADH (lane 5), and NADPH (lane 6).

trypsinolysis under our conditions could not detect conformational changes that may be present.

5. Trypsin Effect on RSO Vesicles

Transhydrogenase-enriched membrane vesicles oriented in a right side out manner were treated with trypsin in a time-course experiment under the same or harsher conditions (ie. 10x higher amount of trypsin to membrane protein ratio, same incubation time-span and points) than that used for ISO vesicles. Figure 18M and 18S shows the results. Over the time-span of this experiment, there were no detectable cleavages of the enzyme at any given time point (Lanes 7-10 of Figures 18M and 18S). Thus, the α subunit is much more accessible from the cytoplasmic side than from the periplasmic side. The β is not cut by trypsin in either orientations. The significance of these observations will be elaborated on in the Discussion section where a possible enzyme topology will be proposed in light of this and other results.

Proteinase K treatment of RSO vesicles gave similar results and does not appear to cleave either subunits (data not shown). See below.

6. Proteinase K Effects

Transhydrogenase-enriched ISO membrane vesicles were treated with the nonspecific protease, proteinase K, in a time-course experiment. The α and β subunits are both cleaved by proteinase K digestion (Lanes 7-11, Figure 19M). The α subunit seems to be cleaved much faster as it had disappeared before 5 minutes of incubation whereas the β band, although diminished in intensity, was still present (Lane 7, Figure 19M). The β band gradually disappeared over the 30 minute time-span of this experiment (Lanes 7-10, Figure 19M). This indicates that a portion of the β subunit is indeed accessible on the cytoplasmic side, which could not be ascertained from the trypsin experimental results. It is very difficult to explain why it is

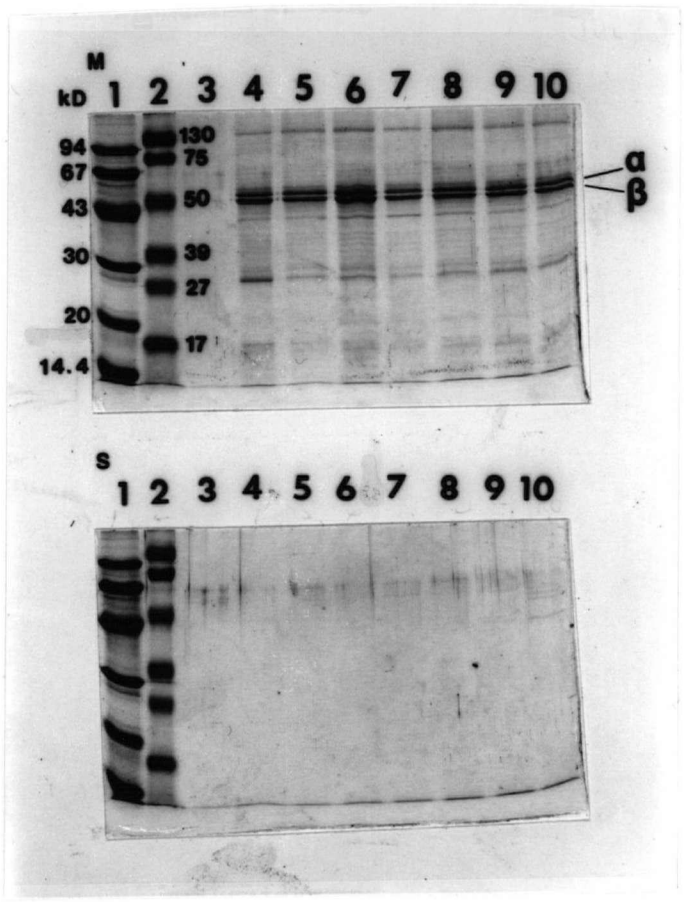

Fig. 18: Tryptic Digestion of RSO Membrane Vesicles

12% SDS-Page of the fractions from tryptic digestion of E. coli JM83pDC21 RSO membrane vesicles: after DPPC-trypsin addition, aliquots were removed after different times of incubation and SBTI was added to stop the reaction. Membranes (M) and released fragments (S) were separated by ultracentrifugation. In this experiment, trypsin was added at a ratio of 1 ug to 12 ug of membrane protein. Lanes 1 and 2, molecular weight markers; lane 3, reaction without membranes stopped after 30 minutes; lane 4, reaction without trypsin but with SBTI after 30 minutes; lane 5, reaction with SBTI-inactivated trypsin added at zero time; lane 6, reaction, with SBTI added to membranes first, followed immediately by trypsin addition at zero time; lanes 7, 8, 9, and 10 are reactions stopped with SBTI after 1, 5, 15, and 30 minutes, respectively. See Materials and Methods for details of protocols..

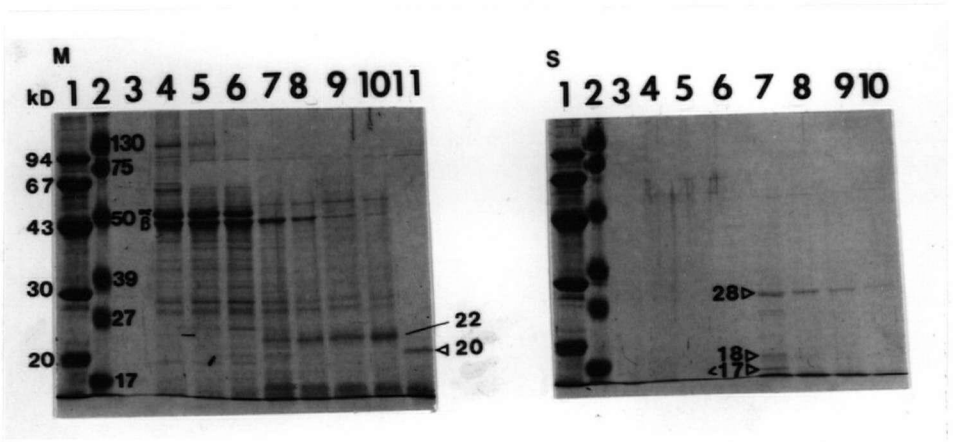

Figure 19: Proteinase K Digestion of ISO Cytoplasmic Membrane Vesicles

12% SDS-Page of the fractions from proteinase K digestion of E. coli JM83pDC21 ISO cytoplasmic membrane vesicles: after proteinase K addition, aliquots were removed after different times of incubation and PMSF was added to stop the reaction. Membranes (M) and released fragments (S) were separated by ultracentrifugation. In this experiment, proteinase K was added at a ratio of 1 ug to 182 ug of membrane protein. Lanes 1 and 2, molecular weight markers; lane 3, reaction without membranes stopped after 30 minutes; lane 4, reaction without proteinase K but with PMSF after 30 minutes; lane 5, reaction with PMSF-inactivated proteinase K added at zero time; lane 6, reaction with PMSF added to membranes first, followed immediately by proteinase K addition at zero time; lanes 7, 8, 9, and 10 are reactions stopped with PMSF after 5, 10, 20, and 30 minutes, respectively; lane 11, reaction unstopped by omission of PMSF. See Materials and Methods for details of protocols.

not cut by trypsin especially when there are numerous basic amino acid residues present in the hydrophilic segment of the β subunit, as predicted by its hydropathy plot. Perhaps, these residues are not exposed due to the folding of hydrophilic β segment. Concomitant with the gradual disappearance of the β band in the proteinase K experiment is the accumulation of a 22 kD fragment in the membrane fraction (Lanes 7-10, Figure 19M). Exhaustive digestion (Lane 11, Figure 19M) left a 20 kD band in the membrane that appears to be protected from proteinase K cleavage. The supposition is that the 22 and 20 kD fragments contain the membrane imbedded parts of the β subunit. This could not be proven as the isolated fragments did not give amino-terminal sequences on analysis (Table III). They did not react with the anti-α,β polyclonals (or the anti-α group) in a Western blot (data not shown).

The most intensely staining bands released into solution were ones of 28 kD, 18 kD, and less than 17 kD molecular size, all of which were observable at the 5 minute time point (Lane 7, Figure 19S). These fragments disappear on further incubation (Lanes 7-10, Figures 19S). None of the fragments reacted with the anti-transhydrogenase polyclonal antibodies (data not shown). These soluble fragments were not stable during prolonged storage except for the less than 17 kD fragment(s) (data not shown). An amino-terminal sequence could not be determined for the 17 kD fragment (Table III). Thus, its identity is unknown.

A similar proteolytic experiment using ten-fold more proteinase K on RSO membranes resulted in no cleavage of the subunits (data not shown), as mentioned previously. This suggests that in the right-side-out orientation, most if not all of both subunits is either imbedded in the membrane bilayer or facing the cytoplasm.

E. Isolation and Identification of Polypeptide Fragments Proteolytically Released from Membrane-Bound Transhydrogenase

1. Amino-Terminal Sequencing of Proteolytically Released Fragments

The 41 and 29 kD fragments that are released into solution from tryptic digestions of transhydrogenase-enriched ISO membranes were initially isolated via diffusive elution into solution from excised SDS-Page gel pieces containing the bands. Figure 20 shows the SDS-Page gel of the final isolates which were used for amino-terminal sequencing (Table III). The initial four positions of both fragments could not be identified with any kind of certainty due to relatively large amounts of glycine which came from the SDS-Page buffer system and was not sufficiently removed from the eluates by dialysis or by Centricon-10 microconcentration and buffer exchange prior to analysis. From the fifth position onwards, a sequence was readable for both polypeptides. The sequences of both, barring the first four residues, lined up with that of the intact amino-terminus of the α subunit. Therefore, these fragments were derived from cuts towards the carboxy-terminal ends of the α subunit.

The interference in the analysis by glycine carried over during the isolation of the fragments was overcome by an isolation method which used electroblotting of SDS-Page bands onto PVDF membranes, which are then sent for sequencing. The amino-terminal sequences at the beginning of the 41 kD and 29 kD fragments isolated in this manner (Figure 21) were then determinable (Table III) and confirmed that both fragments have the same intact amino-terminus of the α subunit.

In addition, the 39, 27, 16, 12, and 11 kD fragments observed under particular tryptic digestion conditions were isolated in the same manner (Figure 21) and their amino-terminal sequences were determined (Table III). All the fragments are derived from α subunit cleavage. The 39 and 27 kD fragments appear to derive from a cut

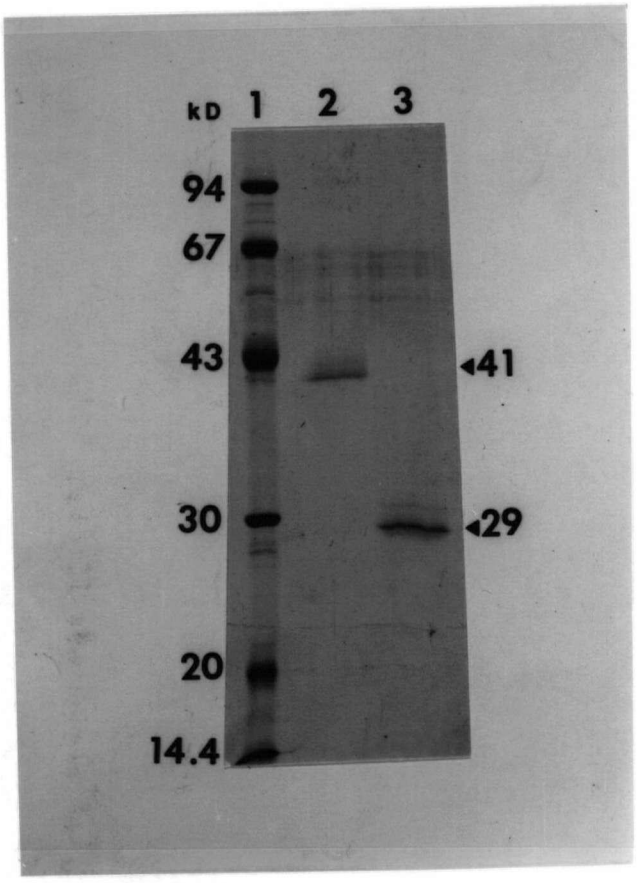

Figure 20: Isolation of the 41 and 29 kD Tryptically Released Fragments Via Diffusive Elution from Excised SDS-Page Gel Pieces

The 41 and 29 kD fragments that are released into solution from tryptic digestions of transhydrogenase-enriched ISO membranes were isolated via diffusive elution from excised SDS-Page gel pieces containing the bands, into solution. Low molecular weight gel contaminants in the eluates were removed from the polypeptide fragments by dialysis or Centricon-10 microconcentration and buffer exchange prior to N-terminal sequence analysis. Lane 1, molecular weight standards; lane 2, "cleansed" eluate containing the 41 kD fragment; lane 3, "cleansed" eluate containing the 29 kD fragment. For details of protocols, see Materials and Methods.

Table III: N-Terminal Sequences of Proteinase K or Tryptically Released Fragments

Molecular Weight (kD)	Method of Isolation	(a) Amino Acid Sequence and (b) Corresponding Transhydrogenase α Subunit Sequence
Trypsin:		
41	D	(a) ?----?----E?---?----I----P----R----E----R----
	E	(a) M----R----I-----G----I----P----R---
		(b) M_1--R_2--I_3----G_4---I_5--P_6---R_7--E_8---R_9--
39	E	(a) V----A----A----T----P----K----T----V----E----Q----
		(b) V_{16}-A_{17}-A_{18}-T_{19}-P_{20}-K_{21}-T_{22}-V_{23}-E_{24}-Q_{25}-
29	D	(a) ?----?-----I-----?----I----P----R----?-----R---L-----
		L----N----E----?----R----V----A----
	E	(a) M----R----I----G----I----P----
		(b) M_1--R_2---I_3---G_4---I_5--P_6---R_7--E_8---R_9--L_{10}--
		T_{11}-N_{12}-E_{13}-T_{14}-R_{15}-V_{16}-A_{17}--
27	E	(a) V----A----A----T----P----K----T----V----E----Q----
		(b) V_{16}-A_{17}-A_{18}-T_{19}-P_{20}-K_{21}-T_{22}-V_{23}-E_{24}-Q_{25}-
16	E	(a) V------M-----S------D-----A------F-----I------K-----A------
		(b) V_{228}-M_{229}-S_{230}-D_{231}-A_{232}-F_{233}-I_{234}-K_{235}-A_{236}-
12*	E	(a) L------I-----T------?-----E------M-----V------D-----S------
		(b) L_{265}-I_{266}-T_{267}-R_{268}-E_{269}-M_{270}-V_{271}-D_{272}-S_{273}-

Molecular Weight (kD)	Method of Isolation	(a) Amino Acid Sequence and (b) Corresponding Transhydrogenase α Subunit Sequence
Trypsin:		
12**	E	(a) E------M-----V------D-----?------M------K-----A------G---- (b) E_{269}-M_{270}-V_{271}-D_{272}-S_{273}-M_{274}-K_{275}-A_{276}-G_{277}-
12***	E	(a) A------G-----S------V-----I------V-----D------L-----A------ (b) A_{276}-G_{277}-S_{278}-V_{279}-I_{280}-V_{281}-D_{282}-L_{283}-A_{284}-
11*	E	(a) V----A----?-----T----P----?----T----V----E----Q---- (b) V_{16}-A_{17}-A_{18}-T_{19}-P_{20}-K_{21}-T_{22}-V_{23}-E_{24}-Q_{25}-
11**	E	(a) A------G-----S------?------I-----V-----D------?-----A------ (b) A_{276}-G_{277}-S_{278}-V_{279}-I_{280}-V_{281}-D_{282}-L_{283}-A_{284}-
Proteinase K:		
20 or 22 (memb frag.)	E	did not sequence
less than 17 (nonmemb fragment)	E	did not sequence

Polypeptide fragments were sequenced on a gas-phase sequenator at the University of Victoria. All tryptic fragments sequenced had been released into solution and were not associated with the membrane fraction. D denotes fragments isolated by diffusive elution from excised gel pieces obtained from SDS-Page gels as shown in Figure 20. E denotes fragments isolated by electroelution of SDS-Page bands (Figure 21) onto PVDF membranes and excised for sequencing. Proteinase K fragments were isolated by method E from gels of samples obtained after proteolytic treatment (Figure 19M, lanes 10, 11 and Figure 19S, lane 7). The one letter amino acid code was used in the representation of sequences. ? indicates where an amino acid assignment could not be made or is questionable. The *, **, and *** denotations indicate fragments of same approximate size but different identities. All relevant procedural details are described in Materials and Methods.

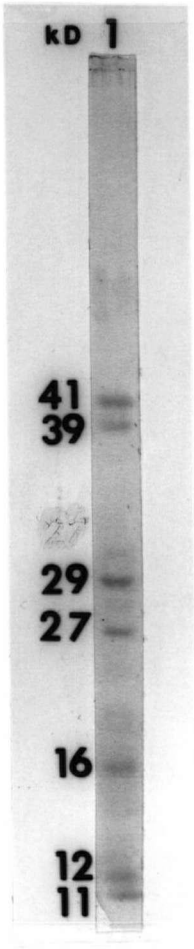

Fig. 21: Isolation of Tryptically Released Fragments Via Electroblotting of SDS-Page Bands onto PVDF Membranes and Subsequent Excision

DPPC-trypsin was used to treat E. coli JM83pDC21 ISO membrane vesicles at a ratio of 1 ug to 255 ug of membrane protein. SBTI was added after 10 minutes to stop the reaction. The polypeptide fragments that were released into solution were removed from the membranes by ultracentrifugation. These fragments were resolved from each other by 12% SDS-Page. The gel containing the fragments was blotted onto Immobilon PVDF transfer paper by electrophoretic elution. The PVDF paper was stained for protein by Coomassie Blue R/Ponceau S. Pieces of PVDF paper containing the individual bands were then excised and subject to N-terminal sequence analysis. Lane 1 is a lane from the electroblotted PVDF paper with the proteins stained prior to excision. For details of protocols, see Materials and Methods.

between arg_{15} and val_{16} of α at its amino-terminal end. These polypeptides may then represent cleavage products of the 41 and 29 kD fragments where the first 15 amino acids have been removed by a second tryptic cut at arg_{15}. The 16 KD fragment appears to arise from one cut at $lysine_{227}$ and another cut farther down the sequence. The 12 kD band actually consists of 3 similar sized polypeptides, each arising from a cut at lys_{264}, arg_{268}, or lys_{275} at their amino-terminal ends. The 11 kD band consists of 2 polypeptides, each resulting from a cut at arg_{15} or lys_{275} at their amino-terminal ends.

As mentioned previously, the proteinase K digested transhydrogenase fragments that could be isolated, did not sequence. The reason is unclear as enough protein was sent for sequencing.

2. Isolation and Characterization of the Tryptically Released Soluble 41 kD α Fragment

2.1 Sephadex-G75 Gel Filtration Chromatography

In an effort to get the relatively large amounts of polypeptide necessary to identify the carboxy-terminus of the tryptically cut fragments by the carboxypeptidase Y sequencing method, Sephadex-G75 gel filtration chromatography was performed on the soluble fraction of the trypsin digest of transhydrogenase-enriched ISO membranes. Sephadex G-75 was chosen because given the SDS-Page estimated molecular weights of the fragments, a column run under properly selected conditions using this filtration material should in theory provide some separation of the fragments and also give another estimate of their sizes.

An SDS-Page gel of the pertinent fractions indicated that the separation was unsuccessful as the 41 and 29 kD fragments were co-eluted (Figure 22). They eluted at the void volume for the column (data not shown) and are therefore outside the column's proper fractionation range, making it impossible to determine the molecular

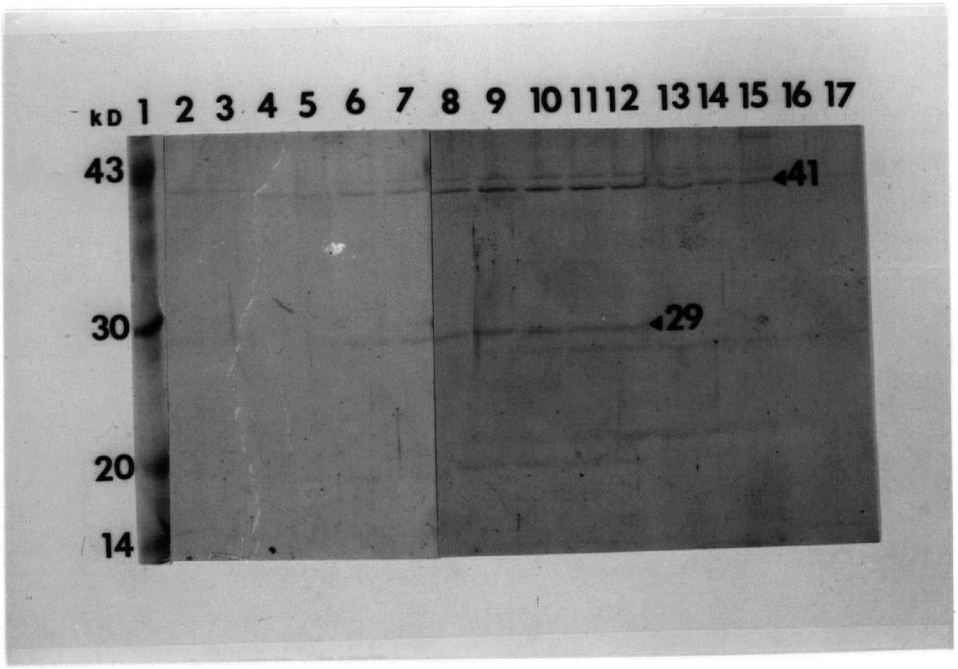

Fig. 22: Sephadex G-75 Gel Filtration Chromatography of Supernatants from Tryptic Digestion of ISO Cytoplasmic Membrane Vesicles

DPPC-trypsin was used to treat E. coli JM83pDC21 ISO membrane vesicles at a ratio of 1 ug to 123 ug of membrane protein. SBTI was added after 5 minutes to stop the reaction. The polypeptide fragments that were released into solution were removed from the membranes by ultracentrifugation. Sephadex G-75 gel filtration was carried out on the supernatant as described in Materials and Methods. 1.5 ml fractions were collected and aliquots from relevant fractions were subjected to 10% SDS-Page. Lane 1, molecular weight markers; lanes 2 to 17, fractions 26 to 41. For procedural details, see Materials and Methods.

weight of the eluted species. Nevertheless, the eluted species appears to be a much higher molecular weight species than either of the constituent 41 and 29 kD fragments that are estimated by subsequent SDS-Page separation. The gel filtration eluted material is probably an aggregate of fragments. This brings us back to the possibility of native α-α interactions occuring in the oligomeric configuration of the membrane-bound transhydrogenase (125). The other explanation for the soluble α-fragment aggregate may be the artefactual complexing of these fragments after cleavage and release into solution.

2.2 MonoQ Ion Exchange Fast Protein Liquid Chromatography

Another method for separating the tryptically cut α fragments was deemed necessary. Figure 23A shows the pertinent fractions of a separation using a MonoQ ion exchange FPLC column. The soluble fraction of a trypsin digest of transhydrogenase-enriched ISO membranes was loaded into the column and eluted with a NaCl gradient. The fragments eluted out together (Lane 4, Figure 23A) in a single sharp peak at a salt concentration of 0.35 M under the conditions of this run (Figure 23B). Thus, the chromatography was not a success. The soya bean trypsin inhibitor was separated from the fragments (Lane 5, Figure 23A).

The separation was repeated incorporating the nonionic detergent, dodecyl-β-D-maltoside. The addition of 1% dodecyl-β-D-maltoside to the soluble fraction of a trypsin digest of transhydrogenase-enriched ISO membranes, was used to hopefully disaggregate the tight aggregation of polypeptides. The fragments still eluted together (Lane 2, Figure 24A) as a sharp peak at a NaCl concentration of 0.035 M (Figure 24B). Again, the chromatography was unsuccessful.

2.3 Superose 12 Gel Filtration Fast Protein Liquid Chromatography

The use of 1% SDS to release the α fragments from each other and subsequent Superose 12 gel filtration FPLC finally effected separation of the 41 kD

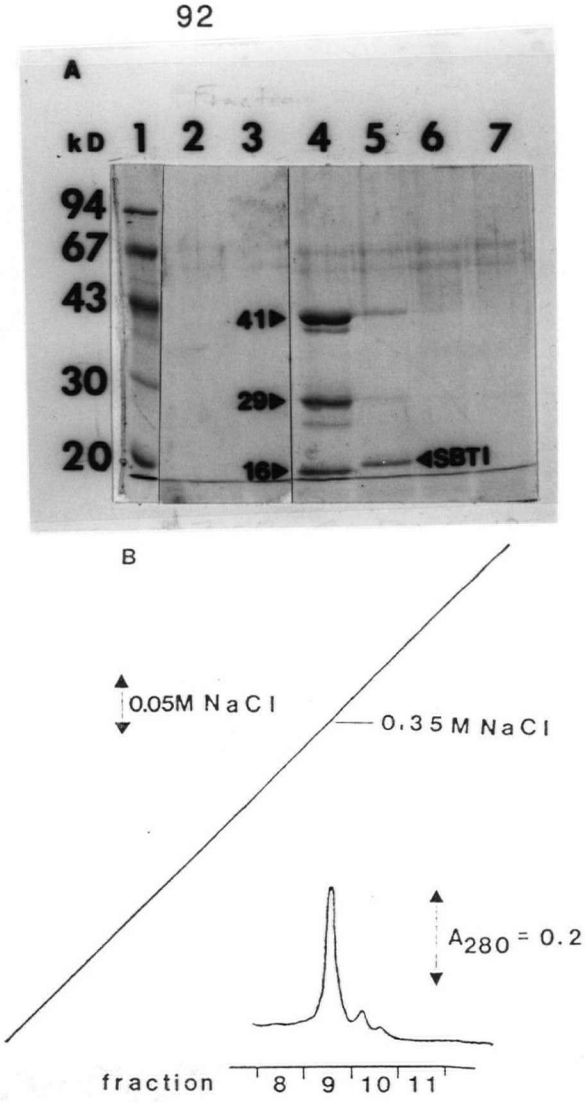

Fig. 23: MonoQ Ion Exchange FPLC Chromatography of Supernatants from Tryptic Digestion of ISO Cytoplasmic Membrane Vesicles

DPPC-trypsin was used to treat E. coli JM83pDC21 ISO membrane vesicles at a ratio of 1 ug to 107 ug of membrane protein. SBTI was added after 5 minutes to stop the reaction. The polypeptide fragments that were released into solution were removed from the membranes by ultracentrifugation. MonoQ ion exchange FPLC chromatography was carried out on the supernatant using a 0-1 M NaCl gradient as described in Materials and Methods. A_{280} was monitored and the elution profile is shown (B). 1 ml fractions were collected and aliquots from relevant fractions were subjected to 10% SDS-Page (A). Lane 1, molecular weight markers; lanes 2 to 7, fractions 7 to 12. For procedural details, see Materials and Methods.

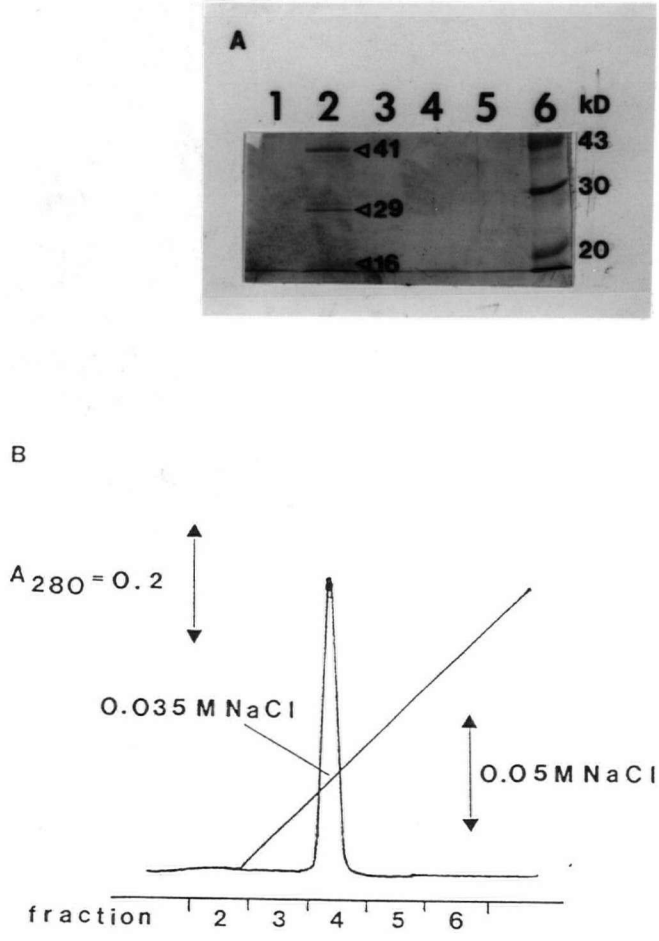

Fig. 24: MonoQ Ion Exchange FPLC Chromatography of Dodecyl-β-D-Maltoside Treated Supernatants from Tryptic Digestion of ISO Cytoplasmic Membrane Vesicles

The fraction from a previous MonoQ ion exchange FPLC run containing the polypeptide fragments that were tryptically released into solution (Figure 23B, lane 4) was solubilized with 1% dodecyl-β-D-maltoside. MonoQ ion exchange FPLC chromatography was carried out on this material using a 0-0.5 M NaCl gradient as described in Materials and Methods. A_{280} was monitored and the elution profile is shown (B). 1 ml fractions were collected and aliquots from relevant fractions were subjected to 10% SDS-Page (A). Lane 6, molecular weight markers; lanes 1 to 5, fractions 3 to 7. For procedural details, see Materials and Methods.

fragment from the other fragments (Figure 25A). It was discovered that upon storage, the 29 kD and lower molecular fragments broke down (Figure 25A and data not shown). The 41 kD polypeptide was more stable and was not cleaved during storage. SDS was removed from the isolated 41 kD fragment using AG11A8 ion retardation chromatography. Lanes 6 and 7 of the SDS-Page gel of collected fractions (Figure 26) both show a single 41 kD band.

2.4 NAD-Affinity Chromatography

The 41 kD α fragment freed of SDS was bound by an NAD-affinity column. A small amount washed through after loading as indicated by a faint band in the washthrough fraction (Lane 3, Figure 27). NADH was used to elute the 41 kD fragment bound by the column (Lanes 4,5). This suggests that SDS has been been removed, allowing some fragments to refold to a state where it will bind NAD(H). More importantly, the NAD(H)-binding capability indicates a possible active site on this α fragment.

Note the slight increase in molecular weight after the fragments have passed through the affinity column (Figure 27). Perhaps, the fragment has been modified or altered during the procedure, changing its migration characteristics on SDS-Page.

2.5 Carboxy-Terminal Sequencing of 41 kD Fragment

The carboxy-terminal sequencing results of the isolated 41 kD fragment (Figure 28) indicate two possible cut sites giving rise to the carboxy-terminal end of the 41 kD polypeptide. One is between arg_{361}-ala_{362} and the other is between arg_{355}-gly_{356} of the α sequence. These two possible cut sites are only separated by six amino acids. The neighbouring sequences going upstream from these cut sites are by coincidence very similar. In fact the first three amino acids upstream from the two cut sites are identical. The pertinent sequence in this region is as follows :

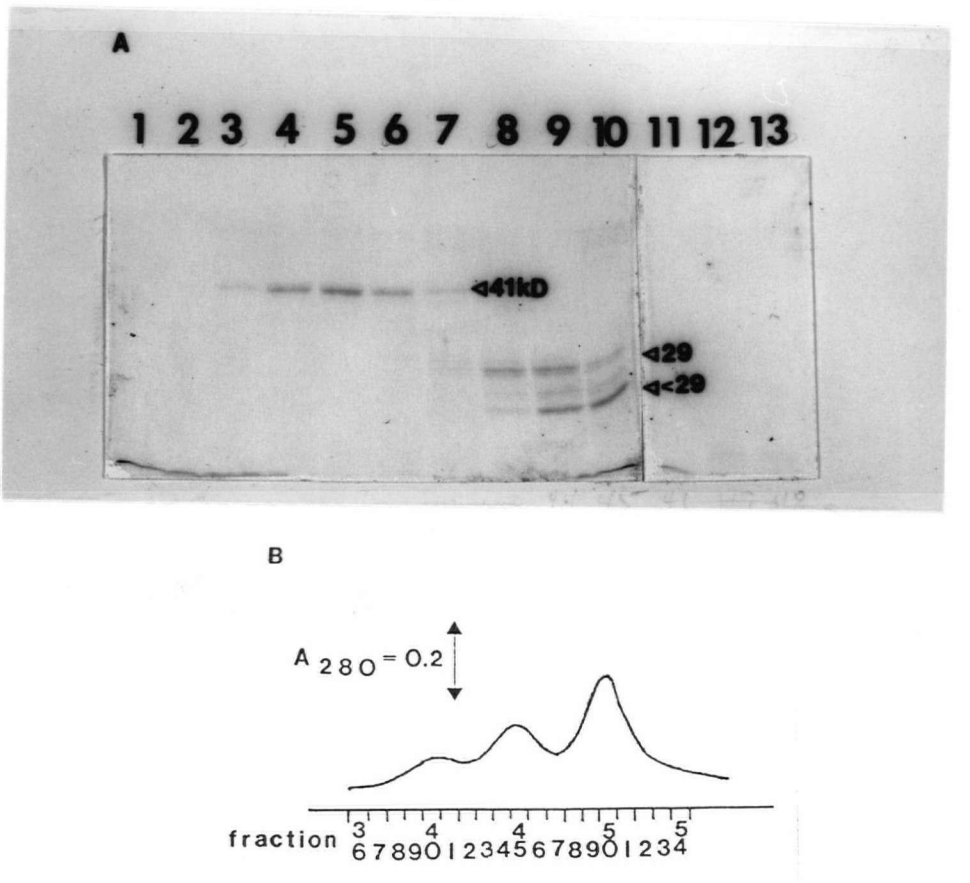

Fig. 25: Superose 12 Gel Filtration FPLC of Supernatants from Tryptic Digestion of ISO Cytoplasmic Membrane Vesicles

DPPC-trypsin was used to treat E. coli JM83pDC21 ISO membrane vesicles at a ratio of 1 ug to 650 ug of membrane protein. SBTI was added after 10 minutes to stop the reaction. The polypeptide fragments that were released into solution were removed from the membranes by ultracentrifugation. The supernatant was solubilized with 1% SDS. Superose 12 gel filtration FPLC chromatography was carried out on this material as described in Materials and Methods. A_{280} was monitored and the elution profile is shown (B). 0.5 ml fractions were collected and aliquots from relevant fractions were subjected to 12% SDS-Page (A). Lanes 1 to 13, fractions 36 to 48. Note the large, third peak of the elution profile (B) is not indicated in the gel (A) and represent low molecular weight tryptic fragments or breakdown products upon storage. The low molecular weight material ran off this particular gel (A) and could not be shown. For details of procedures, see Materials and Methods.

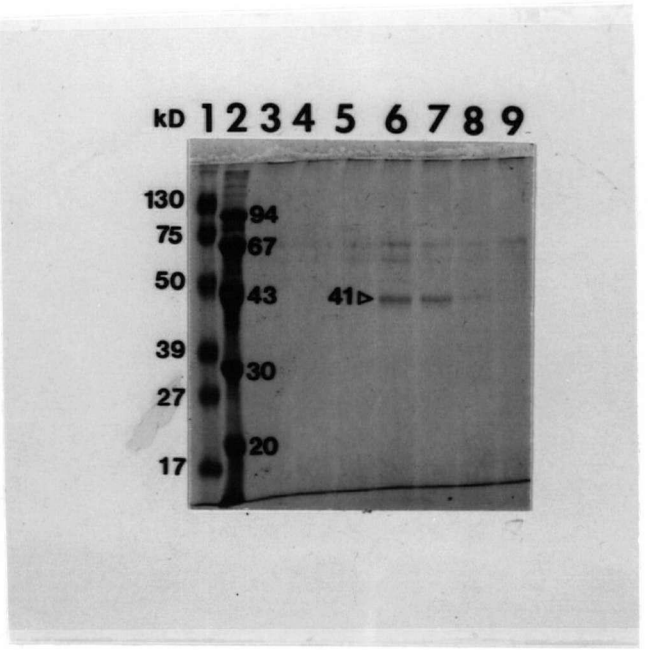

Fig. 26: SDS-Page of the 41 kD Fragment Isolated by Superose 12 Gel Filtration FPLC after Pooling and SDS-Removal

After Superose 12 FPLC, fractions containing the isolated 41 kD fragment were pooled. The pooled sample contained SDS. The SDS was removed by chromatographing the isolate through an AG11A8 ion retardation column as described in Materials and Methods. 0.5 ml fractions were collected and aliquots from relevant fractions were subjected to 12% SDS-Page. Lanes 1 and 2, molecular weight markers; lanes 3 to 9, fractions 1 to 7. For procedural details, see Materials and Methods.

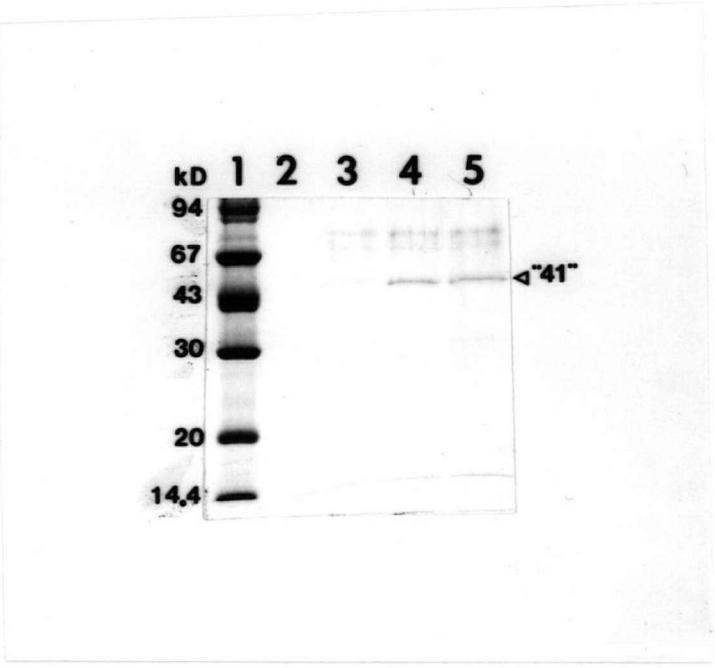

Fig. 27: NAD-Affinity Chromatography of the 41 kD Fragment Isolated by Superose 12 FPLC after SDS-Removal

The Superose 12 FPLC isolated 41 kD fragment was freed of SDS by chromatographing the isolate through an AG11A8 ion retardation column. The SDS-stripped material was subjected to chromatography via binding to an NAD-affinity column and subsequent NADH elution. Fractions were collected in batches and aliquots from relevant fractions were subjected to 12% SDS-Page. Lanes 1 and 2, molecular weight markers; lane 2, washthrough fraction collected prior to sample application; lane 3, material washed through with four bed volumes of buffer after sample application; lane 4, material eluted after first two-bed volumes of 10 mM NADH; lane 5, material eluted after the second two-bed volumes of 10 mM NADH. Note the 41 kD fragment runs a little higher on this gel than it should and is denoted "41". Procedural details are in Materials and Methods.

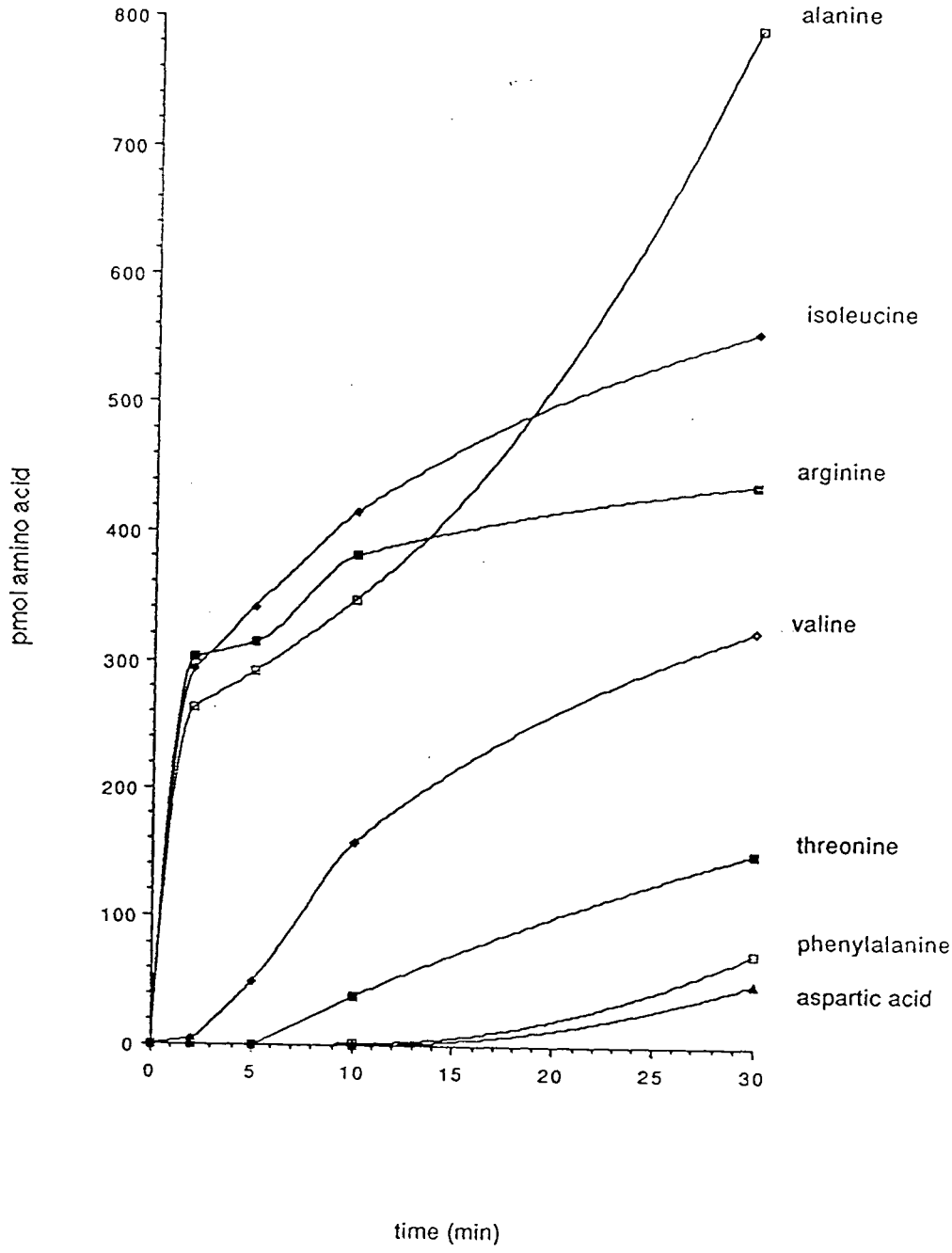

Fig. 28: Carboxy-Terminal Sequencing of the 41 kD Fragment Isolated from Superose 12 FPLC

The entire methodology for carboxy-terminal sequencing of the Superose 12 FPLC isolated 41 kD fragment is outlined in Materials and Methods. The plot indicates the quantitative amounts of each of the amino acids released by carboxypeptidase Y action on the 41 kD fragment's C-terminus as a function of time.

NH_2-----phe_{349}---asp_{350}---asp_{351}---val_{352}---val_{353}---ile_{354}---arg_{355}---gly_{356}---
val_{357}---thr_{358}---val_{359}---ile_{360}---arg_{361}---ala_{362}-----COOH

The kinetic plot of amino acids released from the 41 kD polypeptide as a function of incubation time with carboxypeptidase Y supports both cut sites being present in the 41 kD polypeptide preparation. That would mean the possibility of two polypeptide fragments both of extremely similar but slightly different molecular weights. To determine if this might be the case, the 41 kD fragment preparation was isoelectric focused on an IEF gel (Figure 29). Two bands of very close but still slightly different pIs were observed (Lane 2, Figure 29). The difference in pI would result from the larger polypeptide containing one more arginine residue. Both polypeptides band in the region of the IEF gel having a pH of 4.4. Therefore, one would assume that their pIs are close to this value. An aliquot of the 41 kD fragment preparation was run on a longer (16 cm) SDS-Page gel. This revealed two distinct bands of very close molecular weights (data not shown). Thus, the 41 kD fragment preparation consists of two polypeptides, one of which is shorter than the other by six amino acids on its carboxy-end. The tryptic cutting at sites six amino acids apart in the primary protein structure may mean general exposure of this region of the α subunit to the external medium. Knowing the identity of the two ends of the polypeptide, it was possible to calculate a theoretical molecular weight for both 41 kD fragments, given the gene derived amino acid sequence of the α subunit determined by Clarke (81). They are calculated to be 38.9 and 38.3 kD which compares favourably with the SDS-Page estimated size.

One anomaly in the carboxy-terminal sequencing result is the large amount of alanine that is liberated by carboxypeptidase Y digestion of the 41 kD fragment (Figure 28). There does not appear to be any alanines immediately upstream of either of the two arginines that are left at the carboxy-end of the 41 kD polypeptides after tryptic cleavage. One possible explanation is that there may be low amounts of

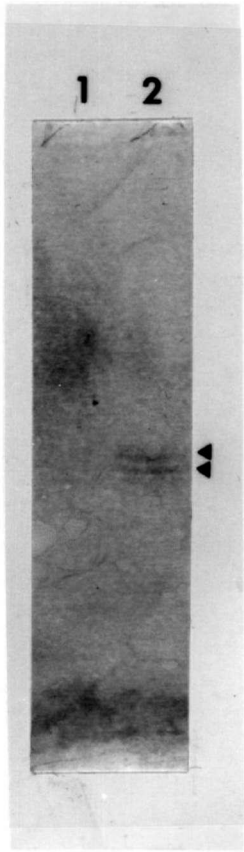

Fig. 29: Isoelectric Focusing Gel Electrophoresis of the Superose 12 FPLC Isolated "41 kD Fragment" Material

The "41 kD fragment" material isolated from Superose 12 FPLC was subjected to isoelectric focusing gel electrophoresis as described in Materials and Methods. Lane 1 is a blank lane of the IEF gel. In lane 2, two protein bands are separated from the "41 kD fragment" sample by isoelectric focusing, as indicated by the arrowheads to the right of these bands.

an ~41 kD α fragment that was cut at lys_{389}. Four out of nine amino acid residues upstream of this site are alanine. This high concentration of alanines may account for the anomaly. This supposition was not tested.

IV DISCUSSION

The transhydrogenase gene has been cloned, expressed and sequenced for the E. coli enzyme (81-82). The molecular weights for the α and β subunits of the enzyme calculated from the two open reading frames of the gene agree well with the 52 and 48 kD molecular weights observed on SDS-Page gels of the gene expressed products in the bacterial cytoplasmic membrane. The amino acid sequences of each subunit were determined from the open reading frames of the gene (Figure 1) (81). Hydropathy plots based on these sequences gave a prediction of possible membrane-traversing hydrophobic segments (Figure 2) (81).

The hydropathy plot for the α subunit indicates that the 100 or so amino acids extending from the C-terminal end of this subunit are organized into four possible transmembranous domains. Because of the large number of hydrophobic residues in this region, it is highly likely that this region is a source of membrane-anchoring for the polypeptide. The remaining 80% or so of the α subunit at the N-terminal end contains many charged and hydrophilic residues although another short potentially membrane-spanning segment is predicted within this long N-terminal tail. From this, three major alternatives can be predicted for the configuration of the α subunit in the membrane. The simplest one is that the subunit is anchored at the C-terminal end by a number of membrane-spanning helices, while the N-terminal region is protruding into solution. Alternatively, the N-terminal region may loop back across the membrane with a smaller portion of the N-terminal end protruding into solution on the other side of the membrane. In other words, there may be a large extramembranous loop and a hydrophilic tail on opposite sides of the membrane connected by the centrally located hydrophobic membrane-spanning sequence. The third possibility is that the large hydrophobic C-terminal tail is not membrane imbedded. Instead, the short centrally-located hydrophobic sequence anchors the subunit to the membrane with N- and C-termini protruding from opposite sides of the membrane.

The hydropathy plot for the β subunit indicates that the first 200 or so amino acids extending from the N-terminal end of this subunit are organized into seven possible transmembranous domains separated by short polar regions containing some charged residues. Since there are large numbers of hydrophobic residues in this region, it is highly likely that this section is a source of membrane-anchoring for the polypeptide. The remaining portion of the β subunit at the C-terminal end contains many charged and hydrophilic residues suggesting that this end is sticking out into solution.

To test whether the predictions made by the hydropathy plots are true or not, the work detailed in this thesis was undertaken. Although this study is far from complete in determining the exact conformation and topography of the transhydrogenase in the membrane or even in verifying all aspects of the predictions made by the hydropathy plots, it did produce results which are consistent with some of the predictions and also results which cannot be predicted from the hydropathy plots alone. An operating model for the enzyme's topography and orientation in the membrane which can be tested and elaborated on with future experimentation, is shown in Figure 30. It is based on the results obtained from these studies and on suppositions made from the hydropathy plot in details where the present results were inadequate.

Partial tryptic digestion of the α subunit from the membrane-bound transhydrogenase released initially, a fragment of 41 kD (as determined by SDS-Page) into solution. This was only observed in the ISO orientation (Figures 12, 13, 17) and not in the RSO case (Figure 18). Because of the impermeability of the trypsin molecule across biological membranes, this suggests that the 41 kD sequence is protruding into the aqueous phase on the cytoplasmic side. That the 41 kD fragment was from the α subunit was verified by its reaction with antibodies reacting to this subunit (Figure 14) and by the sequencing of both of its termini (Figure 28, Table III). As the model (Figure 30) indicates, the 41 kD fragment(s) was determined to have an

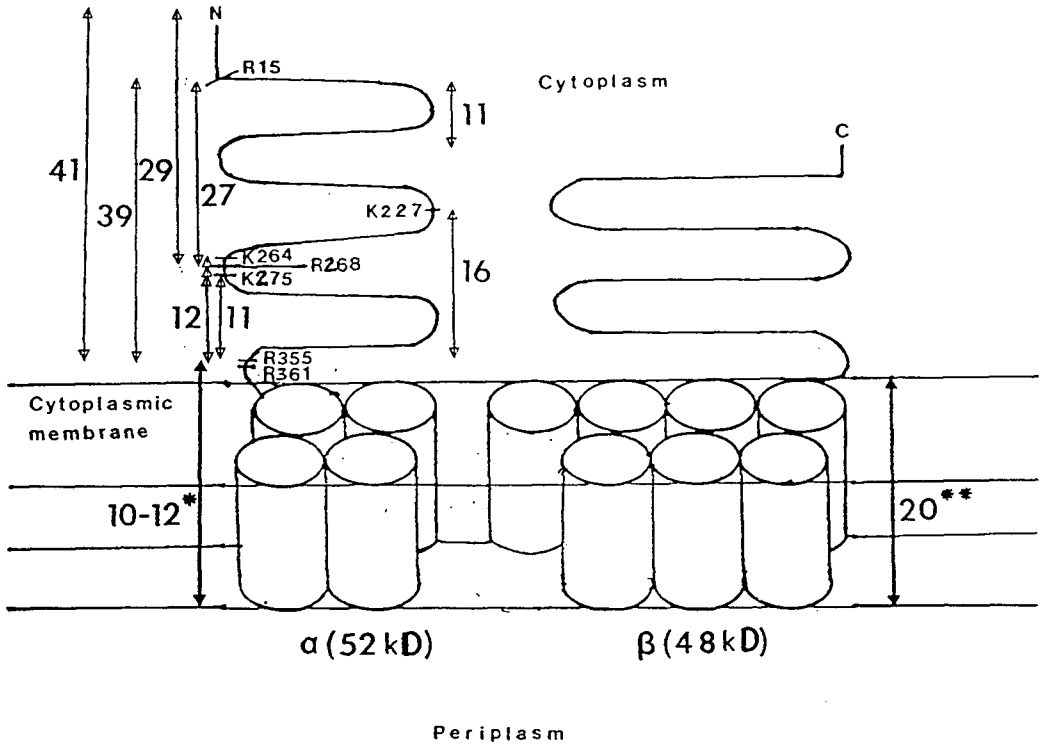

Fig. 30: A Topographical Model of the Transhydrogenase in the E. coli Membrane

The possible topology of the transhydrogenase in the membrane of E. coli is shown. Only one subunit of the α and β type is shown in this diagram, although the native membrane-bound enzyme has an $\alpha_2\beta_2$ structure (125). The trypsin cleavage sites are indicated. K and R denote lysines and arginines, respectively. The numbers that follow their one letter codes represent their position in the primary structure of the subunit. Other than the 41 kD fragment, the C-terminus of fragments may not be exactly where indicated. The prediction of C-terminal sites is based upon the molecular weights (given in kD) and the "fitting together" of fragments. The location and orientation of extracellular domains are based on proteolytic experiments on ISO and RSO transhydrogenase enriched membrane vesicles. * denotes a 10-12 kD membrane-imbedded segment as predicted by Clarke's hydropathy plot for the α subunit (81), but which could not be detected in this thesis. This segment is thought to have 4 transmembranous helices, depicted here as cylinders. ** denotes a membrane-imbedded segment in the β subunit based on Clarke's hydropathy plot predictions (81). The predicted size of such a segment is consistent with the results of proteinase K experiments, although verification could not be obtained due to N-terminal sequencing problems. The cylinders in this region also represent predicted transmembranous helices. N and C denote amino and carboxy termini, respectively.

intact α N-terminus and alternative C-termini corresponding to tryptic cuts after arg_{355} or arg_{361}. The "41 kD fragment" isolated from Superose 12 gel filtration chromatography (Figures 25, 26) was later confirmed to consist of two fragments of very close molecular weight (Figure 29 and data not shown), varying presumably at their C-termini (Results Subsection 2.5). The identity of the 41 kD fragments is consistent with a model for the α subunit topography where there is no intervening transmembranous segment in the hydrophilic N-terminal portion that extends to arg_{361}. Therefore, the possible membrane-spanning segment predicted by hydropathy (Segment I in Figure 2) in this region does not exist. Interestingly enough, this hydrophobic segment does contain within it, an enclave or short sequence of twenty amino acids which shares homology with the pyridine nucleotide binding folds of lipoyl dehydrogenase, glutathione and mercuric reductases (123). The 41 kD fragment(s) was shown to bind to an NAD-affinity column (Figure 27) indicating the location of a possible NAD(H)- binding site in this sequence. This is consistent with the cytoplasmic orientation of the enzymatic activity as well as with the homology observation mentioned above, although verification would have to await nucleotide-labelling and peptide sequencing experiments.

One should note the close proximity of the arg_{361} residue of the 41 kD fragment to where the hydrophilic portion of α is predicted to end and where the first of the four hydrophobic C-terminal segments begins around the 400th amino acid position (Segments II-V of Figure 2). If the hydropathy predictions are correct, a fragment of approximately 12 kD or smaller of the membrane portion is expected to remain after a cut at arg_{355} or arg_{361}. A positive detection of such a fragment was not obtained even after using different staining methods with SDS-Page gels of the membrane portions remaining after tryptic treatment (data not shown). Perhaps the hydrophobicity of the fragment may play a part in its nondetection. The use of polyclonal antibodies against the α subunit in an immunoblot of the membrane portion was also unable to detect membrane fragments from this subunit (Figure 14).

Again, the anti-α antibodies present may not recognize epitopes in the hydrophobic domain of the subunit even if it is present. The validity of the hydropathy plot predictions in the membrane-spanning region still remains to be verified or disputed by further experimentation.

One interesting result that has been obtained is that the α subunit is not cut with either trypsin (Figure 18) or proteinase K (data not shown) in the RSO membrane orientation. This is fully consistent with the hydropathy predictions and with the tryptic results using the ISO membrane vesicles. These suggest that the membrane-spanning domain(s) start right from the C-terminus until where the hydrophilic N-terminal tail protrudes into the cytoplasmic side. Therefore, theoretically, proteases should have no accessibility to the α subunit on the periplasmic side or in the RSO membrane orientation, other than at the short connecting loops. The hydropathy plot of the C-terminal hydrophobic region suggests four possible transmembranous segments that follow each other extremely closely in the primary sequence (Figure 2). This suggests that the very short connecting loops may not be accessible to proteases.

Although the interaction of the subunits in the native $\alpha_2\beta_2$ tetrameric structure (125) is not shown in the model which displays only one monomer with the subunits essentially separate from one another (Figure 30), there is very likely some interaction between the subunits in the native structure. In fact, suggestions of an α–α interaction was evident in the results of a pair of experiments in this thesis. It was observed that after the initial release of the 41 kD fragment from the α subunit, it was first associated with the membrane fraction before it appeared in solution (Figure 13). One possible explanation of this phenomenon is that there is an α–α interaction and a single cut of one subunit of the α–α dimer does not release the 41 kD polypeptide from the membrane until the second α subunit is cut. Another observation consistent with this idea, is that α subunit fragments of 41 and 29 kD that are tryptically released into solution, coelute from a Sephadex G-75 gel filtration column, presumarably as a

complex (Figure 22). The complexing however could be artefactual and occur after the polypeptides are released from the membrane. The indications here of an $\alpha-\alpha$ interaction is nowhere near conclusive but it does raise questions which need to be answered by further experimentation.

Trypsin digestion of ISO membrane vesicles may give rise to fragments of 39, 29, 27, 16, 12, and 11 kD fragments in addition to the 41 kD polypeptide (Figures 12-14, 17, 21). They all appear to arise from further cleavages of the 41 kD fragments. These fragments were sequenced at their N-termini (Table III) but not sequenced at their C-termini. The relationship between these fragments is indicated in the model and is based on their sizes and N-terminal sequencing results (Figure 30).

The 29 kD fragment arises from a second tryptic cut at the C-terminal end of the 41 kD polypeptide as its N-terminus is identical to that of the intact α subunit (Table III). Although the C-terminal end was not directly determined, the amino terminus of three different 12 kD fragments arising from cuts after lys_{264}, arg_{268} and lys_{275} at their N-termini (Table III) suggest these basic residues might make up the C-termini of the 29 kD fragment(s). Indeed, a long SDS-Page gel revealed that the 29 kD "fragment " was actually composed of 3 fragments of very close molecular weights (data not shown). Presumably, they give a single N-terminal sequence on analysis of the mixture and differ only at their C-termini. Based on the molecular weight of the 12 kD fragments, their C-termini may be one of the two arginines that are at the C-terminus of the 41 kD fragment(s). In addition, a 11 kD polypeptide has a N-terminus that corresponds to a cut after lys_{275} (Table III). Because of the 1 kD shortening of a 12 kD fragment having an identical N-terminus, it is speculated that this results from a cut at arg_{355} rather than at arg_{361}, although this was not confirmed.

The 39 and 27 kD fragments appear after tryptic digestion of certain ISO membrane vesicle preparations (Figure 17, 21), but not in others (Figures 12-14), even though there were no apparent differences in conditions during the isolations. In the 39 kD fragment, the first fifteen amino acids have been removed by a tryptic cut

after arg_{15} (Table III). The inconsistency of this arg_{15}-val_{16} cut site being available for tryptic digestion experiments of ISO membrane preparations made under apparently identical conditions, may suggest a flexibility in the conformation at the N-terminus of the α subunit in this region. This flexibility may respond to minute differences in the membrane preparation procedure or to conditions that occur without the experimenter's awareness. The 39 kD fragment may give rise to cleavage products of 11 and 16 kD. The 11 kD polypeptide has an N-terminus identical to the 39 kD fragment, while the 16 kD polypeptide has an N-terminus resulting from a cleavage after lys_{227} (Table III).

Chymotrypsin digestion of ISO membrane vesicles also show the appearance of 41 and 29 kD fragments in solution that occurs concomitantly with the digestion of the α subunit (Figure 15). This study was carried no further even though there is the interesting possibility of chymotryptic and tryptic cut sites being located close together. The exact sites of chymotryptic cleavage has not been determined in this thesis. This must be performed before any conclusion can be made of a general exposure to the external medium of short sequences of the α subunit which may contain vicinal basic and aromatic residues for tryptic and chymotryptic cleavages, respectively.

Interestingly, the β subunit was not affected from tryptic digestion of ISO membrane vesicles (Figures 12-14, 17), suggesting that any large hydrophilic portion which may exist, is protruding from the other side of the membrane, namely the periplasmic side. However, this premature suspicion was put to rest when the nonspecific protease, proteinase K, was found to digest the β subunit in ISO membrane vesicles (Figure 19). The α subunit still appeared to be more sensitive to proteinase K as indicated by its earlier disappearance. The reason why the β subunit is resistant to tryptic attack is unclear since the predicted hydrophilic portion contains many basic residues. Perhaps, the extramembranous portion of the subunit is folded

in such a way that no basic residues are accessible for tryptic cleavage, although the nature of this folding is difficult to envision.

Unlike the digestion of the α subunit by trypsin where no membrane fragments could be detected, the disappearance of the β subunit while under proteinase K attack occurs concomitantly with the appearance initially of a 22 kD membrane fragment (Figure 19). Further digestion gave rise to a 20 kD membrane fragment whose molecular weight would fit in well with that of the hydrophobic span of the β subunit that extends approximately 200 amino acid residues from its N-terminal and is predicted by the hydropathy plot to contain seven possible membrane-crossing domains (Figure 2). These domains lie very close together in the primary structure and any connecting loops between them that might be exposed for proteolytic attack would be very short. This fact may account for why proteinase K could not degrade the 20 kD fragment further. Alternatively, there might be no connecting loops if a large portion of the 20 kD region that did not cross the membrane was sticking out the other side. This alternative is not viable as treatment of the RSO oriented enzyme by either trypsin (Figure 18) or proteinase K (data not shown) resulted in no observable digestion of the β subunit (or of the α subunit, as explained previously). Unfortunately, neither the 22 nor 20 kD membrane fragments could be sequenced at their N-termini or would react with the anti-transhydrogenase polyclonal antibodies (data not shown). It is tentatively assumed that the 20 kD polypeptide represents the hydrophobic N-terminal end of the β subunit with the rest of the hydrophilic C-terminal tail protruding into the cytoplasm (Figure 30).

Two other major results that need to be addressed by further investigations is the negative effect of the detergents, Triton X-100 and sodium cholate, on the transhydrogenase activity (Table II) while apparently not affecting the membrane-bound enzyme's general conformation, as detected by the similarity of the trypsin digestion patterns of native and detergent-cleansed ISO membrane vesicles (Figure 16). Also, another point for consideration is the observation that membrane-bound

enzymes unliganded or liganded with any of its natural substrates showed identical digestion patterns after partial tryptic treatment of ISO membrane vesicles (Figure 17). This suggests a similarity in the general conformation of the enzyme whether liganded or not which is in direct contrast with the results of other workers (63, 79, 88, 107-108, 111-112, 124). Possible explanations and reasons for the substrate effects on enzyme conformation as well as for the aforementioned detergent effects on enzyme activity and conformation, were put forth in the Results section. These hypotheses must be subjected to scientific tests in order to resolve the conundrums.

V. REFERENCES

1. Colowick, S. P., Kaplan, N. O., Neufield, E. F., and Ciotti, M. M. (1952), *J. Biol. Chem.* 195, 95-105

2. Kaplan, N. O., Colowick, S. P., Neufield, E. F. (1953), *J. Biol .Chem.* 205, 1-15

3. Kaplan, N. O., Swartz, M. N., Frech, M. E. and Ciotti, M. M. (1956), *Proc. Natl. Acad. Sci. U.S.A.* 42, 481-487

4. Humphrey, G. F. (1957), *Biochem. J.* 65, 546-550

5. Devlin, T. M. (1958), *J. Biol. Chem.* 234, 952-966

6. Kielly, W. W. and Bronk, J. R. (1958), *J. Biol. Chem.* 230, 521-533

7. McMurray, W. C., Maley, G. F. and Lardy, M. A. (1958), *J. Biol. Chem.* 230, 219-229

8. Fisher, R. R. and Earle, S. R. (1982), in *The Pyridine Nucleotide Coenzymes* (Everse, J., Anderson, B. and You, K.-S., eds.) pp. 279-324, Academic Press, New York

9. Rydstrom, J. (1977), *Biochim. Biophys. Acta* 463, 155-184

10. Rydstrom, J., Hoek J. B., and Ernster, L. (1976), in *The Enzymes* (P.D. Boyer, ed.) vol. 13, pp. 51-88, Academic Press, New York

11. Kyte, J. and Doolittle, R. F. (1978), *J. Mol. Biol.* 157, 105-132

12. Houghton, R. L., Fisher, R. J., and Sanadi, D. R. (1975), *Biochim. Biophys. Acta* 396, 17-23

13. Fisher, R. J., and Sanadi, D. R. (1971), *Biochim. Biophys. Acta* 245, 34-41

14. Bragg, P. D., and Hou, C. (1968), *Can. J. Biochem.* 46, 631-641

15. Bragg, P. D., and Hou, C. (1972), *FEBS Lett.* 28, 309-312

16. Lee, C. P. and Ernster, L. (1964), *Biochim. Biophys. Acta* 81, 187-190

17. Rydstrom, J., Teixeira da Cruz, A., and Ernster, L. (1970), *Eur. J. Biochem.* 17, 56-62

18. Mitchell, P. and Moyle, J. (1965), *Nature* 208, 1205-1206

19. Skulachev, V. P. (1970), *FEBS Lett.* 11, 301-308

20. Mitchell, P. (1972), *Bioenergetics* 3, 5-24

21. Skulachev, V. P. (1974), *Ann. N. Y. Acad. Sci.* 227, 188-202

22. Mitchell, P. (1966), *Biol. Rev.* 41, 445-502

23. Mitchell, P. (1977), *Ann. Rev. Biochem.* 46, 996-1005

24. Mitchell, P. (1961), *Nature* 191, 144-148

25. Williams, R. J. P. (1961), *J. Theor. Biol.* 1, 1-13

26. Williams, R. J. P. (1985), *The enzymology of biological membranes* (Martonosi, A.N., ed.) vol 4, pp. 71-110, Plenum Press, New York

27. Kell, D. B., Clarke, D. J. and Morris, J. G. (1981),*FEMS Microbiol. Letters* 11, 1-11

28. Prats, M., Teissie, J. and Tocanne, J. F. (1986), *Nature (London)* 322, 756-758

29. Nagel, J. F. and Morowritz, H. S. (1978), *Proc. Natl. Acad. Sci. USA* 75, 298-302

30. Westerhoff, H. V., Melandri, B. A., Venturoli G., Azzone, G. F., Kell, D. B. (1984), *Biochim. Biophys. Acta* 768, 257-292

31. Malpress, F. H. (1984), *Biochem. Soc. Trans.* 12, 399-401

32. Skulachev, V. P. (1982), *FEBS letters* 146, 1-4

33. Lee, C. P., Simard-Duquesne, N., Ernster, L. and Hoberman, H. D. (1965), *Biochim. Biophys. Acta* 105, 397-409

34. Louie, D. D. and Kaplan, N. O. (1970), *J. Biol. Chem.* 245, 5691-5698

35. Chung, A. E. (1970), *J. Bacteriol.* 102, 437-438

36. Kaplan, N. O., Colowick, S. P., Neufield, E. F. and Ciotti, M. M. (1953), *J. Biol. Chem.* 205, 17-29

37. Cohen, P. T. and Kaplan, N. O. (1970), *J. Biol. Chem.* 245, 2825-2836

38. Van den Brock, H. W. J., Santema, J. S., Wassink, J. H. and Veeger, C. (1971), *Eur. J. Biochem.* 24, 31-45

39. Middleditch, L. E., Atchison, R. W., and Chung, A. E. (1972), *J. Biol. Chem.* 247, 6802-6809

40. Danielson, L., and Ernster, L. (1963), *Biochem. Biophys. Res. Commun.* 10, 91-96

41. Danielson, L., and Ernster, L. (1963), *Biochem. Z.* 338, 188-205

42. Danielson, L., and Ernster, L. (1963), *Energy-Linked Functions of Mitochondria* (Chance, B., ed.) pp. 157-175, Academic Press, New York

43. Lee, C. P. and Ernster, L. (1966), *Regulation of Metabolic Processes in Mitochondria*, BBA Library, vol 7, pp. 218-234

44. Conover, E. (1971), *Energy Transduction in Respiration and Photosynthesis*, (Quagliariello, E., Papa, S. and Rossi, C. S. eds.) pp. 999-1005, Adriatica Editrice, Bari

45. Kawasaki, T., Satoh, K. and Kaplan, N. O. (1964), *Biochem. Biophys. Res. Commun.* 17, 648-654

46. Lee, C. P., Azzone, G. F. and Ernster, L. (1964), *Nature* 201, 152-155

47. Cox, G. B., Newton, N. A., Butlin, J. D. and Gibson, F. (1971), *Biochem. J.* 125, 489-493

48. Kanner, B. J. and Gutnick, D. C. (1972), *FEBS Lett.* 22, 197-199

49. Van Dam, K. and ter Welle (1966), *Regulation of Metabolic Processes in Mitochondria*, BBA Library, vol 7, pp. 235-245

50. Murthy, P. S. and Brodie, A. F. (1964), *J. Biol. Chem.* 239, 4292-4297

51. Asano, A., Imai, K. and Sato, R. (1967), *Biochim. Biophys. Acta* 143, 477-486

52. Montal, M., Chance, B., Lee, C. P. and Azzi, A. (1969), *Biochem. Biophys. Res. Commun.* 34, 104-110

53. Ernster, L., Juntii, K. and Asami, K. (1972), *J. Bioenerg.* 4, 149-159

54. Asami, K., Juntii, K. and Ernster, L. (1970), *Biochim. Biophys. Acta* 205, 307-311

55. Nordenbrand, K., Hundal, T., Carlsson, C., Sandri, G. and Ernster, L. (1977), *Bioenergetics of Membranes* (Packer, L. et al., eds.) pp. 135-156, Elsevier/North Holland, Amsterdam

56. Persson, B., Berden, J. A., Rydstrom, J. and van Dam, K. (1987), *Biochim. Biophys. Acta* 894, 239-251

57. Chang, D. Y. S. (1990), *Mechanism of Energization of Transhydrogenase in Escherichia coli Membranes*, M.Sc. thesis, University of British Columbia, Vancouver

58. Van de Stadt, R. J., Nieuewenhuis, F. J. R. M. and van Dam, K. (1971), *Biochim. Biophys. Acta* 234, 173-176

59. Teixeria da Cruz, A., Rydstrom, J. and Ernster, L. (1971), *Eur. J. Biochem.* 23, 203-211

60. Rydstrom, J., Teixeria da Cruz, A. and Ernster, L. (1971), *Eur. J. Biochem.* 23, 212-219

61. Rydstrom, J., Teixeria da Cruz, A. and Ernster, L. (1972), *Biochemistry and Biophysics of Mitochondrial Membranes* (Azzone, G. F. et al., eds.) pp. 177-200, Academic Press, New York

62. Hanson, R. L. (1979), *J. Biol. Chem.* 254, 888-893

63. Homyk, M. and Bragg, P. D. (1979), *Biochim. Biophys. Acta* 571, 201-217

64. Rydstrom, J. (1972), *Eur. J. Biochem.* 31, 496-504

65. Chen, S. and Guillory, R. J. (1984), *J. Biol. Chem.* 259, 5945-5953

66. Wu, L. N. Y., Earle, S. R. and Fisher, R. R. (1981), *J. Biol. Chem.* 257, 7401-7408

67. Enander, K. and Rydstrom, J. (1982), *J. Biol. Chem.* 256, 14760-14766

68. Rydstrom, J. and Enander, K. (1983), *J. Biol. Chem.* 257, 14760-14766

69. Carlenor, E., Tang, H.-L. and Rydstrom, R. (1984), *Analyt. Biochem.* 148, 518-523

70. Rydstrom, J., Lee, C. P. and Ernster, L. (1981), *Chemiosmotic Proton Circuits in Biological Membranes* (Skulachev, V. P. and Hinkle, P. C., eds.) pp. 483-508, Addison-Wesley, Massachusetts

71. Wu, L. N. Y. and Fisher, R. R. (1982), *J. Biol. Chem.* 257, 11680-11683

72. Hojeberg, B. and Rydstrom, J. (1977), *Biochem. Biophys. Res. Commun.* 78, 1183-1190

73. Anderson, W. M. and Fisher, R. R. (1978), *Arch. Biochem. Biophys.* 187, 180-190

74. O'Neal, S.G, Earle, S.R. and Fisher, R. R. (1980), *Biochim. Biophys. Acta* 589, 217-230

75. Rydstrom, J. (1974), *Eur. J. Biochem.* 45, 67-76

76. Wu, L. N. Y., Pennington, R. M., Everett, J. D. and Fisher, R. R. (1982), *J. Biol. Chem.* 257, 4052-4055

77. Persson, B., Enander, K., Tang, H.-L. and Rydstrom, J. (1984), *J. Biol. Chem.* 259, 8626-8632

78. Liang, A. and Houghton R. L. (1980), *FEBS Lett.* 109, 185-188

79. Bragg, P. D., Davies, P. L. and Hou, C. (1972), *Biochem. Biophys. Res. Commun.* 47, 1248-1255

80. Clarke, D. M. and Bragg, P. D. (1985), *Eur. J. Biochem.* 149, 517-523

81. Clarke, D. M., Loo, Tip W., Gilliam, S. and Bragg, P. D. (1986), *Eur. J. Biochem.* 158, 647-653

82. Clarke, D. M. and Bragg, P. D. (1985), *J. Bacteriol.* 162, 367-373

83. Earle, S. R., Anderson, W. M. and Fisher R. R. (1978), *FEBS Lett.* 91, 21-24

84. Earle, S. R. and Fisher R. R. (1980), *Biochemistry* 19, 561-569

85. Rydstrom, J. (1979), *J. Biol. Chem.* 254, 8611-8619

86. Mitchell, P. and Moyle, J. (1973), *Biochem. J.* 132, 571-585

87. Chetkausstaite, A. V. and Grinius, L.L. (1979), *Biokhimiya* 44, 1101-1110

88. Clarke, D. M. (1986), *Pyridine Nucleotide Transhydrogenase*, Ph.D. thesis, University of British Columbia, Vancouver

89. Earle, S. R. and Fisher R. R. (1980), *J. Biol. Chem.* 255, 827-830

90. Wu, L. N. Y. and Fisher, R. R. (1982), *Biochim. Biophy. Acta* 681, 388-396

91. Pennington, R. M. and Fisher, R. R. (1981), *J. Biol. Chem.* 256, 8963-8969

92. Phelps, D. C. and Hatefi, Y. (1981), *J. Biol. Chem.* 256, 8217-8221

93. Beechey, R. B., Robertson, A.M., Holloway, C. T. and Knight, J.G. (1967), *Biochemistry* 6, 3867-3879

94. Casey, R. P., Thelen, M. and Azzi, A. (1980), *J. Biol. Chem.* 255, 3994-4000

95. Dontsov, A. E., Grinius, L. L., Jasaitis, A. A., Severina, I. I. and Skulachev, V. P. (1972), *J. Bioenerg.* 3, 277-303

96. Phelps, D. C. and Hatefi, Y. (1984), *Biochemistry* 23, 4475-4480

97. Phelps, D. C. and Hatefi, Y. (1984), *Biochemistry* 23, 6340-6344

98. Robillard, G. T. and Konings, W. N. (1982), *Eur. J. Biochem.* 127, 597-604

99. Hojeberg, B. and Rydstrom, J. (1979), *Methods Enzymol.* 15, 275-283

100. Earle, S. R., O'Neal, S. G. and Fisher, R. R. (1978), *Biochemistry* 17, 4683-4690

101. Yamaguchi, M. and Hatefi, Y. (1989), *Biochemistry* 28, 6050-6056

102. Capaldi, R. A. and Vanderkooi, G. (1972), *Proc. Natl. Acad. Sci. USA* 69, 930-932

103. Anderson, W. M. and Fisher R. R. (1981), *Biochim. Biophy. Acta* 635, 194-199

104. Wu, L. N. Y. and Fisher, R. R. (1983), *J. Biol. Chem.* 258, 7847-7851

105. Pennington, R. M. and Fisher, R. R. (1983), *FEBS Lett.* 164, 345-349

106. Weis, J. K., Wu, L. N. Y., and Fisher R. R. (1987), *Arch. Biochem. Biophys.* 257, 424-429

107. O'Neal, S. G. and Fisher, R. R. (1977), *J. Biol. Chem.* 252, 4552-4556

108. Blazyk, J. F., Zam, D. and Fisher, R. R. (1976), *Biochemistry* 15, 2843-2848

109. Juntti, K., Torndall, U. B. and Ernster, L. (1970), *Electron Transport and Energy Conservations* (Tager, J. M., Papa, S., Quagliarello, E., and Slater, E. C., eds.) pp. 257-271, Adriatica Editrice, Bari

110. Harlow, E. and Lane, D. (1988), *Antibodies: A Laboratory Manual*, Cold Spring Harbor Laboratory, New York

111. Yamaguchi, M., Wakabayashi, S. and Hatefi, Y. (1990), *Biochemistry* 29, 4136-4143

112. Modrak, D. E., Wu, L. N. Y., Alberta, J. A. and Fisher, R. R. (1988), *Biochemistry* 27, 7665-7671

113. Yamaguchi, M., Y. Hatefi, K. Trach and J.A. Hock (1988), *J. Biol. Chem.* 263, 2761-2767

114. Wakabayashi, S. and Y. Hatefi (1987), *Biochem. Int.* 15, 915-924

115. Kozlov, I. A., Milgrom, Y. M., Saburov, L. A. and Sobolev, A. Y. (1984), *Eur. J. Biochem.* 145, 413-416

116. Persson, B., Hartog, A. F., Rydstrom, J. and Berden, J. A. (1988), *Biochim. Biophy. Acta* 953, 241-248

117. Phelps, D. C. and Hatefi, Y. (1985), *Arch. Biochem. Biophys.* 243, 298-304

118. Yamaguchi, M. and Hatefi, Y. (1985), *Arch. Biochem. Biophys.* 243, 20-27

119. Djavadi-Ohaniance, L. and Hatefi, Y. (1975), *J. Biol. Chem.* 250, 9397-9403

120. Wakabayashi, S. and Y. Hatefi (1987), *Biochem. Int.* 15, 667-675

121. Solioz, M. (1984), *Trends in Biochem. Sci.* 9, 309-312

122. Garnier, J., Osguthorpe, D. J. and Robson, B. (1978), *J. Mol. Biol.* 120, 97-120

123. Rice, D. W., Schulz, G. E. and Guest, J. R. (1984), *J. Mol. Biol.* 174, 483-496

124. Houghton, R. L., Fisher, R. J., and Sanadi, D. R. (1976), *Biochem. Biophys. Res. Commun.* 73, 751-757

125. Hou, C., Potier, M. and Bragg, P. D. (1990), *Biochim. Biophys. Acta* 1018, 61-66

126. Kaufman, B. and Kaplan, N. O. (1961), *J. Biol. Chem.* 236, 2133-2139

127. Rydstrom, J., Hoek, J. B. and Hundal, T. (1974), *Biochem. Biophys. Res. Commun.* 60, 448-455

128. Rydstrom, J., Hoek, J. B., Ericson, B. G. and Hundal, T. (1976), *Biochim. Biophys. Acta* 430, 419-425

129. Pesch, L. A. (1964), *Biochim. Biophys. Acta* 81, 229-235

130. Singh, A. P. and Bragg, P. D. (1975), *J. Bioenerg.* 7, 175-188

131. Lazdunski, M. (1972), *Curr. Top. Bioenerg.* 6, 267-310

132. Klingenberg (1981), *Nature* 290, 449-454

133. Phelps, D. C. and Hatefi, Y. (1985), *Biochemistry* 24, 3503-3507

134. Hatefi, Y., Phelps, D. C. and Galante, Y. M. (1980), *J. Biol. Chem.* 255, 9526-9529

135. Guerra, F., Peron, F. G. and McCarthy, J. L. (1966), *Biochim. Biophy. Acta* 117, 433-449

136. Oldham, S. B., Bell, J. J. and Harding. B. W. (1968), *Arch. Biochem. Biophys.* 123, 496-506

137. Sauer, L. A. and Mulrow, P. J. (1969), *Arch. Biochem. Biophys.* 134, 486-496

138. Sauer, L. A. (1970), *Arch. Biochem. Biophys.* 139, 340-350

139. Sauer, L. A. (1972), *Arch. Biochem. Biophys.* 149, 42-51

140. Harano, Y. and Kowal, J. (1972), *Arch. Biochem. Biophys.* 153, 68-73

141. Kaplan, N. O. (1972), *Harvey Lect.* 66, 105-133

142. Ernster, L. and Navazio, F. (1956), *Exp. Cell Res.* 11, 483-486

143. Ernster, L. and Navazio, F. (1957), *Biochim. Biophys. Acta* 26, 408-415

144. Nicholls, D. G. and Garland, P. B. (1969), *Biochem. J.* 114, 215-225

145. Lowenstein, J. M. and Smith, S. R. (1962), *Biochim. Biophys. Acta* 56, 385-387

146. Jocelyn, P. C. and Dickson, J. (1980), *Biochim. Biophys. Acta* 590, 1-12

147. Bellamo, G., Martino, A., Richelmi, P., Moore, G. A., Jewell, S. A. and Orrenius, S. (1984), *Eur. J. Biochem.* 140, 1-6

148. Houghton, R. L., Fisher, R. J., and Sanadi, D. R. (1976), *Arch. Biochem. Biophys.* 176, 747-752

149. Gerolimatos, B. and Hanson, R. L. (1978), *J. Bacteriol.* 134, 394-400

150. Houghton, R. L. (1980), *Fed. Proc.* , 39, 1773

151. Quay, S. C. and Oxender, D. L. (1976), *J. Bacteriol.* 127, 1225-1238

152. Liang, A. and Houghton, R. L. (1981), *J. Bacteriol.* 146, 997-1002

153. Zahl, K. J., Rose, C. and Hanson, R. L. (1978), *Arch. Biochem. Biophys.* 190 598-602

154. Hanson, R. L. and Rose, C. (1979), *J. Bacteriol.* 138, 783-787

155. Hanson, R. L. and Rose, C. (1980), *J. Bacteriol.* 141, 401-404

156. Witholt, B., Boekhout, M., Brock, M., Kingma, J. and Heerikhuizen, H. V. (1976), *Analyt. Biochem.* 74, 160-170

157. Lowry, O. H., Rosegrough, N. J., Farr, A. L. and Randall, A. J. (1951), *J. Biol. Chem.* 193, 265-275

158. Kaplan, N. O. (1967), *Methods Enzymol.* 10, 317-322

159. Laemmli, U. K. (1970), *Nature (London)* 227, 680-685

160. O'Farrell, P. H. (1975), *J. Biol. Chem.* 250, 4007-4021

161. Cleveland, D. W., Fischer, S. G., Kirscher, M. W. and Laemmli, U. K. (1977), *J. Biol. Chem.* 252, 1102-1106

162. Towbin, H., Staehelin, T. and Gordon, J. (1979), *Proc. Natl. Acad. Sci. USA* 76, 4350-4354

163. Rydstrom, J., Persson, B. and Tang, H.-L. (1984), *Bioenergetics* (Ernster ed.) pp. 207-219, Elsevier Science Publisher, B.V.